Université de Montréal

Regulation of HMG-CoA reductase, HSL and ACAT expression and activity in testicular cholesterol metabolism in mink and in mouse following experimental genetic deletion

par

Li Chen

Département de Pathologie et Biologie Cellulaire
Faculté de Médecine

Mémoire présenté à la faculté des études supérieures
En vue de l'obtention du grade de
Philosophiae doctor (Ph.D)

Août 2009

Université de Montréal

Faculté des études supérieures

Cette thèse intitulée:

Regulation of HMG-CoA reductase, HSL and ACAT expression and activity in testicular cholesterol metabolism in mink and in mouse following experimental genetic deletion

présentée par :

Li Chen

a été évaluée par un jury composé des personnes suivantes :

Président-rapporteur :	Dr. Bruce Murphy
Directeur de recherche :	Dr. R-Marc Pelletier
Co-directeur:	Dr. Maria Leiza Vitale
Membre du jury :	Dr. Victor Gavino
Examinateur externe :	Dr. Julie Lafond
Représentant du doyen de la FES :	

List of abbreviations

ACAT-1,2……....acyl-CoA: cholesterol acyltransferase 1,2

BPB…….....……...Bromophenol blue

cDNA……...….complementary DNA

CPMB ……..radiation **c**ounts **p**er **m**inute (cpm) in region **B**

DAB…….…….....diaminobenzidine

DMSO……...dimethylsulfoxide

DNase I……..deoxyribonuclease I

DNA……...deoxyribonucleic acid

dNTP……deoxyribonucleotide triphosphate

DTT……...dithiothreitol

EDTA……..ethylenediaminetetraacetic acid

EGTA…….ethylene glycol-bis-(2-aminoethyl ether)--- N,N,N', N-tetraacetic acid

HMG CoA……...3-Hydroxy-3-methylglutaryl coenzyme A

HMG-CoA reductase……...3-hydroxy-3-methylglutaryl coenzyme A reductase

HPRT-1……...hypoxanthine phosphoribosyltransferase 1

HRP……...horseradish peroxidase

HSL……hormone-sensitive lipase

MVL……...mevalonolactone

ß-NADP……ß-nicotinamide adenine dinucleotide phosphate

NADPH……nicotinamide hypoxanthine dinucleotide phosphate

oleyl CoA……. oleyl-coenzyme A

OCS……....organic counting scintillant

PBS……....phosphate buffer solution

PMSF…….....phenylmethylsulfonyl fluoride

PNPB……..p-nitrophenyl butyrate

RT……..room temperature

SCAP……..…..SREBP clevage-activating protein

SDS…….. sodium dodecyl sulfate

SDS-PAGE……SDS-polyacrylamide gel electrophoresis

SREBP…….....…..sterol resposive element binding protein

SR-BI…….scavenger receptor class B type I

STf……...seminiferous tubule- enriched fractions

ITf……..interstitial tissue-enriched fractions

THF……tetrahydrofuran

Résumé

Introduction: L'homéostasie du cholestérol est indispensable à la synthèse de la testostérone dans le tissu interstitiel et la production de gamètes mâles fertiles dans les tubules séminifères. Les facteurs enzymatiques contribuent au maintien de cet équilibre intracellulaire du cholestérol. L'absence d'un ou de plusieurs enzymes telles que la HMG-CoA réductase, la HSL et l'ACAT-1 a été associée à l'infertilité masculine. Toutefois, les facteurs enzymatiques qui contribuent au maintien de l'équilibre intra-tissulaire du cholestérol n'ont pas été étudiés. Cette étude a pour but de tester l'hypothèse que le maintien des taux de cholestérol compatibles avec la spermatogenèse nécessite une coordination de la fonction intracellulaire des enzymes HMG-CoA réductase, ACAT1 et ACAT2 et la HSL. **Méthodes**: Nous avons analysé l'expression de l'ARNm et de la protéine de ces enzymes dans les fractions enrichies en tubules séminifères (STf) de vison durant le développement postnatal et le cycle reproductif annuel et dans les fractions enrichies en tissu interstitiel (ITf) et de STf durant le développement postnatal chez la souris. Nous avons développé deux nouvelles techniques pour la mesure de l'activité enzymatique de la HMG-CoA réductase et de celle de l'ACAT1 et ACAT2. En outre, l'immunohistochimie a été utilisée pour localiser les enzymes dans le testicule. Enfin, les souris génétiquement déficientes en HSL, en SR-BI et en CD36 ont été utilisées pour élucider la contribution de la HMG-CoA réductase, l'ACAT1 et l'ACAT2 et la HSL à l'homéostasie du cholestérol. **Résultats**: 1) **HMG-CoA réductase**: (Vison) La variation du taux d'expression de l'ARNm de la HMG-CoA réductase était corrélée à celle de l'isoforme de 90 kDa de la protéine HMG-CoA réductase durant le développement postnatal et chez l'adulte durant le cycle reproductif saisonnier. L'activité enzymatique de la HMG-CoA réductase augmentait de façon concomitante avec le taux protéinique pour atteindre son niveau le plus élevé à 240 jours (3.6411e-7 mol/min/μg de protéines) au cours du développement et en Février (1.2132e-6 mol/min/μg de protéines) durant le cycle reproductif chez l'adulte. (Souris), Les niveaux d'expression de l'ARNm et l'activité enzymatique de la HMG-CoA réductase étaient maximales à 42 jours. A l'opposé, le taux protéinique diminuait au cours du

développement. 2) **HSL**: (Vison), l'expression de la protéine de 90 kDa de la HSL était élevée à 180- et 240 jours après la naissance, ainsi qu'en Janvier durant le cycle saisonnier chez l'adulte. L'activité enzymatique de la HSL augmentait durant le développement pour atteindre un pic à 270 jours (36,45 nM/min/μg). Chez l'adulte, l'activité enzymatique de la HSL était maximale en Février. (Souris) Le niveau d'expression de l'ARNm de la HSL augmentait significativement à 21-, 28- et 35 jours après la naissance concomitamment avec le taux d'expression protéinique. L'activité enzymatique de la HSL était maximale à 42 jours suivie d'une baisse significative chez l'adulte. 3) **ACAT-1 et ACAT-2**: Le présent rapport est le premier à identifier l'expression de l'ACAT-1 et de l'ACAT-2 dans les STf de visons et de souris. (Vison) L'activité enzymatique de l'ACAT-2 était maximale à la complétion du développement à 270 jour (1190.00 CPMB/200 μg de protéines) et en janvier (2643 CPMB/200 μg de protéines) chez l'adulte. En revanche, l'activité enzymatique de l'ACAT-1 piquait à 90 jours et en août respectivement durant le développement et chez l'adulte. (Souris) Les niveaux d'expression de l'ARNm et la protéine de l'ACAT-1 diminuait au cours du développement. Le taux de l'ARNm de l'ACAT-2, à l'opposé du taux protéinique, augmentait au cours du développement. L'activité enzymatique de l'ACAT-1 diminuait au cours du développement tandis que celle de l'ACAT-2 augmentait pour atteindre son niveau maximal à 42 jours. 4) **Souris HSL-/ -**: Le taux d'expression de l'ARNm et l'activité enzymatique de la HMG-CoA réductase diminuaient significativement dans les STf de souris HSL-/- comparés aux souris HSL+/+. Par contre, les taux de l'ARNm et les niveaux des activités enzymatiques de l'ACAT-1 et de l'ACAT-2 étaient significativement plus élevés dans les STf de souris HSL-/- comparés aux souris HSL+/+ 5) **Souris SR-BI-/-**: L'expression de l'ARNm et l'activité enzymatique de la HMG-CoA réductase et de l'ACAT-1 étaient plus basses dans les STf de souris SR-BI-/- comparées aux souris SR-BI+/+. A l'opposé, le taux d'expression de l'ARNm et l'activité enzymatique de la HSL étaient augmentées chez les souris SR-BI-/- comparées aux souris SR-BI+/+. 6) **Souris CD36-/-**: L'expression de l'ARNm et l'activité enzymatique de la HMG-CoA réductase et de l'ACAT-2 étaient significativement plus faibles tandis que celles de la HSL et de l'ACAT-1 étaient inchangées dans les STf de souris CD36-/-

comparées aux souris CD36+/+. **Conclusion**: Nos résultats suggèrent que: 1) L'activité enzymatique de la HMG-CoA réductase et de la HSL sont associées à l'activité spermatogénétique et que ces activités ne seraient pas régulées au niveau transcriptionnel. 2) L'ACAT-1 et de l'ACAT-2 sont exprimées dans des cellules différentes au sein des tubules séminifères, suggérant des fonctions distinctes pour ces deux isoformes: l'estérification du cholestérol libre dans les cellules germinales pour l'ACAT-1 et l'efflux du cholestérol en excès dans les cellules de Sertoli au cours de la spermatogenèse pour l'ACAT-2. 3) La suppression génétique de la HSL diminuait la HMG-CoA réductase et augmentait les deux isoformes de l'ACAT, suggérant que ces enzymes jouent un rôle critique dans le métabolisme du cholestérol intratubulaire. 4) La suppression génétique des transporteurs sélectifs de cholestérol SR-BI et CD36 affecte l'expression (ARNm et protéine) et l'activité des enzymes HMG-CoA réductase, HSL, ACAT-1 et ACAT-2, suggérant l'existence d'un effet compensatoire entre facteurs enzymatiques et non-enzymatiques du métabolisme du cholestérol dans les fractions tubulaires. Ensemble, les résultats de notre étude suggèrent que les enzymes impliquées dans la régulation du cholestérol intratubulaire agissent de concert avec les transporteurs sélectifs de cholestérol dans le but de maintenir l'homéostasie du cholestérol intra-tissulaire du testicule.

Mots-clés: Homéostasie du cholestérol, HMG-CoA réductase, HSL, ACAT-1, ACAT-2, Spermatogenèse

Summary

Introduction: Cholesterol homeostasis is essential for the synthesis of testosterone in interstitial tissue and the production of fertile gametes in the seminiferous tubules of the testis. Intracelluar cholesterol equilibrium in the testis is delicately maintained and regulated by enzymatic factors. The absence of one or more enzymes (HMG-CoA reductase, HSL and ACAT) has been implicated in the development of male infertility. However, the enzymatic factors that contribute to the maintenance of cholesterol equilibrium have not been investigated. This study is to test the hypothesis that the coordinated function of intracellular enzymes, HMG-CoA reductase, HSL and ACAT isoforms, are the basis of a system that helps to maintain cholesterol equilibrium during spermatogenesis. **Methods:** We characterized mRNA and protein expression levels of these enzymes in mink seminiferous tubules-enriched fraction (STf) during development and the annual reproductive cycle; or in mouse interstitial tissue-enriched fraction (ITf) and STf during postnatal development. Two novel techniques were developed to measure the HMG-CoA reductase, HSL and ACAT activities in mink and mouse STf. Additionally, immunohistochemistry was used to localize the enzymes in the testis. Finally, HSL knockout (KO) infertile male mice and selective cholesterol transporter (SR-BI, CD36) KO mice were used to elucidate the contribution of HMG-CoA reductase, HSL and ACAT isoforms in testicular cholesterol homeostasis when the enzyme or cholesterol transport system was genetically impeded. **Results: 1) HMG-CoA reductase**: (In mink STf), HMG-CoA reductase mRNA levels were relatively independent of 90kDa protein expression during development and the seasonal cycle. HMG-CoA reductase activity increased independently of its protein expression and reached maximal values by day 240 (3.6411e-7 mol/min/μg protein) during development and peaked in February (1.2132e-6 mol/min/μg protein) during the seasonal cycle. (In mouse STf), HMG-CoA reductase mRNA levels and enzymatic activity peaked by 42 days before decreasing while the protein levels tended to decrease steadily. **2) HSL**: (In mink STf), an increase of 90kDa HSL

protein expression by day 180- and 240 after birth as well as in January in seasonal cycle, was not related to the enzyme mRNA expression. HSL activity increased progressively through development and peaked by 270 days (36.45 nM/min/μg); another high HSL activity was shown in February. (In mouse STf), three significant elevations in HSL mRNA levels by day 21, 28, and 35 corresponded to a steady elevation of HSL protein expression throughout development. HSL activity peaked by day 42 but decreased remarkably in the adult. 3) **ACAT-1 and ACAT-2**: This is the first report to establish the presence of both ACAT-1 and ACAT-2 in the mink and mouse testis. (In mink STf), ACAT-2 activity reached its maximal value at 1190.00 CPMB/200μg protein by day 270 and 2643 CPMB/200μg protein in January. In contrast, ACAT-1 activity peaked by day 90 or in August during the seasonal cycle. (In mouse STf), ACAT-1 mRNA and protein levels were both decreased throughout development; ACAT-2 mRNA levels changes in the opposite direction of the protein levels, increasing throughout development. ACAT-1 activity in STf decreased throughout the development; while ACAT-2 activity increased significantly during development and peaked by day 42. **4) HSL-/- mice**: KO HSL gene caused a decrease of HMG-CoA redutase mRNA expression and enzymatic activity in STf. However, ACAT-1 and ACAT-2 mRNA levels and enzymatic activities significantly increased in STf. **5) SR-BI-/- mice**: The mRNA expression and activity of HMG-CoA reductase as well as ACAT-1 were statistically decreased in STf; whereas HSL mRNA level and activity were increased. **6) CD36-/- mice**: The mRNA expression and activity of HMG-CoA reductase as well as ACAT-2 were significantly decreased in STf; while HSL and ACAT-1 mRNA levels and activities remained constant. **Conclusion:** These results suggest that 1) Activation of HMG-CoA reductase and HSL is associated with spermatogenetic activity, while the enzymatic activities may not only be regulated transcriptionally. 2) ACAT-1 and ACAT-2 are expressed in different cells of the tubules, suggesting distinct functions for these two closely related enzyme isoforms, with ACAT-1 being related to cholesterol esterification in germ cells and with ACAT-2 being associated with the removal of excessive cholesterol by Sertoli cells during spermatogenesis. 3) Genetically blocking HSL reduced the activity of HMG-CoA reductase while increasing

activity of ACAT isoforms, suggesting the turn-off the enzyme in the cholesterol ester cycle may be essential for the accumulation of cholesterol esters in the tubules. 4) The dysfunction of intracellular cholesterol transporters affects regulation of the enzymes (HMG-CoA reductase, HSL and ACAT-1 and ACAT-2), which is presumably in response to compensatory extracellular cholesterol uptake. This study suggests that the enzymes implicated in the regulation of intracellular cholesterol may act cooperatively to maintain cholesterol homeostasis in testis.

Keywords: cholesterol homeostasis, HMG-CoA reductase, HSL, ACAT-1, ACAT-2, spermatogenesis

To my mom, who gave all her life to me

To my father, who guided me to being a good person

Acknowledgement

I wish to express my deep and sincere gratitude to my research supervisor **Dr. R.-Marc Pelletier** and co-supervisor **Dr. María L. Vitale** for being excellent mentors, for their timely advice, for respecting my ideas, for their encouragement and friendship, also for providing me with a great environment for learning and independence. With their support, this work was a pleasure to finalize.

I am deeply indebted **Prof. Julie Lafond** from Department of Biological Sciences of Université du Québec à Montréal for providing me with valuable experimental assistance at all levels of the research project and at times of critical need. I warmly thank **Lucie Simoneau**, the research assistant in Julie's laboratory, for her technical support and friendly help. Her extensive discussions around my work and interesting explorations in operations have been very helpful for this study.

I would like to acknowledge all the lab members in Julie's laboratory for their friendship and help: **Georges Daoud, Charles Marseille, Laurent Perrier, Marie Claude, Ariane Gravel, Maude Éthier, ARFA Omar, Anne Radenne**, **Fédérique le Bellego.** Special mention must also be given to **Aline Schmitt** and **Isabelle Poudrier** who encourage me in so many difficult ways.

I am also grateful to my classmates **Casimir D. Akpovi** and **Sara Solinet**, for their invaluable help and support during my studies. I have collaborated with many colleagues for whom I have great regard, and I wish to extend my warmest thanks to all those who have helped me with my work in the Department of Pathology and Cell biology of University of Montreal.

I would like to thank the jury members for having provided their time and effort in evaluating my thesis. Scholarships from the Canadian Institute of Health Research (CIHR) through the Strategic Training Initiative in Research in the Reproductive Health Sciences

Research (STIRRHS), from Chinese government and from Faculté des études supérieures of University of Montreal are great appreciated.

I am deeply and forever indebted to my father for his love, support and throughout my entire life. I am also thankful to my brother, my sister- in law and my niece for their constant support. I am also grateful to my friends **Chen Qiang, Zhang Jie, Zheng Guifu** and for their generous aid.

Eventually, and most importantly, I would like to thank my husband **Zhou Yu**, whose sacrifices, unconditional love, never-ending support, and tireless encouragement were instrumental in the pursuit of my education.

Previous achievements

1) Published papers

1.1) Published papers

1. **Chen L.**, Zhou Y., Huang D. W., Kennedy M. A. 2009 Differential expression in the brain of the ATP-binding cassette (ABC) transporters ABCG1 and ABCG4, but not ABCA1, during postnatal development in C57BL/6J mice (Submitted to *Brain Res.*).

2. Wu Y., **Chen L.**, Yu H., Liu H., An W. 2007 Transfection of hepatic stimulator substance gene desensitizes hepatoma cells to H2O2-induced cell apoptosis via preservation of mitochondria *Arch Biochem Biophys.* 464:48-56

3. Li Y.J., Cui W., Tian Z.J., Hao Y.M., Du J., Liu. F., Zhang H., Zu X.G., Liu S.Y., Xie R.Q., Yang X.H., Wu Y.Z., **Chen L**., An W. 2004 Crosstalk between ERK1/2 and STAT3 in the modulation of cardiomyocyte hypertrophy induced by cardiotrophin-1 *Chinese Medical Journal* 117:1135-1142

4. Tian Z.J., Cui W, Li Y.J., Hao Y.M., Du J., Liu F., Zhang H., Zu X.G., Liu S.Y., **Chen L**., An W 2004 Different contributions of STAT3, ERK1/2, and PI3-K signaling to cardiomyocyte hypertrophy by cardiotrophin-1 *Acta Pharmacologica Sinica* 25:1157-1164

5. **Chen L**., Sun H.L., Yang L., Du H.J., An W. 2004 Transfection of human hepatic stimulator substance gene could protect BEL-7402 cells against hepatotoxins *Chinese Journal of Hepatology* 12:99-101

6. Wang X.N., Song Z.G., Wu Y., **Chen L**., Zhao Y.Y., An W. 2003 Cloning and structural analysis of 5'-flanking sequence of human hepatic stimulator substance (hHSS) gene *Yi Chuan Xue Bao* 30:1171-1176

7. **Chen L**., Sun H.L., An W. 2003 Increased cellular proliferation and protection of recombined human hepatic stimulator substance *Acta anatomica sinica* 34:162-166

8. Du H.J., Sun H.L., **Chen L**., An W. 2002 Prokaryotic expression and purification of human hepatic stimulator substance *Acta Physiologica Sinica* 54:23-27

9. Zhang M., Zhang B.H., **Chen L**., An W. 2002 Overexpression of heme oxygenase-1 protects smooth muscle cells against oxidative injury and inhibits cell proliferation *Cell Research* 12:123-132

10. Zhang M., An W., Du H.J., **Chen L**., Zhang B.H. 2002 Increased resistance against oxidant injury in the rat vascular smooth muscle cells transfected with human heme oxygenase-1 gene *Acta Physiologica Sinica* 54:12-16

11. **Chen L**., An W., Tan X., Gao D.Ch., Dai J. 2001 Phosphorylation of hepatic stimulator substance on MAPK in BEL- 7402 hepatoma cells *Chinese Journal of Hepatology* 9:22-24

12. An W., Du H.J., **Chen L**. 2001 Increased cellular proliferation in BEL-7402 hepatoma cells transfected by human hepatic stimulator substance gene *Acta Physiologica Sinica* 53:473-477

13. Dai J., An W., Gao D.Ch., **Chen L**. 2000 Influence of hepatic stimulator substance on $p21^{ras}$ expression in human hepatic carcinoma cells BEL-7402 *Acta Physiologica Sinica* 52:225-229

14. Gao D.Ch., An W., Rong Y., Dai J., **Chen L**. 1999 Gene therapy for hepatocellular carcinoma with HSV-TK/GCV System *in vivo* *Chin. J. Appl. Physiol.* 15:77-79

15. Liang F.Y., Rong Y., **Chen L**. 1999 Effect of tamoxifen and interleukin-6 on apoptosis in MCF-7 human breast cancer cells *in vitro*. *Journal of Capital University of Medical Sciences* 20:13-16

16. Liang F.Y., Rong Y., **Chen L**., Gao D.Ch., Dai J., An W. 1999 The killing effect and possible mechanism of norcantharidin on mammalian cells. *Journal of Northwest University* 29:25-28

17. **Chen L**., Cui Y.W., Zou T. 1998 The separation, purification, antisepsis and preservation of biochemical facolony *Research of Chinese Medical Biology* 2:145-148

1.2) Manuscripts in preparation

1. **Chen L**., Akpovi C.D., Vitale M.L., Klint C., Holm C., Simoneau L., Lafond J., Pelletier R.M. Hormone-sensitive lipase deficiency in mice causes cholesterol

accumulation due to a deregulation of HMG CoA reductase and ACAT1 and ACAT2 in the testis.

2. **Chen L**., Vitale M.L., Simoneau L., Lafond J., Pelletier R.M. Acyl-CoA: cholesterol acyltransferase 2 (ACAT2) but not ACAT1 enzymatic activity, increases with the spermatogenic activity in the seminiferous tubules.

3. **Chen L**., Akpovi C.D., Vitale M.L., Simoneau L., Lafond J., Pelletier R.M. Enzymatic activity of HMG CoA reductase increases with the spermatogenic activity but not with intratubular cholesterol levels in the seminiferous tubules.

2) Book chapters:

1. **Chen L.,** Lafond J., Pelletier R.M. 2009 A novel technical approach for the measurement of individual ACAT-1 and ACAT-2 enzymatic activity in the testis. In: Human embryogenesis: Methods and protocols. Julie Lafond & Cathy Vaillancourt (eds) The Humana Press Inc. Press Totowa NJ

3) Abstracts (peer reviewed):

1. **Chen L**., Akpovi C.D., Vitale M.L., Lafond J., Pelletier R.M. 2007 Enzymatic activity of HMG CoA reductase increases with the spermatogenic activity but not with the intratubular cholesterol level *Médecine/Sciences* 34:136.

2. **Chen L**., Vitale M.L., Pelletier R.M. 2005 Changes of the 3-hydroxy-3-methyl glutaryl coenzyme reductase (HMG-CoA red.) expression in the testis during development and adulthood throught the annual reproductive cycle in a seasonal breeder, the mink *(Mustela vison)*. *Biol. Reprod.,* 169:T398

3. **Chen L**., Vitale M.L., Pelletier R.M. 2005 Analysis of the changes in the expression of the HMG CoA reductase in the seminiferous tubules of the mink *(Mustela vison)*. *J. Soc. Obstetricians and Gynaecologists Canada*, 27: 291

4. **Chen L**., Akpovi C.D., Ong H.,Vitale M.L., Pelletier R.M. 2004 CD 36 influences differently the expression of distinct isoforms of the hormone-sensitive lipase in each compartment of the testis. *Biol. Reprod.,* 260:729A

4) Oral presentation:

1. **Chen L** 2008 ATP-binding cassette transporters G1 and G4 mediate cholesterol and desmosterol efflux to HDL and regulate sterol accumulation in the brain Center

for Molecular and Human Genetics, The Research Institute at Nationwide Children's Hospital, August, 2008

.

2**. Chen L**., Akpovi C.D., Vitale M.L., Lafond J., Pelletier R.M. 2007 An increase in the enzymatic activity of HMG CoA reductase is not accompanied by a change of the intratubular cholesterol level in adult mink. Université de Montréal, mai 2007.

3. **Chen L**., Akpovi C.D., Vitale M.L., Lafond J., Pelletier R.M. 2007 HMG CoA reductase enzymatic activity is increase with the expression of the catalytic portion of this enzyme in adult mink. CHU Sainte-Justine, mai 2007

4. **Chen L**., Akpovi C.D., Vitale M.L., Lafond J., Pelletier R.M. 2007 Variation of HMG CoA reductase activity is not coincident with the change of the intratubular cholesterol in adult mink. Université du Québec à Montréal, mai 2007

5. **Chen L**., Vitale M.L., Simoneau L., Lafond J., Pelletier R.M. 2006 ACAT-2, expressed in the mouse testis, is associated with increased esterified cholesterol levels. Université de Montréal, mai 2006.

6. **Chen L**., Vitale M.L., Ong H., Pelletier R.M. 2004 Expression du récepteur CD36 en relation avec le métabolisme du cholestérol dans le testicule. 72^{e} congrès de l'ACFAS Université du Québec à Montréal, mai 2004.

7. **Chen L**., Akpovi C.D., Ong H., Vitale M.L., Pelletier R.M. 2004 The knocking out of CD36 influences differently the expression of hormone-sensitive lipase (HSL) isoforms in mouse testis. 21^{e} journée scientifique du département de pathologie et biologie cellulaire, Université de Montréal, mai 2004

8. **Chen L.**, Akpovi C.D., Ong H.,Vitale M.L., Pelletier R.M. 2004 Differential expression of the hormong-sensitive lipase (HSL) isoforms in CD36-knock out mouse testis. Journée annuelle de la recherche du département d'obstétrique-gynécologie Université de Montréal, avril 2004

List of tables

List of figures

Introduction

1. Testis

1.1 General structure of the testis

Within the mammalian testis are coiled thin tubes called seminiferous tubules bound together by interstitial tissue. The seminiferous tubules and interstitial tissue constitute two morphologically and functionally distinct compartments: namely the site of germ cell production i.e., spermatogenesis; and the site of the primary male sex hormone production, such as testosterone. Inside the tubules, the various germ cells are surrounded and supported by the somatic Sertoli cells. The walls of the tubules are formed by peritubular myoid cells. Next to the myoid cells is the interstitial tissue which includes comprised of blood vessels, lymphatic vessels and nerves, together with the steroid-producing Leydig cells, macrophages, and other cells (Diagram 1).

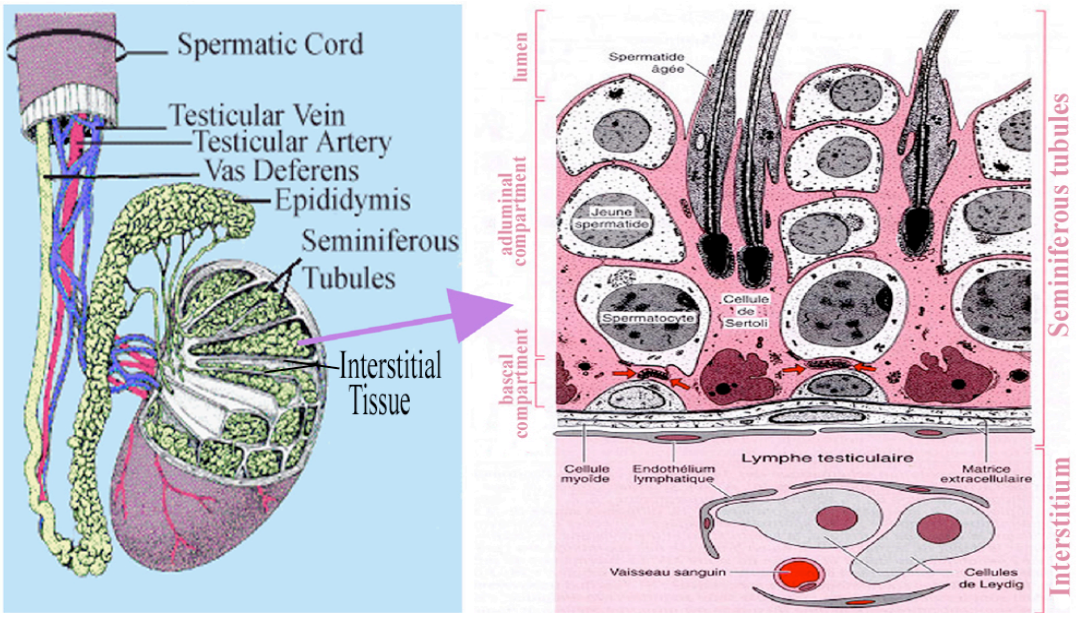

Diagram 1. Schematic drawing of the testis [Taken from (Salasin, 2000)]

1.1.1 Interstitial tissue and testosterone secretion

The connective tissue contains large, prominent Leydig cells which differentiate during puberty (Leydig, 1850); and it also includes a relatively important proportion of macrophage cells (Fawcett et al., 1973; Wing & Lin, 1977) which contacts closely with Leydig cells (Hutson, 1992). 25-hydroxylase in testicular macrophages converts ^{14}C-cholesterol to ^{14}C-25-hydroxycholesterol (Lukyanenko et al., 2001) which is further synthesized to testosterone by Leydig cells (Nes et al., 2000). Leydig cells in most seasonal breeders undertake different appearances depending on breeding season. During breeding season, Leydig cells transform from an "undifferentiated" interstitial cells into active Leydig cells characterized by abundant smooth ER, mitochondria full of prominent tubular cristae, and a large number of medium sized lipid droplets. By the end of breeding season, Leydig cells gradually regress and losing their specific characteristics (Hochereau-de Reviers & Lincoln, 1978; Wing & Lin, 1977).

1.1.2 Seminiferous tubules and spermatogenesis

The seminiferous epithelium is a complex stratified epithelium composed of two functions distinct cell types: Somatic Sertoli cells and germ cells (Diagram 1). In 1865, Enrico Sertoli described columnar cells extending from the basement membrane to the lumen of the seminiferous tubulers and enveloping the neighbouring germ cells while providing physical and "nursing" support (Sertoli, 1865). The Sertoli cells are a nonproliferating population (Clegg, 1963; Steinberger & Steinberger, 1971); and adjacent Sertoli cells are joined to one another by distinct types of junctions: hemidesmosomes, gap

and tight or occluding junctions (Pelletier & Byers, 1992; Pelletier & Friend, 1983). Physiological and morphological studies have established that the Sertoli- Sertoli tight junctions are the site of the blood-testis barrier (Pelletier & Byers, 1992). The blood-testis barrier divides the germinal epithelium into a basal cellular compartment adjacent to the basal lamina and in contact with the blood-borne substances and a luminal cellular compartment sequestered from the blood. Pelletier et al. (1986) demonstrated that the establishment of the blood-testis barrier is correlated with the development of the lumen and the establishment of gradients between the apical and the basolateral fluid compartments, and not necessarily with the presence of a particular generation of germ cells in the seminiferous epithelium.

Spermatogenesis is the developmental process in seminiferous tubules whereby the germ cells are undergo the undifferentiated spermatogonia to spermatozoa (Clermont, 1972). Spermatogenesis consists of three principal phases and each involving a distinct class of germ cells (Clermont, 1972). (1) Spermatogonial phase, the diploid spermatogonia proliferate by mitosis. The spermatogonia reside in the basal compartment of the seminiferous epithelium where they perpetuate their own numbers to give rise to spermatocytes (De Rooij et al., 1989; Leblond & Clermont, 1952). The germ cells located in the basal compartment migrate into the luminal compartment to complete meiosis and undergo cellular differentiation. This migration of the germ cells occurs at a precise moment, the early zygotene spermatocyte stage in most species (Cavicchia & Miranda, 1988; Cavicchia & Sacerdote, 1991; Dym & Cavicchia, 1977; Dym & Cavicchia, 1978). (2) Meiosis: This phase is characterized by the reduction of the number of chromosomes

from diploid (2n) to haploid (n) (Diagram 1). (3) Spermiogenesis: Spermatids differentiate in this stage. The main features include formation of the acrosome, development of a flagellum, condensation of the chromatin and loss of residual cytoplasm containing lipids and organelles (Leblond & Clermont, 1952).

1.2 Cholesterol in testis

Previous observations showed that cholesterol is an important structural component of cellular membranes and myelin and the precursor of oxysterols, steroid hormones and bile acids (Goldstein & Brown, 1990). Cholesterol is composed of four hydrocarbon rings, a hydroxyl group and a hydrocarbon tail. The 4-ring region of cholesterol is the signature of all steroid hormones (such as testosterone in the testis) (Xu et al., 2005). The hydroxyl group in cholesterol converts the otherwise highly hydrophobic molecule into an amphiphile modecule, and orients its position in the membranes. In addition, it can mediate hydrogen bonding with water and possibly other membrane lipids (Bittman et al., 1994; Boggs, 1987). Both the hydrocarbon tail and the ring region are non-polar. These specific structures are critical for cholesterol solubility in fatty and oily substances while not mixing with water.

In testis, cholesterol is mainly distributed in the microsomal fraction (Ichihara, 1969) and is involved in testosterone synthesis (Shikita & Tamaoki, 1965) and spermatogenesis (Armstrong, 1970). The concentration of cholesterol in testis exhibits considerable variations in prebubertal as well as adult animals (Aoki & Massa, 1975). Cyclic changes in testicular cholesterol distribution have also been detected in a seasonal mammal (*Talpa*

europaea) (Lofts & Boswell, 1960). The physiological fluctuations of testicular cholesterol concentration absolutely require efficient mechanisms to maintain cholesterol equilibrium that is crucial for normal testis functions and spermatogenesis. Recent studies on hyper- and hypocholesterolemia added new evidence showing the physiological significance of cholesterol homeostasis in the testis: hypercholesterolemia caused spermatogenesis inhibition (Bataineh & Nusier, 2005) and hypocholesterolmia impaired fertility (Wechsler et al., 2003). The regulation of intracellular cholesterol metabolism for the maintenance of spermatogenesis needs future investigation.

Cholesterol participates in testosterone production and spermatogenesis (Armstrong, 1970). These important physiological events occur in two distinct compartments of testis: the interstitial tissue and seminiferous tubules.

1.2.1 Cholesterol in the interstitial tissue

Testosterone is synthesized and secreted in the interstitial tissue. The precursor of testosterone is cholesterol. The possible sources of cholesterol could be either plasma lipoprotein or *de novo* synthesized cholesterol (Fofana et al., 1996). For example, in rat interstitial tissue, 40% of cholesterol is derived from plasma and 60% from *de novo* synthesis (Morris & Chaikoff, 1959). Cholesterol synthesis is mediated by a series of enzymes located in the endoplasmic reticulum of the Leydig cells. Among these enzymes, 3-hydroxy-3-methylglutaryl coenzyme A (HMG-CoA) reductase is the rate-limiting enzyme which converts HMG-CoA to mevalonate, an intermediate associated with testosterone production (Hou et al., 1990). HMG-CoA reductase activity increased dramatically in agreement with the elevation of testosterone production after experimental

hormone treatment on cultured Leydig cells *in vitro* (Hou et al., 1990). HMG-CoA reductase activity reached highest levels at the onset of sexual maturation when testosterone levels reach their maximum in rat testis (Ness & Nazian, 1992). These findings suggest that *de novo* cholesterol synthesis might be the main source of testosterone production.

On the other hand, plasma derived cholesterol for testosterone production must be hydrolysed by Hormone-sensitive lipase (HSL), one of the cholesteryl ester lipases that free esterified cholesterol (Holm et al., 2000). Observations from our lab showed that HSL protein levels and enzymatic activity are positively correlated with serum testosterone levels during development in the Guinea pig (Kabbaj et al., 2001). In addition, HSL-enzymatic activity is high in the interstitial tissue during periods of high serum testosterone levels in mink testis (Kabbaj et al., 2003). Furthermore, the cholesterol ester hydrolase inhibition experiments showed increasing esterified cholesterol in mouse testis and decreasing testosterone levels in serum (Bartke et al., 1973). All these observations suggested HSL hydrolyses esterified cholesterol from plasma and provides free cholesterol for the production of testosterone.

The process of providing free cholesterol is reversed at resting states. The excess of cholesterol is esterified and stored in lipid droplets by acyl-CoA: cholesterol acyltransferase (ACAT). The esterification activity of ACAT provides protection against excessive cholesterol. It has been reported that hypercholesterolemia-induced testicular damage is probably due to the compromised cholesterol esterification activity of ACAT (Fogari et al., 2002). However, the role of individual isoforms of the enzyme (ACAT) in the maintenance of cholesterol homeostasis in the interstitial tissue has never been addressed.

1.2.2 Cholesterol in the seminiferous epithelium

Cholesterol content in seminiferous tubules is indispensable for gamete development and fertility in most male animals (Hermo et al., 2008, Osuga et al., 2000; Vallet-Erdtmann et al., 2004; Wechsler et al., 2003). However, the origins of cholesterol in seminiferous tubules remain elusive.

In contrast to the liver and other extrahepatic tissues which acquire cholesterol carried by lipoprotein in the circulation, the transport of lipoprotein cholesterol from the circulation to the testis is reduced because the blood-testis barrier effectively limits its uptake (Setchell, 1975). In fact, the basement membrane of the seminiferous tubules, which separates each tubule from capillaries, blocks the entry of low-density lipoprotein (LDL) (Fofana et al., 2000). It has been reported that Sertoli cells may possess the capacity to synthesize cholesterol from acetate *in vitro* (Wiebe & Tilbe, 1979). Thus, cholesterol synthesis may constitute one origin of cholesterol in the seminiferous tubules. Because of different metabolic demands imposed on Sertoli cells by cyclic production of germ cell, the ability of Sertoli cells to synthesize cholesterol must be precisely regulated. Additionally, close to 75% of the germ cells will die by apoptosis before reaching maturity in the normal testis, and most of them will be phagocytosed by Sertoli cells, leaving an accumulation of cellular debris including lipids and cholesterol (Pelletier & Vitale, 1994). Thus, the apoptotic germ cells or their cell membrane remnants become a crucial source of cholesterol in the seminiferous tubules. Because cholesterol is a component of all germ cell membranes, including spermatozoa (Pelletier & Friend, 1983a), the cyclical release of

spermatozoa offers a constant challenge to the homeostasis of cholesterol in the tubules that demands the action of regulatory mechanisms.

An additional source of cholesterol for Sertoli cells may originate from the cyclical phagocytosis of esterified cholesterol-rich lipid droplets contained within the spermatids' residual bodies (Pelletier & Vitale, 1994). The residual bodies are lobes of excess of cytoplasm that are detached from spermatozoa prior to their release from the seminiferous tubules (Smith & Lacy, 1959).

The source of cholesterol in the seminiferous tubules is different from the interstitial tissue. However, the observation that free cholesterol concentration in tubules equals that in interstitial tissue (Kabbaj et al., 2001; Kabbaj et al., 2003; Marshall, 1957) entails factors regulating cholesterol homeostasis to maintain this equilibrium. Enzymatic factors involved in cholesterol homeostasis include HMG-CoA reductase, HSL and ACAT.

The *in vitro* studies on HMG-CoA reductase confirmed the high rate of acetate incorporation into cholesterol during spermatogenesis (Potter et al., 1981). The rate of acetate incorporation into cholesterol is high in pachytene spermatocytes, but returns to very low levels in mature spermatozoa (Potter et al., 1981). Other evidence showed that the rate of [^{14}C] acetate incorporation into cholesterol increases 4- to 5-fold as spermatocytes mature to pachytene spermatocytes (Hou et al., 1990). These findings suggest that the cholesterol synthesis is closely associated with spermatocytes and meiosis. Thus, the function of HMG-CoA reductase in the regulation of tubular cholesterol metabolism for the maintenance of spermatogenesis is worth investigating.

It has been suggested that Sertoli cell phagosomes contain lipases that could process lipids borne from residual bodies and liberate the subunits or " building blocks" necessary for new lipid synthesis (Kerr et al., 1984). Kabbaj et al. (2001; 2003) demonstrated that hormone sensitive lipase (HSL) was present in Sertoli cell lysosomes; and that HSL may induce hydrolysis of esterified cholesterol in the tubules to maintain optimal cholesterol concentrations. The present study focuses on testicular HSL because of the manifest importance of the enzyme in male fertility. The HSL knockout mice results in male sterility, suggesting a key role of the enzyme in the testis (Osuga et al., 2000). A significant rise in cholesterol ester levels concomitantly with the absence of cholesterol esterase activity was reported in HSL knockout mice testes and a decrease in testosterone concentration of peripheral plasma (Bartke et al., 1973; Osuga et al., 2000; Vallet-Erdtmann et al., 2004). In contrast, expression of transgene HSL_{tes} in HSL-null mice provoked the restoration in cholesteryl ester hydrolase activity and the rescue of infertility (Vallet-Erdtmann et al., 2004). These studies attest to the utmost biological significance of the enzyme in the maintenance of adequate cholesterol content in testicular cells.

Cholesterol is indispensable to all cells; however, the cholesterol concentration must be regulated to prevent excessive accumulation of the compound within the cell, which would compromise vital cellular functions and eventually be lethal. Cholesterol esterification serves both as a means to store cholesterol for later use and as a detoxification reaction to protect cells from excess free cholesterol (Simons & Ikonen, 2000). Yet, no reports describe the metabolism process of the esterification of excessive cholesterol in the Sertoli cells or germ cells. It has been reported that acyl-CoA: Cholesterol acyltransferase 1

(ACAT-1), the enzyme converting cholesterol into cholesteryl esters, is expressed in testis (Chang et al., 1997). Thus thesis investigates the behavior and the role of ACAT-mediated modulation of cholesterol metabolism in testis during different phases of spermatogenic activity.

1.2.3 Cholesterol in spermatozoa

The lipidic component in spermatozoa enables specialized activities in these cells. For example, lipid composition is a major determinant of the membrane rigidity and permeability (Stubbs & Smith, 1984). A loss of cholesterol allows for changes in the permeability of the cell membrane which are required for the characteristic flagellar movement of spermatozoa and also of the fusogenic properties of the cell membranes associated with the acrosome reaction and fertilization (Bearer & Friend, 1982). In addition, the removal of membrane cholesterol and the resulting decrease in the cholesterol/phospholipid (C/PL) ratio in the membrane constitutes an important step of capacitation in human spermatozoa (Hoshi et al., 1990).

Changes in the proportion of various lipids in spermatozoa were reported throughout the reproductive period (24-72 wk of age) in male chickens (Cerolini et al., 1997). Cholesterol esters and free fatty acids increased continuously with age while the relative free cholesterol and triacylglycerols content showed no change in spermatozoa or in relation to fertility (Cerolini et al., 1997).

Several enzymatic factors potentially involved in cholesterol homeostasis in spermatozoa have been detected. HSL was reported in epididymal spermatozoa (Kabbaj et al., 2003). And HSL_{tes}, one of the HSL isoforms, was expressed in early and elongated

spermatids. HSL_{tes} transgene expression reversed the cholesteryl ester accumulation in HSL-null mice (Vallet-Erdtmann et al., 2004). Expression of HSL_{tes} and cognate cholesteryl ester hydrolase activity leads to a rescue of the infertility observed in HSL-deficient male mice (Vallet-Erdtmann et al., 2004). On the other hand, male germ cells highly expressed the intermediates in the cholesterol biosynthetic pathway including HMG-CoA reductase, while the role of the enzyme has not yet been evaluated (Tacer et al., 2002). To date, ACAT isoforms have not been detected in the spermatozoa.

2. Enzymatic factors regulating intracellular cholesterol to maintain cholesterol equilibrium in the testis

2.1. 3-hydroxy-3-methyl-glutaryl-CoA (HMG-CoA) reductase

2.1.1 Composition, structure and orientation

HMG-CoA reductase is an integral glycoprotein (Mr 90,000-97,000) of the endoplasmic reticulum (ER) with an extended, carboxy-terminal, and a cytosolic domain that harbors the catalytic site (Chin et al., 1984; Hardeman et al., 1983). HMG-CoA reductase is also synthesized inside the mitochondria of Leydig cells in rat (Pignataro et al., 1983). Modeling studies (Liscum et al., 1985) on the primary structure of mammalian HMG CoA reductase localized the enzyme in ER membrane and suggested that NH_2-terminal of the reductase contains seven hydrophobic segments embedded in the membrane of ER and that the COOH-terminal of the protein, which contains a long relatively hydrophilic domain, extended into the cytoplasm (Liscum et al., 1985). The link region between NH_2-terminal and COOH-terminal is composed of proteolytic sites. Hence, the action of endogenous and exogenous proteases can release a water-soluble 53-kDa fragment into the cytoplasm (Miller et al., 1989). The findings suggest that the hydrophilic COOH- terminal includes the 53-kDa water-soluble enzymatically active site, while the NH_2-terminal portion of the reductase would fix HMG-CoA reductase to the ER membrane (Gibson & Parker, 1986) (Diagram 2).

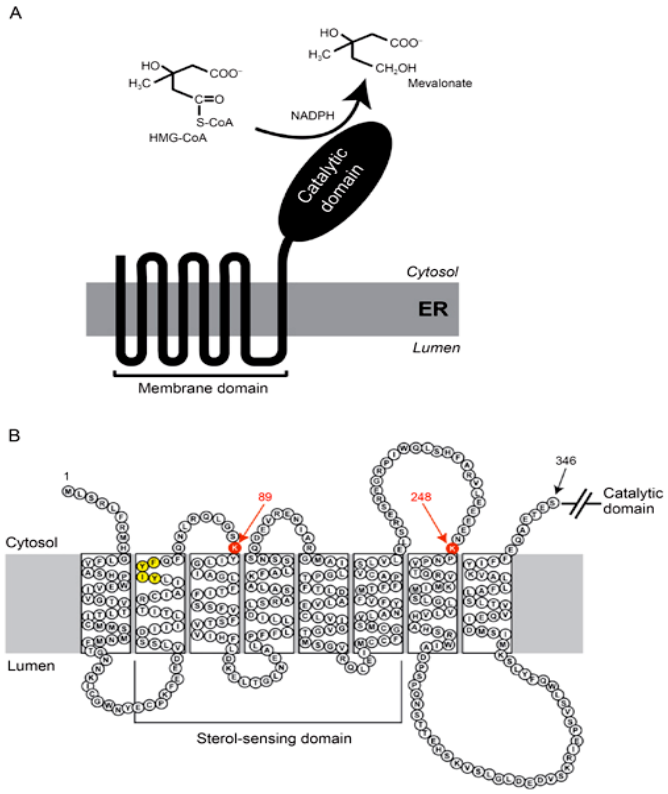

Diagram 2. Topological model of HMG-CoA reductase. This figure showed a model of the orientation of HMG-CoA reductse in the ER membrane. **(A)** HMG-CoA reductase includes two distinct domains: a hydrophobic N-terminal domain with eight membrane-spanning segments that anchor the protein to ER membranes, and a hydrophilic C-terminal domain that projects into the cytosol and exhibits all of the enzyme's catalytic activity. **(B)** Amino acid sequence and topology of the membrane domain of HMG-CoA reductase. The lysine residues implicated as sites of Insig-dependent, sterol-regulated ubiquitination are highlighted in red and denoted by arrows. The YIYF sequence in the second membrane-spanning helix that mediates Insig binding is highlighted in yellow [Taken from (DeBose-Boyd, 2008)].

2.1.2 Physiological roles of HMG-CoA reductase in tissue and in testis

HMG-CoA reductase is present as a single enzyme irrespective of the species. HMG-CoA reductase is the rate-limiting enzyme, and catalyzes the main step in cholesterol

synthesis which is the conversion of HMG-CoA to mevalonate (Brown & Goldstein, 1980; Kennelly & Rodwell, 1985) (Diagram 3).

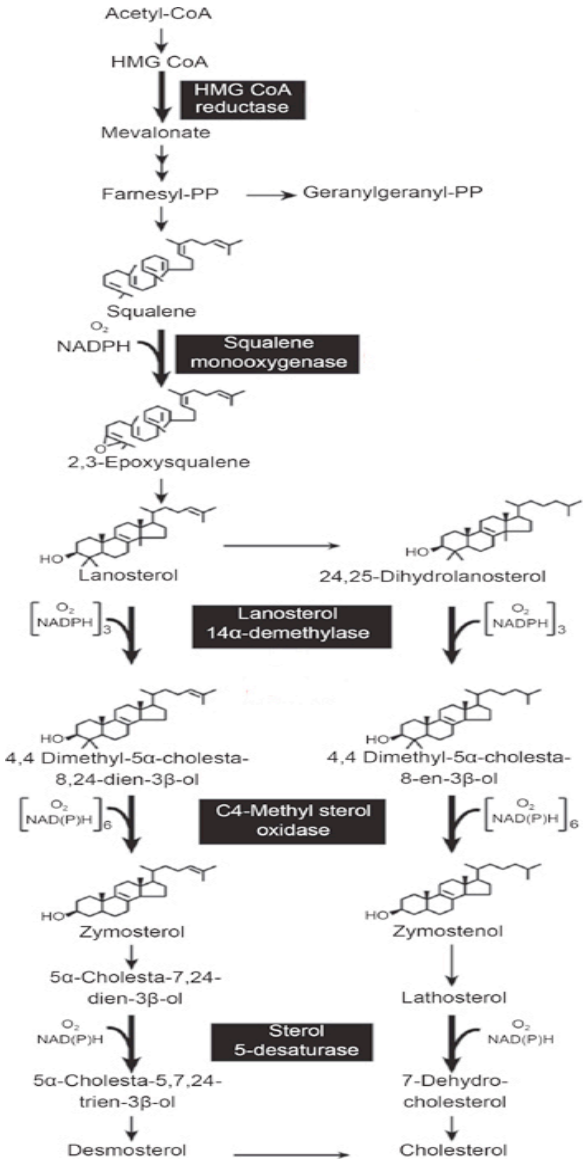

Diagram 3. The progress of biosynthesis of cholesterol. The rate-limiting step is 3-hydroxy-3-methylglutaryl-CoA (HMG-CoA) reductase activity. Intermediates are used as attachments to different proteins and enzymes. CoA, coenzyme A; PP, pyrophosphate. [Taken from (DeBose-Boyd, 2008)]**.**

The physiological significance of HMG-CoA reductase was demonstrated by the observation that the loss of HMG-CoA reductase resulted in cell death and early embryonic lethality (Nwokoro et al., 2001; Porter, 2002). Therefore, no direct in-depth study is feasible on the cholesterol metabolism in HMG-CoA reductase deficient animals. Instead, another gene, Dhcr24, knockout mice was produced (Wechsler et al., 2003). Dhcr24 encodes the cholesterol biosynthetic enzyme desmosterol reductase which catalyses the last step in the cholesterol synthesis. The study showed that Dhcr 24 knocking out mice was associated to a marked decrease (90%) in the intracellular and plasma membrane cholesterol levels (Wechsler et al., 2003). Both male and female Dhcr24-/- mice were reported infertile (Wechsler et al., 2003). Therefore, one could speculate that HMG-CoA reductase contributes to the endogenous cholesterol pool which is essential for the production of viable germ cells in the tubules and fertile male gametes.

It has been reported that the liver expresses the highest level of HMG-CoA reductase activity in the rat, but not in the hamster, rabbit or Guinea pig in which the adrenals, intestine, skin and carcasses exhibited still higher levels of cholesterol synthesis (Hamilton et al., 1994; Ness, 1994). For decades, HMG-CoA reductase inhibitors have been used in the treatment and prevention of cardiovascular diseases (Davignon, 2004; Martens & Guibert, 1994). It has also been demonstrated that HMG-CoA reductase is involved in mevalonation and proteins farnesylation and geranylgeranylation, which is essential for cellular proliferation and survival (Duncan et al., 2005). In addition, the enzyme could induce human breast cancer cells grown in culture and as in tumors grown in

nude mice (Duncan et al., 2005; Graaf et al., 2004). Therefore, HMG-CoA reductase inhibitors may be used for the treatment of malignancies (Brown, 2007).

Studies on the influence of HMG-CoA reductase inhibitors in testis demonstrated that inhibitors of hypercholesterolemia administrated to male rats improved their reproductive function by providing protection against the reduced fertility induced by hypercholesterolemia (Shalaby et al., 2004). This observation attests to the physiological significance of HMG-CoA reductase in the physiology of the testis. Yet, HMG-CoA reductase-mediated modulation of cholesterol metabolism in the testis has not been studied. HMG-CoA reductase activity was reported to be highest from 21-26 days after birth in rat testis then, tended to decline in adulthood, suggesting a major role of HMG-CoA reductase in *de novo* cholesterol synthesis in developing testis (Ness, 1994). However, since this enzymatic activity measurement was performed in whole testis extracts not on components of individual compartments of the testis, the results do not provide precise information on the enzyme involved in either spermatogenesis or the production of testosterone.

In the liver and intestine, the highest specific activity of HMG-CoA reductase was recorded in the endoplasmic reticulum subsfraction (Field et al., 1982; Zammit et al., 1991). However, the highest activity of HMG-CoA reductase in rat Leydig cells was associated with highly enriched mitochondrial fractions and located on the inner mitochondrial membrane (Pignataro et al., 1983), suggesting that much of the cholesterol biosynthesis that takes place in Leydig cells is carried out within the mitochondria. No studies have yet localized HMG-CoA reductase in the seminiferous tubules. Previous reports showed that the rate of [^{14} C] acetate incorporation into cholesterol increased with the onset of meiosis

(Hou et al., 1990), suggesting HMG-CoA reductase may be involved in meiosis. However, within the tubules where spermatozoa are generated, there is no evidence that the biosynthesis pathway makes a physiologically significant contribution to cholesterol in the tubules. Instead, the previous observation revealed the rate of acetate incorporation into cholesterol significantly decreased within the tubules when spermatozoa are generated (Potter et al., 1981). Thus the physiological significance of HMG-CoA reductase in the testis remains unclear.

Recent observations open a new view into the role of the cholesterol synthesis in the maturing germ cells. The cholesterol biosynthetic genes are expressed discontinuously in the testis (Tacer et al. 2002). The testis-specific expression of pre-testis meiosis-activating sterol (T-MAS) genes but not post-T-MAS genes is the primary regulatory checkpoint that caused the accumulation of the meiosis-signaling sterol T-MAS during maturation of male germ cells (Diagram 4). The discrepancy between pre-MAS and post-MAS genes expression suggested that the principal role of male germ cells may not be to synthesize cholesterol but rather to produce T-MAS (Tacer et al. 2002). Thus, the development of a tissue-specific transcriptional regulatory system to produce a cholesterol biosynthetic pathway intermediate in the male gonad suggested that HMG-CoA reductase may have a role besides or in addition to the biosynthesis cholesterol. This hypothesis remains to be confirmed, and the role of Sertoli cell in the biosynthesis of cholesterol will be one of the focuses of my study.

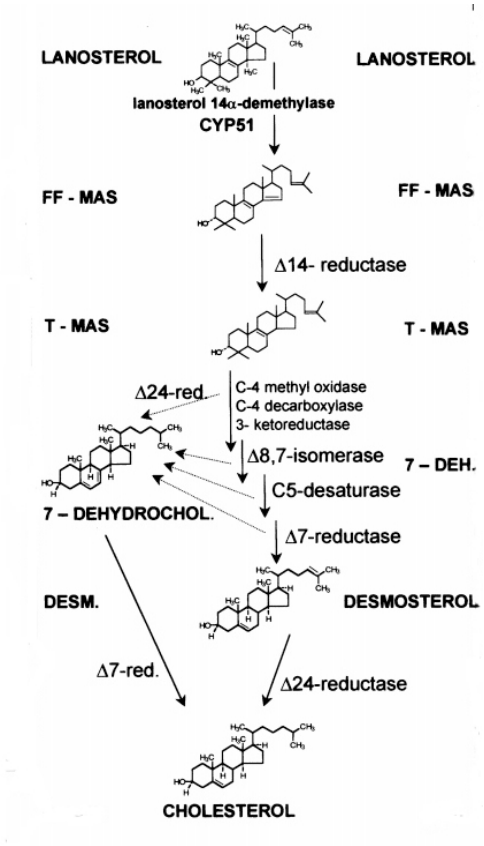

Diagram 4 . Postlanosterol part of the pathway of biosynthesis of cholesterol. T-MAS, testis meiosis-activating sterol; FF-MAS, follicular fluid meiosis-activating sterol [Taken from (Tacer et al., 2002)].

2.1.3 Regulation of HMG-CoA reductase activity

The mechanism of the regulation of HMG-CoA reductase activity in the testis has received little attention. In most tissue, HMG-CoA reductase is regulated at various levels: transcription, phosphorylation/dephosphorylation, translation and protein degradation (Panda & Devi, 2004).

1) Transcription

The mRNA level of reductase has been shown to vary in parallel with the enzyme activity in rat liver (Clarke et al., 1984). Feeding diets containing 2% cholesterol to Syrian hamsters was reported to reduce hepatic HMG-CoA reductase mRNA levels 6-fold (Gil et al., 1986). In addition, HMG-CoA reductase is transcribed at relatively high rate when cells are starved for cholesterol and other mevalonate-derived products (Luskey et al., 1983). Transcription is repressed by over 80% when cholesterol and other mevalonate-derived products are supplied (Osborne et al., 1985). However, few studies described the details of mRNA expression of HMG-CoA reductase gene in the testis besides the observation that expression of HMG-CoA reductase gene is upregulated during the maturation of the testis (Tacer et al., 2002).

HMG-CoA reductase is generally regulated on the transcriptional level by membrane bound transcription factors of the sterol responsive element binding protein (SREBP). SREBPs are a family of proteins that regulate the transcription of a range of genes involved in the cellular uptake and metabolism of cholesterol and lipids (Brown & Goldstein, 1997). SREBP1 isoforms are responsible for the energy metabolism, including fatty acid synthesis and glucose/insulin metabolism, whereas the role of SREBP2 is in the activation of genes (e.g. HMG-CoA reductase) involved in cholesterol biosynthesis (Shimano, 2001).

Regulation of genes including HMG-CoA reductase in cholesterol synthesis and the mechanism by which cells sense the level of cholesterol have been extensively studied in liver. SREBP1 and 2 are synthesized as the precursor proteins residing in endoplasmic

reticulum (ER) membranes (Brown & Goldstein, 1997). SREBPs are bounded to SREBP cleavage-activating protein (SCAP), which is required for the movement of SREBPs from the ER to the Golgi apparatus (Goldstein et al., 2002; Horton et al., 2002). When cholesterol is scarce in the ER, the SREBP-SCAP complex migrates from ER to Golgi apparatus where SREBP is subjected to proteolysis. The cleavage of SREBP is carried out by 2 distinct enzymes (S1P and S2P). The result of the cleavage is the release of the N-terminal transcriptionally active part of SREBP into the cytosol. Then the active portion of SREBP migrates to the nucleus where it will dimerize and form complexes with transcriptional coactivators leading to the activation of genes containing HMG-CoA reductase (Yang et al., 2002). In contrast, when cells contain sufficient levels of cholesterol, the SREBP-SCAP complex will be maintained in the ER. Thus, cholesterol biosynthesis will not be continued (Diagram 5). The cholesterol-level/SREBP-dependent transactivation of cholesterolgenic genes is believed to serve primarily to increase production of mRNAs encoding for HMG-CoA reductase and other cholesterolgenic enzymes, which causes the increase of cholesterol synthesis (Eberle et al., 2004; Shimano, 2002). In the testis, another type of regulation for HMG-CoA reductase mRNA expression was the cholesterol level-independent/SREBP-independent regulation (Fon Tacer et al., 2003). The role of SREBP2 in cholesterogenesis of germ cells and testis was recently investigated, when an unique isoform of male germ cell-enriched transcription factor SREBP2 was identified in rat and mouse spermatogenic cells (McPherson & Gauthier, 2004; Wang et al., 2002). The testis-specific SREBP2 was reported to be expressed as SREBP2gc, in mouse or rat spermatogenic cells in a stage-dependent manner and insensitive to the levels of cholesterol

(Wang et al., 2002). SREBP2gc is translated as a soluble and mature form of SREBP2, missing the SCAP-SREBP binding domain (Wang et al., 2002) . The role of SREBP2gc is unclear. The physiological function of regulating HMG-CoA reductase by SREBP2gc remains to be elucidated.

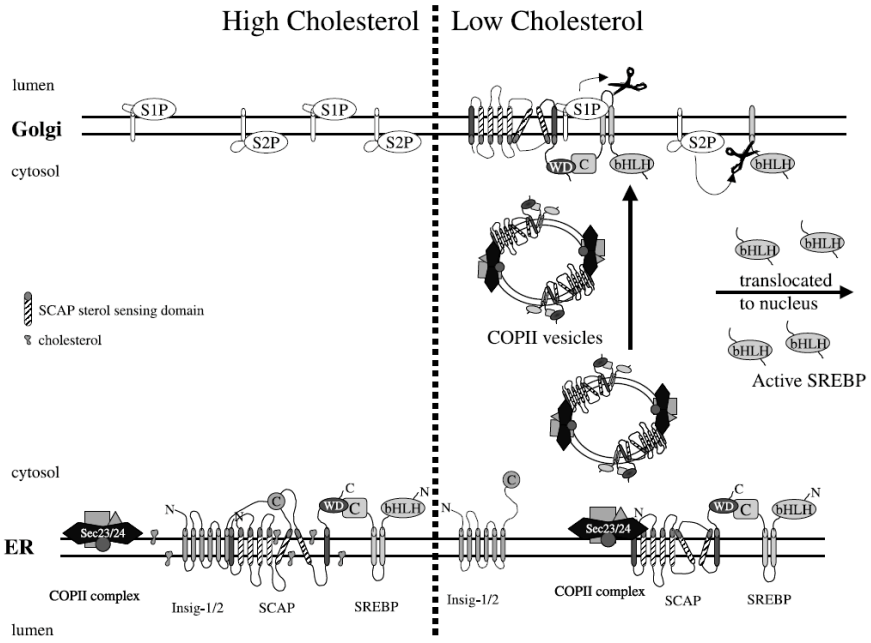

Diagram 5. Model for the cholesterol regulation of SREBP trafficking [Taken from (McPherson & Gauthier, 2004)].

2) Phosphorylation/dephosphorylation

Beg *et al.* suggested that the catalytic efficiency of HMG-CoA reductase might be regulated by phosphorylation/dephosphorylation in rat liver cytosol (Beg et al., 1973). It has been reported that phosphorylation of HMG-CoA reductase decreases its activity (Istvan et al., 2000). Phosphorylation of the enzyme is catalyzed by the reductase kinase (RK), which itself undergoes reversible phosphorylyation. RK is phosphorylated by a

cAMP-independent cytosolic kinase (RKK) or a cAMP-dependent RKK (Goldstein & Brown, 1990). Since cAMP is regulated by hormonal stimuli, regulation of cholesterol biosynthesis is hormonally controlled (Easom & Zammit, 1987). Insulin causes a decrease in cAMP, causing HMG-CoA reductase to be activated and cholesterol biosynthesis to be increased (Easom & Zammit, 1987). On the other hand, glucagon and epinephrine are hormones that increase the level of cAMP, which results in the HMG-CoA reductase being inactivated and in the cholesterol biosynthesis being decreased (Easom & Zammit, 1987). Alternatively, RKK is dephosphorylated by phosphoprotein phosphatase (Beg et al., 1973). Protein phosphatase is inhibited by phosphoprotein phosphates inhibitor 1 (PPI-1), which may be activated by a cAMP-dependent kinase (Beg et al., 1973). The elements required for modulation of HMG-CoA reductase by activation-inactivation cycles are illustrated in Diagram 6. However, this type of regulation for HMG-CoA reductase has not been confirmed in the testis.

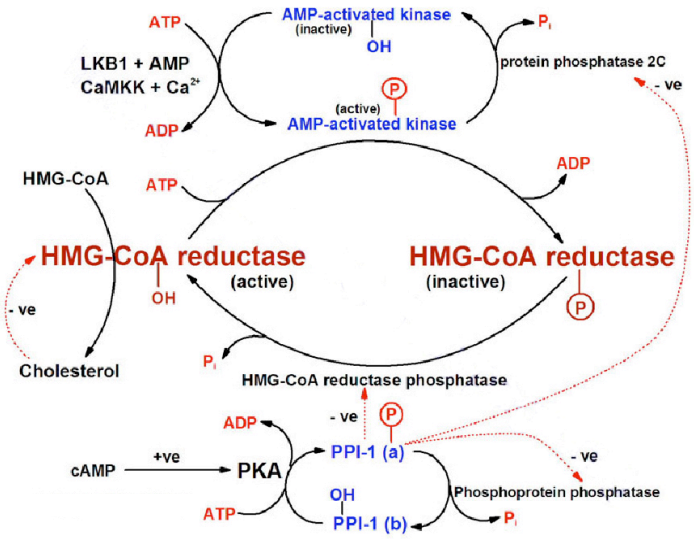

Diagram 6. Regulation of HMG-CoA reductase by **phosphorylation/dephosphorylation** [Taken from (Michael King 2009)].

3) Translational rgulation

One mode of post-transcriptional regulation of HMG-CoA reductase is translation. Interest in translation as a site for feedback regulation by dietary cholesterol emerged from studies showing a much greater decline in hepatic reductase immunoreactive protein than in mRNA levels (Ness et al., 1994). It was observed that feeding diets including 2% cholesterol to rats for 48h caused a 6-fold decrease in the rate of synthesis of HMG-CoA reductase protein (Chambers & Ness, 1998). Higgins *et al.* (1971) showed that the increasing of HMG-CoA reductase activity was accompanied by a rise in the synthesis of the reductase protein in rat liver and that synthesis completely stops several hours after the activity peaked (Higgins et al., 1971). A 200-fold increase in HMG-CoA reductase protein was reported within a few hours when the potent reductase inhibitors blocked the synthesis of mevalonate in the culture cells (Goldstein & Brown, 1990). Translational regulation of HMG-CoA reductase in the testis remains to be determined.

4) Protein degradation

The level of HMG-CoA reductase protein could also be determined by changes in the rate of its degradation (Ness & Chambers, 2000). It was found that feeding diets supplemented with potential HMG-CoA reductase inhibitor, mevinolin, caused the increasing of the half-life of HMG-CoA reductase protein in mammalian liver (Goldstein & Brown, 1990). However, investigations into the molecular mechanism by which cholesterol exerts feedback regulation on rat testis HMG CoA reductase have led to the conclusion that no obvious decreases of protein levels are seen in the testes when rats are placed on diets

supplemented with cholesterol (Ness et al., 2001). The protein degradation of HMG-CoA reductase in the testis remains unclear.

There are two mechanisms for protein degradation. The first one is the state transition, in which the intrinsic degradation motif is exposed to the degradation substrate when a stable state changes to a degraded state. In the second mechanism, the degradation motif is already exposed, but it is blocked by regulatory molecules and the degradation is inhibited. The mechanism of the degradation of HMG-CoA reductase is unclear. Hampton *et al*. (2002) presented the ubiquitin-mediated degradation of a number of ER-associated misfolded protein (Hampton, 2002). In 2003, Sever et al. (Sever et al., 2003) reported that the degradation of HMG-CoA reductase was mediated by the binding of Insig-1. As mentioned above, HMG-CoA reductase contains a sterol sensing domain and is negatively regulated by binding to Insig-1, which accelerates ubiquitination and proteasomal degradation of the enzyme (Song et al., 2005).

5) Nonsterol- mediated regulation of HMG-CoA reductase

Oxysterols, such as 25-hydroxycholesterol, was shown to bind to a cytosolic protein in cultured cells and to act as a potent repressor at the levels of transcription (Gibbons et al 1980). Oxylanosterols were also reported to act as potent repressors, but only at the level of translation (Gibbons et al., 1980; Panini et al., 1992; Taylor et al., 1984).

2.2 Hormone-sensitive lipase (HSL)

Hormone-sensitive lipase (HSL) is an intracellular neutral lipase that is capable of catalyzing the hydrolysis of triglycerides, diglycerides, monoacylglycerols, and cholesterol esters and retinyl esters (Holm et al., 2000).

2.2.1 Structure and biochemical properties

The HSL gene is located on human chromosome 19q13.3 (Holm et al., 1988) and contains 9 exons (1-9) spanning approximately 11kb in humans and 10 kb in mice, respectively (Langin et al., 1993). These nine exons encode a mRNA of 2.8 kb (Grober et al., 1997) which is translated into a 775-amino acid-long protein (Langin et al., 1993) in human adipose tissue. Subsequently, two additional noncoding exons (A and B) spanning approximately 12.5 and 1.5kb were identified upstream exon 1, respectively (Grober et al., 1997). The transcription starting site of HSL mRNA (2.8 kb) was mapped in the exon B, whereas exon A was represented in a minor fraction of adipocyte HSL transcripts (Grober et al., 1997). Two testicular forms of HSL have been characterized in human and rodent testes (Holst et al., 1996; Mairal et al., 2002). A testis-specific exon 15.5 kb upstream of exon 1 of human and rat adipocyte HSL produces a 3.9 kb testicular HSL mRNA (Holst et al., 1996). HSL_{tes} mRNA is translated into 1068- and 1076-amino-acid proteins in human and rat (Blaise et al., 2001). Compared with rodents, where only HSL_{tes} mRNA of 3.9 kb is expressed (Holst et al 1996), a second testicular mRNA, 3.3 kb mRNA was found in human (Mairal et al 2002) . This specific exon is located 12kb upstream of exon 1 and encodes a protein which is identified to the adipocyte HSL. The transcription of the HSL gene is

under the regulation of two promoters: the promoter upstream exon B which regulates HSL transcription in adipocytes and other tissues, the other promoter upstream exon T regulates HSL transcription specifically in the testis (Blaise et al., 2001) (Diagram 7).

The purified human adipose HSL has a molecular weight of approximately 88 kDa on SDS-PAGE, corresponding to the 775-amino-acid protein with a molecular mass of 84 kDa predicted (Langin et al., 1993). The adipose HSL in rat has an 84 kDa immunoreactive band seen on SDS-PAGE (Shen et al., 1999). In the testis, several protein species with apparent molecular weight ranging from 26 to 130 kDa are expressed (Holm et al., 1987; Kabbaj et al., 2001; Kraemer et al., 1993b). These forms may come from the 3.9 kb HSL mRNA in rodents and form two mRNA species of 3.9 and 3.3 kb in human (Blaise et al 2001; Holst et al 1996). The large form encodes the predicted protein of 120 kDa, HSL_{tes}, whereas the 3.3 kb from encodes a small protein of 88 kDa, that is similar to the adipose HSL (Langin et al., 1993).

HSL has been shown to be a muti-domain structural protein by limited proteolysis studies and spectroscopic analyses (Holm, 2003). HSL consists of two major structural domains: a C-terminal catalytic domain common to all HSL isoforms, and an N-terminal domain, different among all HSL isoforms. The C-terminal portion of the protein comprises two distinct domains, one containing the catalytic triad and a second that constitutes a regulatory "loop". The regulatory loop, from residue 521 to residue 669, contains all of the known phosphorylation sites and is specific to HSL in rat (Holm, 2003). The function of N-terminal domain is poorly understood but is has been implicated in protein-protein and protein-lipid interactions (Osterlund et al., 1996; Smith et al., 1996). It has been

demonstrated that the N-terminal portion of the adipocyte enzyme mediates interaction with adipocyte lipid binding protein (ALBP), an intercellular fatty acid carrier (Shen et al., 1999). Compared to the normal adipose HSL protein structure, HSL_{tes} protein is composed of an additional 300 or 301 amino acids N-terminal in rat and human respectively (Mulder et al., 1999) (Diagram 7).

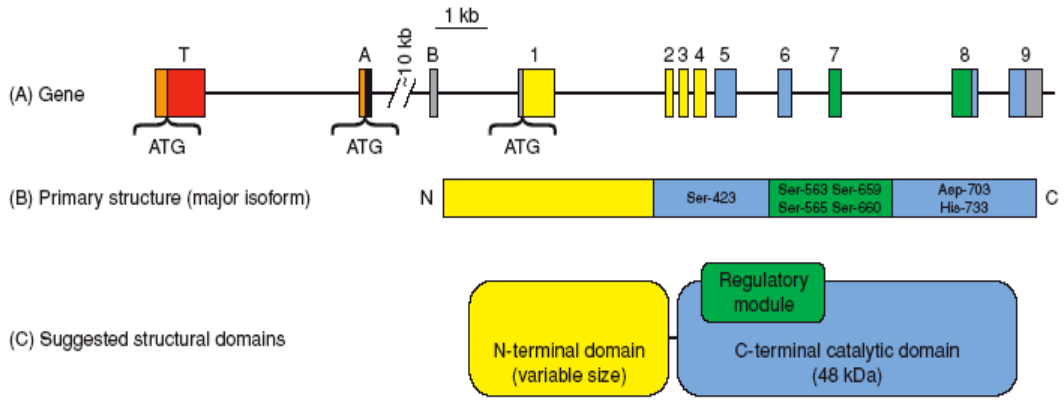

Diagram 7. The structure of the human HSL gene and the corresponding protein. (A) The organization of human HSL gene. Testis-specific exon T encodes additional 300 amino acids at the N-terminus. (B,C) The primary amino acids sequences of HSL are described accordingly in (A). Three functional regions are given: an N-terminal protein binding domain, a C-terminal catalytic domain and a regulatory module contaning multiple phosphorylation sites. [Taken from (Holm et al., 2003)].

2.2.2 Cholesteryl ester hydrolase (HSL) in tissue and in testis

HSL is an intracellular neutral enzyme which is expressed in adipose and steroidogenic tissues, cardiac and skeletal muscle, macrophages, and pancreatic islets

(Holm et al., 1988; Kraemer & Shen, 2002). In adipose tissue, the primary action attributed to HSL is hydrolysis of stored triglycerols, named lypolysis (Londos et al., 1999). HSL plays a crucial role in regulating the accumulation of triglyceride droplets and in energy utilization in cardiac and skeletal muscle (Kraemer et al., 1993a; Langfort et al., 1999). The neutral cholesterol ester hydrolase activity purified from the adrenal gland has been shown to be similar to that in adipose tissue (Cook et al., 1982). However, the role of HSL in macrophages remains to be investigated. It has been found that the neutral cholesterol ester hydrolase activity does not change in peritoneal macrophages in HSL knockout mice (Contreras, 2002; Osuga et al., 2000); the cholesterol ester stores in HSL-deficient macrophages are identical to wild type macrophages. These findings hint that one or several additional intracellular lipases could exist and this (these) lipase(s) could in part compensate for the lack of HSL.

In rat testis, HSL mRNA and protein expression showed marked developmental changes, and HSL mRNA levels were low in the first week after birth and increased several fold in the adult between days 20 and 90 (Kraemer et al., 1991). Conflicting observations have been reported for HSL mRNA and protein expression in testis. HSL has been reported in human Leydig cells by immunohistochemistry (Mairal et al., 2002) while Holst et al. (Holst et al., 1996) said HSL was not expressed. Studies in our laboratory revealed that testicular macrophages contain active HSL in mink (Kabbaj et al., 2003), which challenges the hypothesis regarding the function of HSL in the production of testosterone in Leydig cells (Mairal et al., 2002) and entails an important contribution of the testicular macrophages in the modulation of the amounts of the cholesterol to be used for testosterone

production by the Leydig cells (Kabbaj et al., 2003). Moreover, HSL has been observed in Sertoli cells and spermatozoa in Guinea pig (Kabbaj et al., 2001) and mink (Kabbaj et al., 2003) and human testes (Mairal et al., 2002). *In situ* hybridization showed strong labeling of germ cells in the seminiferous tubules at stage X-XIV in rat testis (Holst et al., 1994). Immunohistochemistry revealed HSL immunoreactivity in the germ cells at stages XIII-VIII in rat testis (Holst et al., 1996). The data suggested that HSL mRNA and protein were expressed in haploid germ cells but with a delay between mRNA and protein expression as many other genes expressed during spermatogenesis (Blaise et al., 1999; Blaise et al., 2001).

The functions of HSL have been further identified by generating HSL-null mice. Basal lipolysis has been reported to be unchanged in these mice (Haemmerle et al 2002; Mulder et al 2003). The findings suggest the presence of one or more additional intracellular triglyceride lipases in the adipose tissue as well as in macrophages, which could partly compensate for the lack of HSL (Haemmerle et al., 2002; Mulder et al., 2003; Osuga et al., 2000; Wang et al., 2001).

The most striking aspect of HSL-null mice was male sterility due to oligospermia (Osuga et al 2000), which evidences a crucial contribution of HSL in male fertility. The testis weight of HSL-null mice is 40 percent lower than that of the wild type mice (Vallet-Erdtmann et al., 2004). Decreased numbers of early and late spermatids were reported in the seminiferous tubules, no spermatozoa were found in the epididymes (Vallet-Erdtmann et al., 2004). Additionally, neither immunoreactive HSL nor neutral cholesteryl ester hydrolase activity was detected in testis of HSL-deficient mice (Osuga et al., 2000).

Therefore, it appears that HSL is responsible for all of the neutral cholesteryl hydrolase activity and the defect in cholesterol metabolism may contribute to the abnormalities in late spermatids of the knockout mice. Consistent with the lack of HSL in Leydig cells, HSL-/- mice have normal plasma testosterone levels, follicle-stimulating hormone and luteinizing hormone (Osuga et al., 2000). One could speculate that the oligospermia does not result from hypogonadism, but rather, result from cholesterol inequilibrium by HSL-deficiency in seminiferous tubules. Thus, HSL may be directly involved in the cholesterol homeostasis in the testis and contributed to the male fertility.

To further elucidate the physiological significance of HSL, especially HSL_{tes}, in male sterility, a transgenic mice strain ($HSL_{tes}^{+/+}$ or $HSL_{tes}^{+/-}$) expressing the human HSL_{tes} under the control of its own promoter was generated, through crossing transgene animals with HSL-null mice. The remodeling mice show a lack of HSL in all tissues except haploid germ cells (Osuga et al., 2000; Vallet-Erdtmann et al., 2004). Rescue of spermatogenesis in HSL-/- HSL_{tes}+/+ mice demonstrated that the lack of the mature spermatids and spermatozoa was due to the absence of the correct HSL_{tes} transcription (Vallet-Erdtmann et al., 2004). Interestingly, the presence of two alleles of HSL_{tes} led to a rescue of infertility observed in HSL-null male mice (Vallet-Erdtmann et al., 2004). The findings point to the unique function of HSL_{tes} in the testis and its quantitative demand for normal spermatogenesis. HSL has been shown in most tissues to be crucial for the cholesteryl ester hydrolase (CEH) activity (Arenas et al., 2004; Kraemer & Shen, 2002). In HSL-deficient testis, a relationship was established between CEH activities, cholesteryl ester level and fertility. HSL-/- testis showed very low levels of CEH activities and accumulation of

cholesterol esters in the tubules (Osuga et al., 2000). On the other hand, the finding in HSL_{tes} transgenic mice showed that the increasing of CEH activity was necessary to restore spermatozoa and resume fertility. Thus, the HSL_{tes} transgene experiments indicated that male infertility in HSL deficient mice was due to the lack of expression of HSL_{tes}, the testicular form of HSL in the spermatids, and suggests that the absence of spermatozoa was mediated in part by repressing the CEH activity.

The studies in our laboratory extended over previous studies by showing that HSL activity and protein levels increased in parallel in the tubules and in the interstitial tissue with development but that HSL activity was higher in interstitial tissue where testosterone is synthesized (Kabbaj et al., 2003). In addition, our laboratory showed that the modulation of cholesterol metabolism in individual testicular compartments may be regulated by HSL isoforms expressed in distinct cells. Interstitial macrophages may be part of a system involved in the synthesis of steroid hormones and in the recycling of sterols in interstitium whereas in the tubules, recycling could be ensured by Sertoli cells. Moreover, our laboratory suggested that HSL may be the only cholesterol esterase in the seminiferous tubules (Kabbaj et al., 2001; Kabbaj et al., 2003).

Previous studies done in our laboratory had used enzymatic digestion to generate the different tissue fractions (Kabbaj et al., 2001; Kabbaj et al., 2003). This might have caused a possible destruction of various phosphorylated forms of HSL. Recently, a separation technique has been developed in our laboratory and this approach apparently allows to be better preserve the HSL enzymatic activity and the phosphorylated forms of proteins (Akpovi et al., 2006). Nevertheless, the interrelationship between HSL and other

enzymes that directly or indirectly contribute to the cholesterol metabolism in the testis remains to be elucidated. Moreover, there are no data on the activities of other enzymes when HSL activity is either decreased or rendered inefficient.

HSL has broad substrates, which includes retinyl esters. The absence of the function of retinoic acid has been described in the dysfunction of spermatogenesis. Retinoic acid is the acid form of vitamin A (Djakoure et al., 1996). Vitamin A– deficient male rats developed sterility (Griswold et al., 1989) and male sterility was the major phenotype in retinoic acid nuclear receptor, RARą knockout mice (Lufkin et al., 1993). However, no studies focussed on the impairment of retinoic acid production and spermatogenesis. Further studies are needed to elucidate the mechanism by which HSL deficiency results in male sterility.

2.2.3 Regulation of HSL activity

2.2.3.1 Transcriptional regulation

HSL activity is modulated at the transcriptional and post-transcriptional levels. HSL mRNA level is correlated with the maximal lipolysis rate in human fat cells (Large et al., 1998). Changes in adipose HSL mRNA levels have also been reported in humans with familial combined hyperlipidemia (Reynisdottir et al., 1995).

During spermatogenesis, specialized transcriptional mechanisms ensure a stage-specific gene expression in the germ cells. Some germ cell-specific transcriptional factors have been described and shown to function on few target genes. CREMγ is a product of the

CREM gene that acts as a transcriptional activator associated to the cAMP signaling pathway (Foulkes et al., 1992). And protamin 1, a nucleoprotein that replaces histones and promotes nuclear condensation, has been identified to be the target gene for CREMγ – mediated activiation of HSL_{tes} promoter in post-meiotic germ cells (Delmas et al., 1993).

2.2.3.2 Post-transcriptional regulation

Lipolytic and anti-lipolytic hormones as well as neurotransmitters and other effector molecules regulate adipocyte lipolysis. Catecholamines, adrenaline and noradrenaline belong to this group of hormones that are crucial for lipolysis, whereas insulin and adenosine are the most important anti-lipolytic stimulators (Londos et al., 1999). A well-known mechanism regulating lipolysis is the cAMP pathway (Carmen & Victor, 2006; Haemmerle et al., 2003; Holm, 2003). Catecholamine agonists bind to the β-adrenergic receptors, coupled to adenylate cyclase via the stimulatory G-protein, then cause an increase in cAMP and an activation of a cAMP-dependent protein kinase (PKA) (Holm, 2003). The two main substrates, HSL and perilipins, are phosphorylated by PKA (Osterlund, 2001). PKA phosphorylation of HSL causes translocation from the cytosol to the lipid droplet, whereas phosphorylation of perilipin by PKA alleviates the barrier function of this protein and prompts its active participation in the lipolytic process (Holm, 2003) (Diagram 8). On the other hand, other signaling pathways were also reported to be involved in the lipolytic response. For instance, PKC can be stimulated and mediated by both independent and dependent mitogen-activated protein kinases (extracellular signal regulated kisnases, ERK-1/2) way (Haemmerle et al., 2003; Holm, 2003) (Diagram 9).

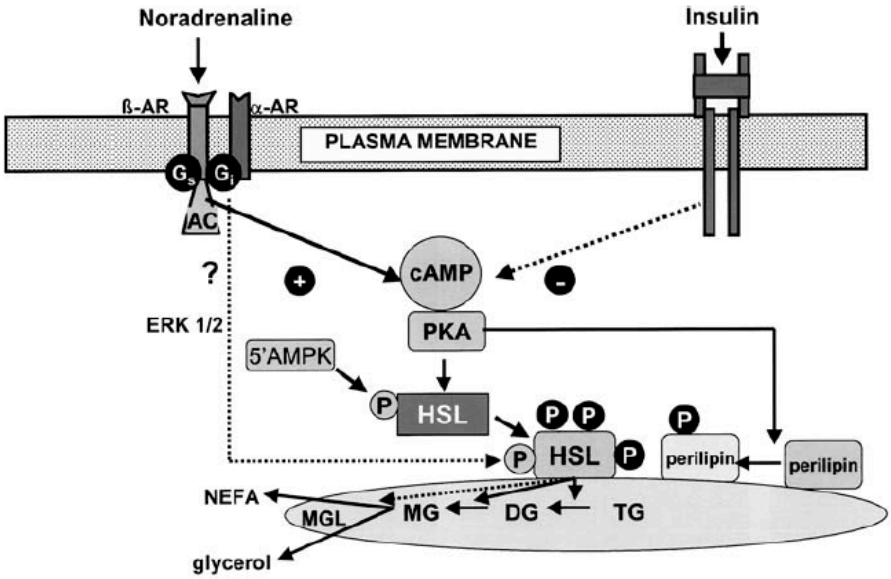

Diagram 8. The classified cAMP pathway for regulation of HSL activity. TG, triglycerides; DG, diglycerides; MG, monoglycerides; MGL, monoglyceride lipase. [Taken from (Holm et al., 2003)].

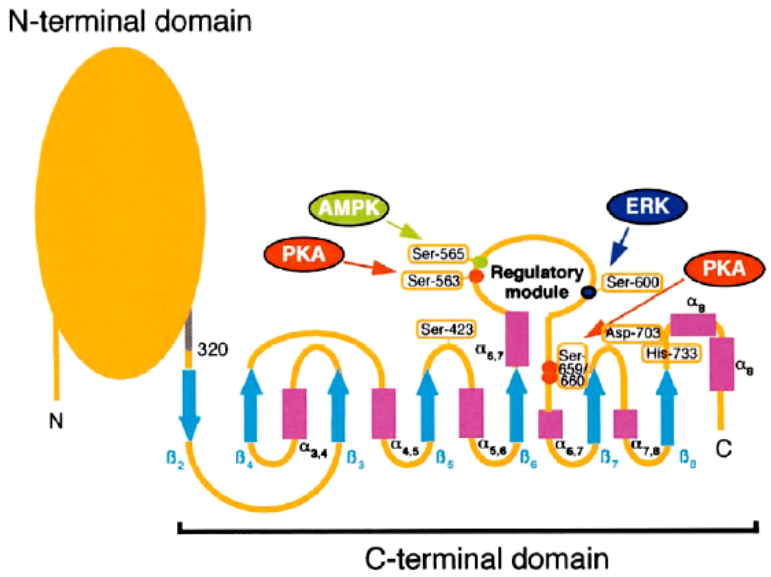

Diagram 9. Schematic structure of phosphorylation sites of HSL. The N-terminal amino acids are described as a globular structure and the important serine residues can be phosphorylated by the different kinases are shown in the C-terminal portion. [Taken from (Kraemer & Shen, 2002)].

PKA phosphorylates HSL at three serine residual sites: S563, S659 and S660 (Anthonsen et al., 1998). Activation of ERK pathway appears to be able to regulate adipocyte lipolysis by phosphorylating HSL on the residue S600 (Greenberg et al., 2001). In contrast to the activated sites of HSL seen in PKA and ERK phosphorylation, one additional serine residual site in HSL, S565, has been shown to be phosphorylated by other kinases such as Ca^{++}/calmodulin-dependent protein kinase II and AMP-activated protein kinase (Garton & Yeaman 1990). Phosphorylation HSL at S565 prevents the phosphorylation of S563 by PKA and inactive HSL (Diagram 9) (Garton et al., 1989; Garton & Yeaman, 1990).

2.3 Acyl-CoA: cholesterol acyltransferase 1 (ACAT-1) and 2 (ACAT-2)

Acyl-coenzyme A: cholesterol acyltransferase (ACAT) is an ER membrane bound enzyme that catalyzes the transfer of a long-chain fatty acyl residue from acyl-CoA to the β-hydroxyl group of cholesterol to form a cholesteryl ester (Diagram 10). Two isoforms of the enzyme, ACAT-1 and ACAT-2 have been described (Chang et al., 1993; Chang et al., 1998).

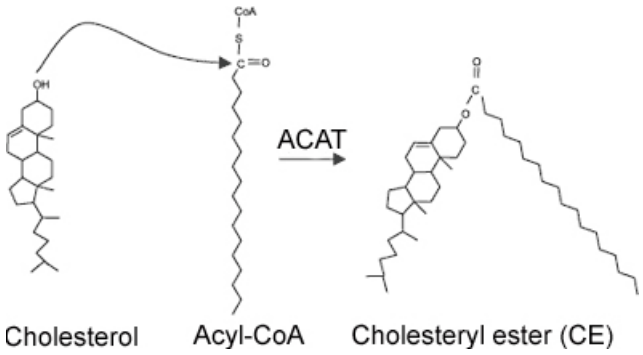

Diagram 10 . The ACAT reaction of cholesterol esterification in cells. CoA, coenzyme A; ACAT, Acyl-coenzyme A: cholesterol acyltransferase [Taken from (Brown & Goldstein, 1986)].

2.3.1 Comparison between ACAT-1 and ACAT-2

1) Historical perspective

Cholesterol esterase was first reported in the blood in 1895 (Hürthle KZ 1895). It was defined as lecithin: cholesterol acyltransferase (LCAT). Around the 1950's, another intracellular cholesterol esterase was found in rat liver cells and was identified as acyl-coenzyme A: cholesterol acyltransferase (ACAT) (Goodman et al., 1964). By 1993, Chang et al. (1993) cloned the human ACAT gene using a combination of somatic cells and molecular genetic approaches and they named it ACAT-1. A second mammalian acyl-coenzyme A: cholesterol acyltransferase, named ACAT-2 was identified on the basis of its protein sequence homology with ACAT-1 close to the C terminal (Cases et al., 1998a).

2) Tissue distribution

In human, rabbit and mouse, ACAT-1 protein has been localized in virtually all tissues examined including: hepatocytes, Kupffer cells, adrenal, skin cells, intestinal enterocytes, neurons, and macrophages (Chang et al., 1993; Pape et al., 1995; Uelmen et al., 1995). However, the localization of ACAT-2 was said to be restricted. In humans, ACAT-2 was localized in the intestinal mucosa and hepatocytes (Anderson et al., 1998; Lee et al., 1998), and under pathological conditions (Sakashita et al., 2003) in macrophages. ACAT-2 was said to be absent from testis (Fazio et al., 2001; Lee et al., 2000; Rudel et al., 2001). The distribution of ACAT-1 and ACAT-2 was not identical in mouse and humans. ACAT-2 is the major isoenzyme in mouse hepatocytes, whereas in adult humans, hepatocyte ACAT-1 is the major isoenzyme. Additionally, ACAT-1 mRNA was reported to be relatively abundant in steroidogenic tissues, including the adrenal gland, testis, and ovary (Chang et al., 1993).

3) Structures of the gene and protein

The human ACAT-1 gene is located on two different chromosomes (Li et al., 1999). The coding region and the proximal promoter are located on chromosome 1, whereas the 5' noncoding region and distal promoter that control the expression of the noncoding region are located on chromosome 7 (Li et al., 1999). The mouse gene is located on chromosome 1 (Uelmen et al., 1995). However, the human ACAT-2 gene is located on chromosome 12, and the mouse ACAT-2 gene is located on a homologous region of chromosome 15 (Cases et al., 1998a).

ACAT-1 and ACAT-2 may both contain multiple hydrophobic transmembrane regions consistent with their being integral membrane proteins (Joyce et al., 2000; Lin et al., 1999) (Diagram 11). Depending the method used, ACAT-1 was said to span the ER membrane 5 to 7 times (Chang et al., 1993), whereas ACAT-2 includes 5 to 10 (usually 6 to 9) hydrophobic domains capable of serving as trans-membrane regions (Cases et al., 1998a).

The ACAT-1 cDNA encodes a protein of 550 amino acids in human and of 540 amino acids in mouse (Chang et al 1993). ACAT-2 cDNAs encode proteins of 522 and 525 amino acids, respectively (Anderson et al., 1998; Lee et al., 1998). The amino acid sequence of human ACAT-2 show more than 40% identity with human ACAT-1. The most highly conserved regions are in the carboxyl terminal. The predicted molecular weight of ACAT-1 is approximately 65kDa, while the molecular weight viewed in SDS-PAGE is roughly 50kDa (Chang et al., 1993). The predicted molecular weight of ACAT-2 is around 50kDa, but the one viewed in SDS-PAGE is roughly 46kDa (Cases et al., 1998a).

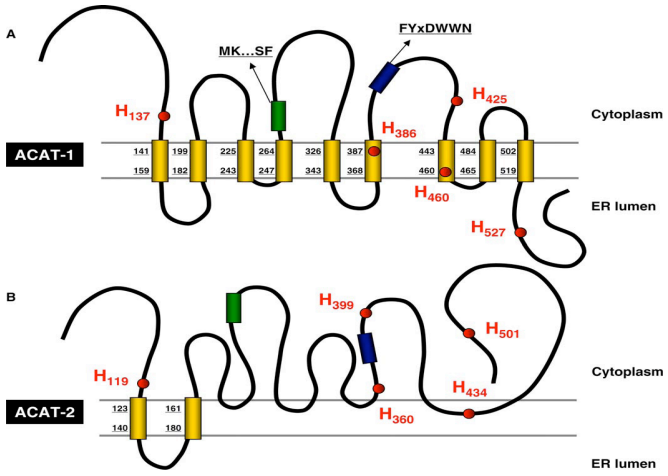

Diagram 11. The transmembrane topology model of ACAT-1 and ACAT-2. The histidine residues are depicted. [Taken from (An et al., 2006)].

2.3.2 Physiological roles of ACAT-1 and ACAT-2 in tissue and in testis

The function of ACAT is to convert cholesterol into cholesteryl esters by using a long chain fatty acyl conenzyme A, so as to eliminate free cholesterol in excess (Suckling & Stange, 1985). ACAT-1 produces cholesterol ester as cytoplasmic lipid droplets (Chang et al., 2001a). Cholesterol ester droplets serve as the major reservoir for free cholesterol, an essential component of cell membranes. In steroidogenic tissues, cholesterol ester provided by ACAT-1 is stored and will be used as a source of free cholesterol that will serve as the precursor for steroid hormones biosynthesis (Chang et al., 2001a). ACAT-2 is expressed in the liver and small intestine, where it esterifies newly synthesized or dietary cholesterol prior to incorporation into lipoproteins and thereby regulates plasma cholesterol levels (Cases et al., 1998a; Rudel et al., 2001).

The functional analyses of ACAT-1 and ACAT-2 have been provided by individual gene-deficient mice. The phenotypes of ACAT-1 and ACAT-2 knockout mice show tissue-specific decreases in cholesterol esterification (Meiner et al., 1996). In ACAT-1 deficient mice, phenotypic changes did not affect the intestine or liver. The cholesterol absorption, cholesterol ester formation and the incorporation of esters into nascent chylomicrons were normal in ACAT-1-/- mice fed a regular chow diet (Dove et al., 2006; Meiner et al., 1996). In addition, ACAT-1 deficient mice had normal plasma cholesterol level. The major findings in ACAT-1-/- mice was the lack of cholesterol ester droplets in adrenal glands and zona fasciculata cells of the cortex and in cultured peritoneal macrophages (Meiner et al., 1996), suggesting functional redundancy of cholesterol esterification for steroidogenesis. ACAT-1-deficient macrophages promoted the formation of atherosclerosis in

hyperlipidemic mice (Fazio et al., 2001). ACAT-1 deficiency in macrophage had a variety of effects on cholesterol homeostasis including the paradoxical acceleration of foam cell lesions in the absence of cholesterol esterification (Meiner et al., 1996). These changes included decreased efflux of cellular cholesterol, increased uptake of modified lipoproteins, increased cholesterol biosynthesis, accumulation of membrane-bound vesicles, and increased turnover of lipoprotein-derived cholesterol (Dove et al., 2006).

On the other hand, in ACAT-2 deficient mice, cholesteryl ester formation was fully abolished in both the liver and small intestine with a regular chow diet feeding (Buhman et al., 2000), suggesting that the importance of ACAT-2 activity in regulating cholesterol absorption and hepatic cholesterol homeostasis might change depending on dietary cholesterol intake. Moreover, ACAT-2 deficiency prevented atherosclerosis in the apolipoprotein E null mice (Willner et al., 2003). Therefore, at present, ACAT-2 is considered the most potential target for treatment of coronary heart disease associated with hypercholesterolemia (Willner et al., 2003).

ACAT has been studied mainly in the gut and liver. The role of individual isoforms of the enzyme in the maintenance of cholesterol homeostasis in the gonad has not yet been studied. ACAT-1 has been reported in Leydig cells where it was suggested to contribute to the testosterone-production (Sakashita et al., 2000). The role of ACAT-1 in the tubules has not been investigated. There is at present no study on whether ACAT-2 is or not expressed in the testis nor on its putative role in testicular cholesterol homeostasis.

2.3.3 Regulation of ACAT-1 and ACAT-2 activity

The mechanism of the regulation of ACAT1 and ACAT-2 enzymatic activity has not yet been studied in the testis. In other tissues, ACAT enzymatic activity was shown to be regulated at distinct levels: phosphorylation/dephosphorylation, transcription and post-transcription.

1) Phosphorylation/dephosphorylation

ACAT activated by phosphorylation and inhibited by dephosphorylation *in vitro* as well as *in vivo* (Suckling et al., 1983b; Suckling et al., 1983a). *In vitro*, the ACAT phosphorylation by microsomal protein kinase is stimulated by ATP-Mg, whereas dephosphorylation may be obtained by cytosolic phosphatase. However, other studies have argued the role of dephosphorylation in the regulation of ACAT activity (Corton & Hardie, 1992; Einarsson et al., 1989). Thus, the regulation of ACAT by protein phosphorylation cannot be completely ruled out yet.

2) Transcriptional regulation

The ACAT-1 gene is not transcriptionally regulated by cholesterol and the sterol regulatory element present within the promoters of many cholesterol-regulated genes, could not be found within the ACAT-1 gene promoters (Brown & Goldstein, 1997). Similarly to the ACAT-1 promoter, the sterol regulatory element also could not be found within human ACAT-2 promoter (Song et al., 2001). However, a recent study has identified an important liver-specific *cis*-acting element in the promoter region of ACAT2 that acts as a putative

binding site for the hepatic nuclear factor 1 (HNF1) (Song et al., 2006). This element serves as a positive regulator of ACAT-2 gene expression and is functionally active. Significantly, HNF1 beta expression was highest in the testis (Harries et al., 2004). Thus, one could speculate that HNF1 is likely involved in the regulation of ACAT-2 gene expression in the testis, but this remains to be confirmed.

3) Post-transcriptional regulation

Both ACAT-1 and ACAT-2 appear to be regulated by post-translational mechanisms (An et al., 2006; Chang et al., 1997; Chang et al., 2001b). *In vitro* studies on the regulation of ACAT-1 enzymatic activity have shown that cholesterol esterification was increased without showing changes in the mRNA or protein expression levels (Chang et al., 1994; Yu et al., 1999). The mode of cholesterol-dependent regulation is by allosteric control of the sterol substrate (An et al., 2006; Chang et al., 1998; Chang et al., 1997; Chang et al., 2001b). It has been found that ACAT-1 has two distinct sterol-binding sites: a substrate-binding site and an allosteric-activator site (Chang et al., 1997). Combination of cholesterol with ACAT-1 allosteric-activator site caused a ligand-induced structural/configurational change in its protein, which converts the enzyme from inactive to active (Chang et al., 1997). ACAT-2 is also allosterically regulated by cholesterol, with cholesterol serving as an activator (Liu et al., 2005). The putative activator sites of ACAT isoforms may only recognize cholesterol (An et al., 2006; Chang et al., 1998; Chang et al., 1997; Chang et al., 2001b; Liu et al., 2005). ACAT-2 was less likely than ACAT-1 to use

cholesterol as substrate because ACAT-2 is less responsive to cholesterol-dependent activation (Temel et al., 2003).

The two ACAT isoforms have different substrate specificities and catalytic cores corresponding to their different physiological functions and specific tissue expression (Zhang et al., 2003). ACAT-1 was reported to esterify cholesterol and various oxysterols, such as 7-ketocholesterol and 7α-hydroxycholesterol, though at very low rates compared to cholesterol (Zhang et al., 2003). However, 25-hydroxycholesterol was esterified more efficiently by ACAT-2 than by ACAT-1; and ACAT-2 was more selective than ACAT-1 relative to substrate (Liu et al., 2005).

With regard to the ACAT active site, a conserved serine residue was reported in both ACAT-1 and ACAT-2 (Cases et al., 1998b). Replacing this conserved serine with leucine led to a loss of ACAT activity in mammalian cells, suggesting that the conserved serine residue may be part of the enzymatic active site (Joyce et al., 2000). Membrane topographical studies of ACAT-1 and ACAT-2 suggest that the putative active site ACAT-1 serine (Ser269) is located on the cytoplasmic side of the ER, whereas the analogous serine residue of ACAT-2 (Ser 249) is located on the luminal side of the ER (Joyce et al., 2000). Another conserved region in ACAT-1, ACAT-2, DGAT and 20 other enzymes have been identified (Hofmann, 2000). The conserved region was located on histidine 460 of ACAT-1 and histidine-434 of ACAT-2. H460 and H434 residues have both been located in the interior of the ER membrane (Guo et al., 2005). It has been confirmed that H460 is the key active site residue of ACAT-1 (Guo et al., 2005). The complete ACAT activity was completely lost when the histidine 460 gene was mutated (Guo et al., 2005; Lin et al.,

2003). H360 and H399, cytoplasmic histidine residues, were shown to be essential for the catalysis of ACAT-2 (An et al., 2006) (Diagram 11).

3. Justification of the animal models used in the study

Two different animal models were used, mink (*Mustela vison*) and mouse (*Mus musculus*). The mink is a seasonal breeder, while the mouse is a continual breeder.

3.1 Seasonal breeder animal model: mink (*Mustela vison*)

Our laboratory has utilized mink (*Mustela vison*) as animal model since 1979 and has provided ample results on the cholesterol metabolism in the testis (Akpovi et al., 2006; Kabbaj et al., 2001; Kabbaj et al., 2003; Pelletier, 1986; Pelletier & Friend, 1986; Pelletier & Vitale, 1994).

The mink has several advantages. It shows a seasonal initiation of spermatogenesis in addition to the initiation of spermatogenesis during post-natal development. Additionally, this model allows us to distinguish the dynamic expression of the enzymatic factors during different phases of spermatogenic activity. The mink is a seasonal breeder which includes an 8-month-long active spermatogenic phase that produces spermatozoa followed by an inactive spermatogenic phase that does not (Fig. 1). During the active spermatogenic phase, mitotic and meiotic activities are increased; spermatogenesis was completed. During the inactive phase, there is no spermatid differentiation, no meiotic

activity and reduced mitotic activity. The animal model allows distinguishing the mechanisms underlying the seasonal testicular regression from those involved during the natural seasonal initiation of spermatogenesis. Besides, in mink the neonatal period expands from birth (usually in May) to about Day 90 after birth. This is followed by puberty, which extends from Day 91 to Day 252 after birth; this period includes the completion of spermatogenesis by Day 240 after birth and the apprearance of spermatozoa in the epididymis some 12 days later in January. The use of the mink model provides the unique advantage of distinguishing factors that regulate testicular cholesterol metabolism during postnatal sexual maturation of the developing testis from those acting during the seasonal annual reproductive cycle in tehadult testis. Here, all measurements were performed during the neonatal period, puberty, and adulthood, thus allowing for correlation of a physiological event typical with a particular phase of testicular development.

3.2 Continual breeder animal model: mouse (*Mus musculus)*

In most previous studies, the mouse was used because of its rapid maturation from birth to sexual maturity. In mouse, spermatogenesis was found to start by day 7 after birth. The neonatal period covers the first 7 days after birth, and it is followed by puberty, which lasts up until day 52 from day after birth. Spermatogenesis is completed by 35 days after birth (De Rooij et al., 1989). Since the 1970's, studies already confirmed that a large amount of lipid droplets appeared in both seminiferous tubules and the interstitial tissue of the mouse, and that the lipid droplet content varied greatly with development (Bell et al., 1971; Ohata, 1979). Being a continual breeder, the mouse shows similarities with the

humans. Recent technological advances have dramatically increased our ability to create analyses for human diseases. For instance, previous observations showed that male sterility in HSL-deficient mice is due to the lack of expression in spermatids of the testicular form, HSL_{tes} (Vallet-Erdtmann et al., 2004). The dramatic effect of the absence of HSL_{tes} leads to the question of whether mutations in the HSL gene may be the reason for male infertility in humans.

Objectives

Cholesterol homeostasis is essential for the synthesis of testosterone in the interstitial tissue and the production of fertile gametes in the seminiferous tubules of the testis. The expression of enzymatic factors (HMG-CoA reductase, HSL and ACAT) that regulated cholesterol equilibrium in the testis has been recently described. The absence of one or more of these enzymes has been implicated in the development of male infertility. However, the enzymatic factors that determine the fate of cholesterol in the testis, especially, the inter-relation between individual enzymatic factors that directly contribute to the maintenance of the cholesterol equilibrium has not been extensively investigated in the testis. The present work is directed towards this task and aims to: **1) to elucidate the behaviour and the contribution of HMG-CoA reductase, ACAT-1, ACAT-2 and HSL in the modulation of cholesterol metabolism in each of the two compartments of the testis and 2) to identify the inter-relationship in the action of these enzymes in the maintenance of cholesterol equilibrium in the testis.** My project will test the hypotheses (Model 1) that 1) to preserve the integrity of functions typical of each compartment of the testis, the three main enzymes implicated in the regulation of intracellular cholesterol have to act in coordination with each other in order to maintain viable cholesterol concentrations locally; 2) each of the two ACAT isoforms are both expressed and active in the seminiferous tubules and the interstitial tissue; 3) genetic HSL perturbation in the mouse will result in changes in the function of remaining enzymes involved in the regulation of the cholesterol equilibrium in the tubules; 4) the disruption of the cholesterol transporters

genes (SR-BI and CD36) would cause compensatory effects on the remaining enzymes involved in the "cholesterol ester cycle". The project will allow identifying enzyme-induced changes that contribute to the maintenance of cholesterol metabolism for the maintenance of normal spermatogenic activity. These studies will hopefully lead to a better understanding in male infertility where aberrant cholesterol metabolism has been implicated.

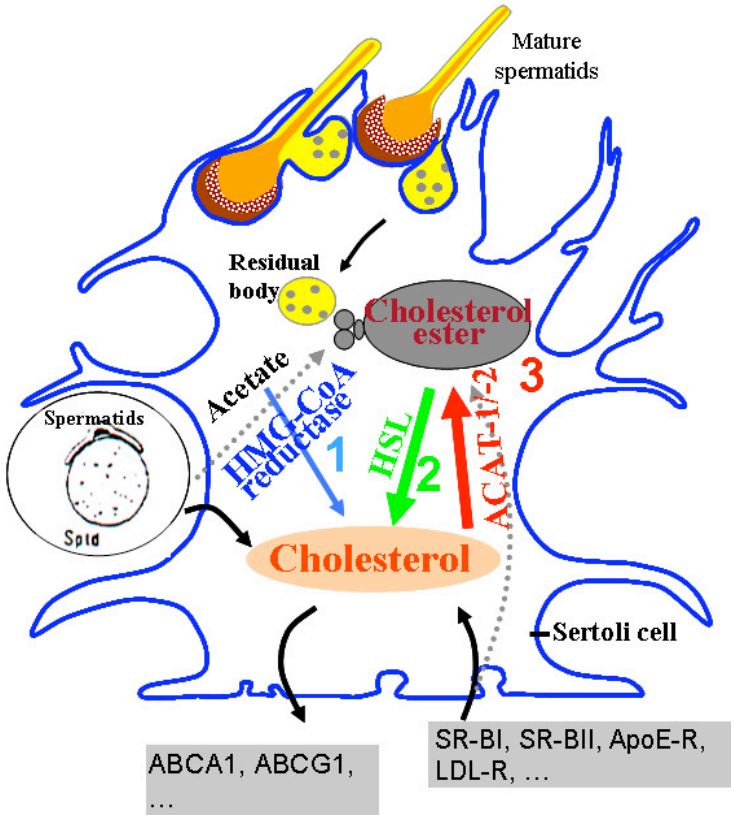

Model 1. Schematic drawing of HMG-CoA reductase, HSL and ACAT in intracellular cholesterol metabolism during normal spermatogenesis.

Materials and methods

1. Reagents

1.1 Chemicals and enzymes

Chemical enzymes and supplies were obtained as following:

acetonitrile, agarose, anhydrous petroleum ether, bromophenol blue (BPB), bovine serum albumin (BSA), cholesteryl oleate, diaminobenzidine (DAB), dimethylsulfoxide (DMSO), dithiothreitol (DTT), ethylenediaminetetraacetic acid (EDTA), ethylene glycol-bis-(-aminoethyl ether)--- N,N,N',N'-tetraacetic acid (EGTA), glucose-6-phosphate, glucose-6-phosphate dehydrogenase, KCl, K_2HPO_4, KH_2PO_4, β-mercaptoethanol, ß-nicotinamide adenine dinucleotide phosphate (ß-NADP), NaF, Na_3VO_4, $Na_4P_2O_7$, oigo-dT, triphenylphosphine (Tris), (Sigma-Aldrich, Oakville, ON, Canada); acrylamide, Bio-Rad protein assay, nitrocellulose membranes, sodium dodecyl sulfate (SDS), SDS-PAGE standards (high and low range) (Bio-Rad, Mississauga, ON, Canada); aprotinin, leupeptine (Boehringer-Mannheim, Laval, PQ, Canada); cholesterol (ICN Biomedicals Inc. Irvine CA USA); Diethyl ether, heptane, hexane, Na_2HPO_4, trichloroacetic acid (TCA), tetrahydrofuran (THF), xylene (Fisher Scientific, Montreal, QC, Canada); DNase I (Rnase-free), ECoR II, lumi-light western blotting substrate, phenylmethylsulfonyl fluoride (PMSF), SYBR Premix Ex Taq^{TM} (Roche, Laval, QC, Canada); ethanol (Commercial Alcohols, Brampton, ON, Canada); hydrogen peroxide (H_2O_2), NaCl (J.T. Baker,

Phillipsburg, NJ, USA); [^{14}C]-3-Hydroxy-3-methylgluatryl coenzyme A (HMG CoA), OCS (Organic counting scintillant) scintillation cocktail, [^{14}C]-oleyl-coenzyme A (oleyl CoA) (GE Healthcare, Baie d'Urfe, QC, Canada); isopropanol, mehylene blue (BDH, Toronto, ON,Canada); Film-classic Blue (EBA 45) (Universal X-ray Company of Canada Ltd., Dorval, QC, Canada); RNase inhibitor (Amersham Biosciences, Baie d'Urfe, QC, Canada); silica gel solid-phase extraction (SPE) column (Waters Corporation, Toronto, ON, Canada); TLC plates (silica gel 60 F254) (EMD Chemicals Inc., Gibbstown, NJ, USA); RNeasy Mini kit, Omniscript RT kit, Taq PCR core kit (Qiagen, Mississauga, ON, Canada).

1.2 Antibodies

As following were the sources of antibodies:

ACAT-1 polyclonal antibody (rabbit polyclonal IgG), ACAT-2 polyclonal antibody (rabbit polyclonal IgG) (Cayman Chemical, Ann Arbor, MI, USA); HMG-CoA reductase polyclonal antibody (rabbit polyclonal IgG) (Upstate, Lake Placid, NY, USA); HSL polyclonal antibody (rabbit polyclonal IgG) (Dr. Cecilia Holm from Lund University, Lund, Sweden); myosin (light chain) monoclonal antibody (IgM) (Sigma-Aldrich, Oakville, ON, Canada); anti-rabbit IgG horseradish peroxidase-conjugated, anti-mouse IgM horseradish peroxidase-conjugated, biotin-SP-conjugated affinity puried F(ab')$_2$ fragment anti-rabbit IgG (H+L) (goat), HRP-conjugated streptavidin (Jackson ImmunoRes Lab, West Grove, PA, USA).

2. Apparatus

The following instruments were utilized:

EPSON perfection 3200 photo scanner (Epson Ltd. Hemel Hempstead, Herts, UK); XL-70 Beckman ultracentrifuge, Optima™ MAX ultracentrifuge, GS-6R Beckman centrifuge, Life science UV/Vis spectrophotometer (DU® 530) (Beckman Coulter™, Fullerton, CA, USA); Precision 180 Series Water Bath (Precision, Winchester, VA, USA); β–counter (Perkin Elmer, Tri-Carb 2800 TR), Thermal Cycler GeneAmp PCR System 2400 (Perkin Elmer, Markham, ON, Canada); IEC micro-centrifuger (IEC International Equipment Company, Nepean, ON Canada); Light cycler II-real time PCR equipment (Roche, Laval, QC, Canada); Light microscopy (Axiophot II) (Carl Zeiss, Hawthorne, NY, USA); Perkin Elmer GeneAmp PCR System 2400 (Garner, North Carolina USA); pH meter, Vortex Genie 2™ (Fisher Scientific, Montreal, QC, Canada); 2011 UV transilluminator (UVP Inc., Upland, CA, USA); Ultraviolet spectrophotometer (UV 160) (Shimadzu Scientific Instruments, Columbia, MD, USA).

3. Softwares

The following computer programs were used:

Primer Premier Probe Design Software 5.0 (Premier Biosoft International, Palo Alto, CA, USA); Scion Image Software (Scion Corporation, Frederick, MD, USA); Sigma plot 7.0 software (SPSS Inc., Chicago, IL, USA); The Light cycler Software 3.5 (Roche, Laval, QC, Canada); Relative quantification software, version 1.01 (Roche, Laval, QC,

Canada); Alphalmager 2200 (documentation & analysis system) (Alpha Innotech Corporation, San Leandro, CA, USA).

4. Animals

Mink (*Mustela vison*, a seasonal breeder) and mouse (*Mus musculus*, a continual breeder) were used in this study.

4.1 Mink *(Mustela vison)*

All mink, purchased from Visonnière St. Damase (St. Damase, QC, Canada), were individually caged, kept under natural lighting conditions, and allowed food and water ad libitum. After anaesthesia by an intraperitoneal injection of sodium phenobarbital (Somnotol) (0.9 ml/kg of body weight) (MTC Pharmaceutical, Cambridge, ON, Canada) and of a solution of 0.3g/ml chloral hydrate (MTC Pharmaceutical, Cambridge, ON, Canada) in sterile saline (0.15 ml/kg body weight), mink were decapitated and tissues were collected. For studies on development, testes were harvested at each 30 day interval 1) during the neonatal period (90 days old), 2) puberty (120, 150, 180, 210, and 240 days old), and 3) by the onset of adulthood (270 days old). Adult mink testes were collected for each 30 day interval during the last week of each month throughout the annual reproductive cycle from 1-2 year old mink. The dynamics of the germ cell population during development and the annual reproductive cycle were identified by the methods of Pelletier (Pelletier, 1986), and are depicted in figure 1. Six normal mink per age group were used except when testes were small during puberty, when 6-10 mink were used.

Fertility was tested as follows: the ejaculated semen recovered from vaginal smears was evaluated with a light microscope, and the morphology, motility, and number of spermatozoa was assessed by the farmer from Visonnière St. Damase (St. Damase, QC, Canada) for each male mink during the mating season in March.

4.2 Mice *(Mus musculus)*

4.2 .1 Normal mice

BALB/c mice were obtained from Charles River Laboratories, St-Constant, QC, Canada. Animals were killed at 7 day intervals up to adulthood. The testes were harvested. Each age group consisted of no less than 20 animals. The testes of more than 20 mice at days 14, 21, 28, 35, 42, and adult were prepared to generate tissue fractions to be used to prepare microsomes. All the assays were carried out on enriched tissue fractions rather than on whole testis preparations. Therefore, a high number of mice were required in the mRNA, protein expression and enzymatic activity measurements.

4.2 .2 SR-BI and CD36 and HSL knockout mice

SRBI and CD36 knockout mice were used as animal models in which a selective transporter was blocked. Both, SRBI and CD36, knockout mice were generously supplied by Dr. Louise Brissette from Université du Québec a Montréal (UQÀM). For SR-BI knockout mice, the SR-BI gene had been inactivated in embryonic stem cells by standard homologous recombination methods (Rigotti et al., 1997). A portion of exon 1 and the additional sown stream intron was mutated. The mutated locus is expected to encode a

transcript that would not translate or would be translated into nonfunctional, nonmembranous and presumably unstable, protein. CD36 knockout mice were also generated by targeted homologous recombination (Febbraio et al., 1999).

HSL knockout mice were generously supplied by Dr.Cecilia Klint from Lund University in Sweden. In brief, the gene encoding HSL was disrupted in embryonic stem cells by homologous recombination. A portion of exon 5, and the entire exon 6, which encodes the catalytic domain, was replaced by the cDNA encoding the *Aequorea victoria* green fluorescent protein and a neomycin resistance gene (Grober et al., 2003; Lipsett et al., 1966; Mulder et al., 2003).

5. Preparation of seminiferous tubule (STf) and interstitial tissue enriched fractions (ITf)

The seminiferous tubule-enriched fractions (STf) and the interstitial tissue enriched fractions (ITf) were generated according to the method of Akpovi et al., (Akpovi et al., 2006). Briefly, freshly decapsulated testes were placed in cold PBS (137mM NaCl, 3mM KCl, 8mM NA_2HPO_4, pH 7.4) or in PBS containing protease and phosphatase inhibitors (4mM Na_3VO_4, 80mM NaF, 20mM $Na_4P_2O_7$ (pH 8.5), 2 mM ethylene glycol-bis-(-aminoethyl ether)--- N,N,N', N-tetraacetic acid (EGTA), 5mM leupeptine, 5 mM aprotinin and 2 mM phenylmethylsulfonyl (PMSF)). The tissue fractions were generated by mechanical techniques. Further separation was achieved by centrifugation at 600 rpm for 20 min in a GS-6R Beckman centrifuge equipped with a GH 3.8 rotor. The resulting STf, in the pellet, and ITf, in the supernatant, were washed three times in the corresponding buffer (PBS or PBS containing protease and phosphatase inhibitors). Purity of the enriched fractions was evaluated by light microscopy. This represents a modification of a previously

published isolation method in which mild enzymatic digestion with collagenase D and soybean trysin inhibitor was used to separate tubules from the interstitial tissue (Kabbaj et al., 2001).

6. Epididymal spermatozoa

Epididymal spermatozoa were obtained by dicing adult mink caudae epididymides in cold PBS. The resulting cell suspension was filtered through a 74-mm mesh and centrifuged at 2000 rpm for 15 min in a GS-6R Beckman centrifuge to recover spermatozoa. The gametes were suspended in Tris buffer (10 mM Tris-HCl, pH 8.0 , 1 mM EDTA) for 5 min to lyse contaminating epithelial and blood cells (Herrada & Wolgemuth, 1997; Kabbaj et al., 2003).

7. Real time polymerase chain reaction (real time PCR)

7.1 Isolation of ribonucleic acid (RNA)

Total tissue RNA was isolated using RNeasy Mini kit (Qiagen, Mississauga, OH, Canada) according to the manufacturer's instructions. Briefly, the tissues were homogenized in 600 μl RLT buffer (Qiagen, Mississauga, OH, Canada). The homogenates were transferred into the RNeasy mini column placed in a 2 ml collection tube with addition of 600μl of 70% ethanol. The homogenate was centrifuged 15 sec at 10,000g in a micro-centrifuge. The RNeasy columns binding ribonucleic acid (RNA) were washed with buffer RW1 and RPE and transferred into a new 1.5 ml collection tube. The RNA was dissolved with 40μl RNase-free water and detached from the columns by centrifugation.

RNase-free DNase I (10U/μl) at a final volume of 4μl was added and heated at 75°C for 30 min. The quality and quantity of isolated RNA were measured using a spectrophotometer. The RNA solution was checked for presence of residual amounts of DNA by performing PCR amplification.

7.2 Preparation of complementary DNA (cDNA)

Complementary DNA (cDNA) was obtained by reverse transcription in the presence of random polydT using Omniscript RT kit. The reaction mixture consisted of a reverse transcriptase (RT) buffer (10X), 10 mM oligo-dT, 5mM deoxyribonucleotide triphosphate (dNTP) mixture, RNase inhibitor (32,600 U/ml), Omniscript RT enzyme (4 U/ml) and RNA samples. The total amount of 5 μg RNA was reverse transcribed into cDNA at 37°C for 1h in a 50 μl final volume.

7.3 Quantification of gene expression

The mRNA expression of HMG-CoA reductase, HSL, ACAT-1 and ACAT-2 were measured using primers designed for mouse and mink genes (Table 1). All primers sequences were generated using Primer Premier Probe Design Software 5.0 and checked for specificity using BLAST analysis on NCBI webiste. All these primers were purchased from Invitrogen company. For expression screening, PCR reactions were performed in the presence of 0.2 μM dNTP, 0.5 μM of each primer and 2.5 U Taq DNA polymerase (Taq PCR core kit) at a final volume of 25 μl. Products of reaction were visualized by electrophoresis in a 1.5-3% agarose gel, stained with ethidium bromide and photographed under a UV transilluminator.

Table1. Specific primers designed for mink and mouse HMG CoA reductase, ACAT-1, ACAT-2 and HSL

Gene	GeneBank accession numbers	Primers		Product size (bp)
		sense	Anti-sense	
HMG CoA red. (mouse)	NM_008255	5'CAGGATGCAGCACAGAATG3'	5'AGGCAGGCTTGCTGAGGTA3'	175
HMG CoA red. (mink)	NM_000859	5'CTTCCTCGTGCTTGTGACTC3'	5'GACGTGCAAATCTGCTCG3'	105
ACAT-1 (mouse)	NM_009230	5'CTGTAAGATGGGGTTATGTCGC3'	5'CACTGAAGGGCTCCTGTTTG3'	126
ACAT-1 (mink)	NM_003101	5'TTGGAATGGCTTTCAACT3'	5'AAACACGTAACGACAAGTCC3'	185
ACAT-2 (mouse)	AF078751	5'TGGGAGTGTTCCTGGTGTCT3'	5'CCCGAAAACAAGGAATAGCA3'	101
ACAT-2 (mink)	AF059203	5'GCAAGTCCCTGCTTGATGAGC3'	5'CCAGCGATGAACATGTGGTAGAT3'	70
HSL (mouse)	NM_010719	5'TTCGCCATAGACCCAGAGTT3'	5'GACGACAGCACCTCAATCTCA3'	113
HSL (mink)	NM_0053572	5'GGAGCACTACAAACGCAACG3'	5'TCTCAAAGGCTTCGGGTG3'	250
HPRT-1	NM_013556	5'TGACACTGGCAAAACAATGCA3'	5'GGTCCTTTTCACCAGCAAGCT3'	93

The real time PCR reactions were performed in the presence of 0.5 μM of each primer according to the manufacturer's instructions (SYBR Premix Ex Taq^{TM}). In all PCR reactions, a negative control corresponding to RT reaction without the reverse transcriptase enzyme and a blank sample were carried out. Amplification of the housekeeper gene hypoxanthine phosphoribosyl transferase 1 (HPRT-1) cDNA was used as internal control to quantify the expression of a given gene in real time PCRs. For quantification studies, melting curves were performed at the end of the real time PCRs to ensure amplification of a single product with the appropriate melting temperature. Quantification was done with the

Relative quantification software, version 1.01. The specificity of real time PCR products was evaluated through enzymes restriction according to manufacturer's instructions.

7.4 Restriction digestion of PCR and real time PCR products

To identify the PCR or real time PCR product, the amplified DNA fragments were digested with restriction enzymes. Alu I and EcoR II were used to cleave ACAT-2 amplified fragments in mink STf or mouse STf respectively. The reactions were performed in presence of 1U Alu I or ECoR II restriction enzyme, digestion buffer (10 X) and DNA fragments at the final volume of 10 µl. The mixture was digested at 37°C overnight. Digestion and PCR products were analyzed by electrophoresis in a 3% agarose gel, stained with ethidium bromide and photographed under UV transilluminator.

8. Western Blot Analyses

8.1 Protein measurements

Protein in the tissue enriched fractions were measured according to the method of Bradford (1976) by using a dye-binding assay, and BSA as a standard. Samples were prepared for electrophoresis by boiling them in the corresponding volume of sample buffer 2X (8 M urea, 70 mM Tris-HCl pH 6.8, 3% SDS, 0.005% BPB, and 5% β-mercaptoethanol) for 5 min.

8.2 Electrophoresis and transfer

Proteins (20-40 µg) were resolved on a 10% sodium dodecylsulfate-polyacrylamide gel electrophoresis (SDS-PAGE) at 70 V to 120V. After migration, the proteins in the gel

were electro-transferred at 300 mA for 1.5 h or at 27 V overnight at 4°C onto nitrocellulose membranes using a transfer buffer (25mM Tris-HCl pH 8.3, 150mM glycine and 20% (v/v) methanol). The nitrocellulose membranes were colored with Ponceau red (0.2% Ponceau red and 3% TCA in distilled water) for 10 seconds at room temperature (RT) until the bands were visualized and then rinsed with distilled water. The molecular mass of the bands corresponding to the proteins of interest was determined by comparison with the migration of molecular mass standards (SDS-PAGE Standards, High and Low Range). Thereafter, the membranes were washed with PBS at RT for 10-15 minutes under agitation to remove the Ponceau red.

8.3 Immunoblotting

To block nonspecific binding, the membranes were incubated in PBS-containing 3% skim milk at 37°C for 1 hour. Next, the membranes were incubated with one of the following primary antibodies: anti-HMG CoA reductase (1:500), anti- ACAT-1 (1:50), anti-ACAT-2 (1:200), anti-HSL (1:500) overnight at 4°C under agitation. After the incubation, the membranes were washed with 0.05% Tween20- PBS 15 min each for 4 times at 37 °C and incubated with the corresponding (anti-rabbit IgG, or anti-mouse IgM) secondary horseradish peroxidase-conjugated antibody (1:2000) for 1 h at RT with agitation. All antibodies were prepared in 1% skim milk-PBS. The membranes were rinsed three times in 0.05% Tween 20-PBS for 15 min and one time in TBS buffer (137 mM NaCl, 2.7 mM KCl, 24.8 mM Tris-base, pH 7.4) for 15 min at RT with agitation.

Immunoreactive bands were revealed by chemiluminescence and the membrane were exposed to film-classic Blue (EBA 45).

9. Preparation of the microsomal fraction and enzyme activity measurement

9.1 Microsome preparation and protein determination

Microsomes from mink or mouse seminiferous tubule enriched fractions were prepared by differential centrifugation as described by Stalhberg et al. (Stahlberg et al., 1997). The STf were homogenized with the homogenization solution (15mM Tris-HCl pH 7.4, 300mM sucrose, 10mM mercaptoethaol, 1mM PMSF, 10mM aprotinin and 10mM leupeptin) in a Glass-Col homogenizer on ice. The homogenate was centrifuged at 19,600 g for 15 min at 4°C with Optima^{TM} MAX ultracentrifuge. The upper supernatant layer was carefully removed. The pellet was discarded and the microsomes sedimented by ultracentrifugation (XL-70 Beckman ultracentrifuge) at 100,000 g for 60 min at 4°C. The pellet was resuspended in phosphate buffer (1M K_2HPO_4, 1M KH_2PO_4(pH 7.4), 30mM EDTA, 5mM dithiothreitol (DTT) and 250 mM NaCl, 1mM PMSF, 10mM aprotinin and 10mM leupeptin). The microsome protein content was evaluated according to the method of Bradford, using BSA as a standard (Bradford, 1976).

9.2 Determination of HMG-CoA reductase activity

Microsomes (200 μg) were added to 150 μl phosphate buffer [50 mM K_2HPO_4 (pH 7.4), 30 mM EDTA and 70 mM KCl] and pre-incubated for 5 min at 37°C (Shapiro et al., 1974). Microsomes pre-heated for 5min at 95°C were used as control. The reaction was

triggered by the addition of nicotinamide hypoxanthine dinucleotide phosphate (NADPH) generator system (25.3mM glucose-6-phosphate, 1U glucose-6-phosphate dehydrogenase and 29 mM NADP and the radioactive substrate [200 μM 3-Hydroxy-3-methylgluatryl coenzyme A (HMG-CoA) containing 19 nCi (1.11%) of [^{14}C]-HMG-CoA]. The mixture was incubated at 37°C for 15 min, to produce [^{14}C]-mevalonic acid, and stopped by the addition of 20 μl of 5 N HCl. The reaction mixture was then incubated for 30 min at 37°C to allow lactonization of [^{14}C]-mevalonic acid into [^{14}C]- mevalonolactone (MVL). The reaction mixture (100 μl) was evaporated to dryness at RT and then suspended in 150 μl of acetonitrile by sonication and centrifuged for 5 min at 13,000g. The suspensions (100 μl) were seeded into a silica gel solid-phase extraction (SPE) column (previously conditioned with 3 X 1ml of anhydrous petroleum ether). Thereafter, 1ml anhydrous petroleum ether was added onto the SPE column, followed by 2X-1ml of THF. All the solutions were collected and evaporated to dryness at RT. The scintillation cocktail was added and the radioactivity was measured using a β–scintillation counter. The [^{14}C]-HMG-CoA, a polar molecule, binds to the silica gel, whereas the [^{14}C]-MVL, a non-polar molecule, is easily eluted by petroleum ether and tetrahydrofuran (THF) (Nguyen et al., 1990).

9.3 Determination of ACAT activity

9.3.1 Total ACAT enzymatic activity measurement

Total ACAT enzymatic activity was determined by assessing the production of cholesteryl[^{14}C] oleate (Chang et al., 1998; Erickson et al., 1980). The microsome preparation (200 μg) was added to 100 μl assay buffer [0.2 mM KH_2PO_4 (pH 7.4), 2mM

DTT] containing 0.4 mg/ml of cholesterol and 6mg/ml of BSA. After a preincubation at 37°C for 20 min, the reaction was triggered by the addition of 10 μM [^{14}C]-oleyl-CoA (specific activity of 56.0 nCi/nmol). Then, the mixture was incubated at 37°C for 25 min and the reaction was stopped by addition of 1ml isopropanol-heptane (4:1, v/v). The final reaction mixture was vortexed and 0.6 ml heptane and 0.4 ml assay buffer were added. The upper heptane phase (100 μl) was transferred into a vial containing liquid scintillation cocktail and the radioactivity was measured in a β–scintillation counter. Separation of cholesteryl [^{14}C] oleate from residual substrate, [^{14}C] oleoyl-CoA, and side-products was performed by solvent partitioning between an upper heptane phase and a lower isopropanol-water phase (Jeong et al., 1995).

Since some of the radioactivity recovered in the upper phase was due to the enzymatic incorporation of radioactive fatty acid into products other than cholesteryl oleate, to specifically measure ACAT activity, the partitioned heptane phase was separated by thin layer chromatography (TLC) (Silica gel 60 F_{254}) using a solvent mixture made up of n-hexane-diethyl ether-acetic acid (90:10:1). Cholesteryl ester standard (choleseryl oleate) was used on several lanes across each plate in order to identify the region of cholesteryl ester. The separated free and esterified cholesterol were visualized by staining with iodine vapour and the radioactive content of the excised bands of free and esterified cholesterol was determined by scintillation counting.

9.3.2 Individual ACAT-2 enzymatic activity measurement and ACAT-1 enzymatic activity assay

We provide a novel technical approach for the measurement of individual ACAT-2 enzymatic activity and individually determine the activity of ACAT-1 in seminiferous tubules and interstitial tissue during postnatal development and adulthood something which had never been reported before. The technique is based on the use of a selective ACAT-1 inhibitor, K-604.

The assay buffer (100μl) was the same as in the total ACAT enzymatic activity measurement except for the addition of the ACAT-1 inhibitor (K-604) (100 μM diluted in 5ml of dimethylsulfoxide (DMSO)). The steps to measure the ACAT-2 enzymatic activity were the same as in the total ACAT enzymatic activity measurements. The concentration of K-604 used in the assay was determined according to a dose-dependent inhibition curve. Various concentrations (0-1000μM) of inhibitor were added to the assay buffer. A concentration-enzymatic activity inhibition curve was established and the inhibitor concentration that inhibits all ACAT-1 activity but not ACAT-2 activity was selected for the study.

Thereafter, ACAT-1 enzymatic activity was calculated by subtracting ACAT-2 enzymatic activity from total ACAT enzymatic activity.

9.4 Determination of HSL activity by spectrophotometric esterase assay

To assess the HSL activity, a spectrophotometric esterase assay based on the hydrolysis of PNPB was used (Holm & Osterlund, 1999). Kabbaj et al, applied this method

to the seminiferous tubules and interstitial tissue during postnatal development and adulthood (Kabbaj et al., 2001; Kabbaj et al., 2003). STf were homogenized on ice in 0.25 M sucrose, 1 mM EDTA, pH 7.0, 1 mM dithioerythreitol, 20 μg/ml leupeptin, 2 μg/ml antipain, and 1 μg/ml pepstatin. Aliquots of 10–20 μg of protein of each sample were incubated with PNPB (diluted in acetonitrile) and buffer (0.1 M NaH_2PO_4, pH 7.25, 0.9% NaCl, 1 mM dithioerythreitol) at 37°C for 10 min. The reaction was stopped by addition of 3.25 ml of methanol: chloroform: heptane (10:9:7). After centrifugation at 800×g for 20 min, solutions were incubated for 3 min at 42°C and the absorbance of the supernatant was measured at 400 nm in a light spectrophotometer. The enzymatic activity was expressed in units, one unit being equivalent to the release of 1 μmol of p-nitrophenol/min. All samples were analyzed in triplicate and the HSL activity was related to the total protein concentration of each sample.

To determine the best protein concentration for the assay, various concentrations (0-400μg) of protein in the samples were incubated with PNPB. After the reaction was completed, a protein concentration enzymatic activity curve was made and the proper protein concentration was chosen for the study.

10. Immunohistochemical analyses

10.1 Tissue preparation for immunohistochemistry

Testes were perfused-fixed through the testicular artery, first with PBS and then with Bouin's fixative, and were immersed for 48 hours in the same fixative at RT as described by Pelletier (Pelletier et al., 1995; Pelletier, 1995; Pelletier et al., 1997). Tissues

were dehydrated with series of ethanol (70%, 95% and 100%) and xylene. Next, the tissues were embedded with paraffin and sectioned to 5 μm thick. The sections were mounted on glass slides and dried at 40°C overnight.

10.2 Immunolocalization of the enzymes

The mounted sections were deparaffinized with xylene and rehydrated with series of ethanol (100%, 95%, 70%, 50%) followed by water (Pelletier, 1995; Pelletier et al., 1997). Then, the sections were boiled in citrate buffer (10mM citric acid, 0.05% Tween 20, pH 6.0) for 8 min at 95°C and exposed to 0.6% H_2O_2 in TBS for 10 min to inhibit endogenous peroxidase activity and rinsed with TBS containing 0.1% Tween-20 (0.1% TBST). Next, the sections were incubated with 0.5% skim milk in TBST for 30 min at RT to block non-specific binding followed by incubation with anti-HMG-CoA reductase (1:50) or anti-ACAT1 (1:100) or anti-ACAT2 (1:50) overnight at RT. Subsequently, the sections were rinsed and incubated with biotinylated anti-rabbit IgG Fab (1:10,000) for 1 h at RT. All antibodies were prepared in 1% skim milk-PBS. After washing, the sections were incubated with horseradish peroxidase (HRP)-conjugated streptavidin (1:200 1% milk-PBS) for 1h at RT and rinsed. The reaction was detected by 0.05% diaminobenzidine tetrachloride (DAB) containing 0.03% H_2O_2 and counterstained with 0.05% methylene blue. The sections were dehydrated with series of ethanol (70%, 95% and 100%) and xylene.

11. Analysis of data and statistical analysis

The immunoreactive bands of enzymes in Western blots obtained for each time interval studied were scanned with a laser scanner. The values were normalized to the 90

day values for developmental studies or to August values for the studies on mink adults; the values were also normalized to the 14 day values for the studies of development or the wild-type for the mice studies. The data are expressed as the mean ± standard error of the mean (SEM). Student's *t*-test was used for comparisons between two groups. Differences were considered statistically significant as $P<0.05$.

Data were expressed as the mean ± SEM for real time PCR and enzymatic activity analyses followed by Student's *t*-test at a $P<0.05$ level of significance. All analyses were carried out with Sigma plot 7.0 software.

Results

1. HMG-CoA reductase

1.1 Mink

Measurements in mink were performed in seminiferous tubule-enriched fractions (STf) obtained each 30 day- (d) interval throughout postnatal development (from 90d to 270d after birth), and throughout the twelve-month seasonal reproductive cycle in the adult (Fig. 1). The histological changes during postnatal development are similar to those of the active spermatogenic phase in mink testis (Pelletier et al., 2009). The neonatal period expands from birth to about day 90 days after birth, the puberty from day 90 to day 252 after birth; this period includes the completion of spermatogenesis by Day 240 after birth and the appearance of spermatozoa in the epididymis some 12 days in January (252 days after birth).

Here, it must be stressed that the enzymatic activity measurements were carried out on microsomes that were obtained from seminiferous tubule-enriched fractions. This procedure necessarily requires using much greater numbers of animals or big amount of tissues than if the procedure used whole testis extract as is done in most studies. Thus, the experiments were not carried out in the interstitial tissue fractions since not enough interstitial tissue could be gained.

1.1.1 Real time quantitative PCR, Western blot and enzymatic activity measurements in STf

1.1.1.1 mRNA

The mRNA expression profile of HMG-CoA reductase was evaluated by real time PCR using total RNA isolated from mink STf during development and the annual reproductive cycle. HPRT-1, a house-keeper gene, was used as internal control since it is expressed constitutively and constantly in all samples. It corresponded to a 93bp single band (Fig. 2A). HMG-CoA reductase primers (Table 1) amplified a single product with an expected size of 105bp by real time PCR (Fig. 2A). The 105bp HMG-CoA reductase and the 93bp HPRT-1 product were detected throughout development and the annual reproductive cycle (data not shown). A negative control corresponding to RT reaction without the reverse transcriptase enzyme was carried out and showed no PCR product amplification (data not shown). Figure 2B shows that HMG-CoA reductase mRNA levels varied distinctly during development and the annual cycle. The HMG-CoA reductase mRNA levels significantly increased toward the end of development. The levels increased significantly from 180 to 210 days and then decreased significantly from 240 to 270 days (Fig. 2B). The levels increased significantly by the end of testicular regression in the seasonal cycle. The mRNA levels peaked from April to May, and then significantly decreased from June to July (Fig. 2B).

1.1.1.2 Protein

Western blot analyses performed with anti-HMG-CoA reductase antibody revealed several bands in mink STf during development and the annual reproductive cycle (Fig. 3A). Adsorption of anti-HMG-CoA reductase with an HMG-CoA reductase peptide caused the disappearance of the 90kDa immunoreactive band and a decrease of the 53kDa band (Fig. 3A). Because the 53kDa band did not completely disappear with the pre-adsorption, the 90kDa was considered the HMG-CoA reductase immunoreactive band and will be analyzed in our study. Representative Western blots of HMG-CoA reductase are shown in Figure 3B. The 90 kDa HMG-CoA reductase expression showed different tendencies between development and the reproductive cycle. In addition, the protein level profiles (Fig. 3) did not parallel the mRNA level profiles (Fig. 2B). The 90kDa HMG-CoA reductase significantly increased with the initiation of meiosis particularly from 150 to 180 days. In the adult, the 90kDa band tended to decrease during testicular regression but not significantly. Myosin light chain (MLC) was used as an internal loading control. MLC has a molecular mass of 20 kDa, and the intensity of the band did not change in the different experimental conditions (data not shown).

1.1.1.3 Enzymatic activity

The HMG-CoA reductase enzymatic activity was measured by quantifying its reaction product mevalolactone (MVL) using an alternative chromatographic technique developed in Dr. Julie Lafond's lab (Montoudis et al., 2004). HMG-CoA reductase

activity tended to increase throughout development (Fig. 4) and this increase does not parallel the profile in the levels of the 90 kDa immunoreactive band during development and the annual cycle (Fig. 3). The enzymatic activity at 120 days averaged 6.4071e-8 ± 5.5729e-8 (mean ±SEM) mol/min/μg protein in three group experiments. The enzymatic activity was significantly increased from 210 to 240 days, and reached the maximal value at 3.6411e-7 ± 3.3718e-9 mol/min/μg protein (mean ±SEM) at 240 days, but significantly decreased afterwards (Fig. 4). During the annual reproductive cycle, HMG-CoA reductase activity firstly and significantly increased by December and again increased significantly from December to January and from January to February. The maximal value was at 1.2132e-6 ± 2.9000e-7 mol/min/μg protein (mean ±SEM) by February. HMG-CoA reductase enzymatic activity decreased from June to July but not significantly (Fig. 4).

1.1.2 Immunohistochemical localization in the testis

HMG-CoA reductase positive labeling was found throughout development and the annual reproductive cycle within the seminiferous tubules. HMG-CoA reductase–positive dots were detected in Sertoli cells, and spermatids. Endothelial cells of capillaries and other interstitial tissue cells are also positive (Fig. 5).

1.2 Mouse

1.2.1 Real time quantitative PCR, Western blot analyses in ITf

1.2.1.1 mRNA

A single product was amplified by real time PCR using HMG-CoA reductase primers to mouse (Table 1). The product had the expected size of 175bp (Fig. 6). During development, mRNA expression levels were sharply and significantly increased from 21 to 28 days after birth, and then significantly decreased from 28 to 35 days and from 35 to 42 days after birth (Fig. 6A).

1.2.1.2 Protein

Pre-adsorption of anti-HMG-CoA reductase with the HMG-CoA reductase peptide caused the disappearance of the 90 kDa immunoreactive band (Fig. 6B-1). Thus the 90 kDa band was considered the HMG-CoA reductase immunoreactive band in our study. The 90kDa immunoreactive band remained more or less constant throughout development (Fig. 6B-2) contrary to the mRNA levels (Fig. 6A) which did not.

1.2.2 Real time quantitative PCR, Western blot and enzymatic activity measurements in mouse STf

1.2.2.1 mRNA

In the mouse STf, the size (175bp) of HMG-CoA reductase amplicons was the same as the one produced in mouse ITf (Fig. 7A). The mRNA expression levels significantly increased from 14 to 21 days, from 21 to 28 days and again from 35 to 42 days, but decreased with adulthood (Fig. 7A).

1.2.2.2 Protein

In pre-adsorption experiments, the 90 kDa band almost disappeared, indicating that this is the HMG-CoA reductase immunoreactive band (Fig. 7B-1). The 90kDa immunoreactive band was detected in the STf (Fig. 7B-2). The 90kDa HMG-CoA reductase protein levels in STf increased early during development and the intensity of the 90kDa immunoreactive band was the strongest at 28 days, and then tended to decrease afterwards (Fig. 7B-2). In epididymal Spz however the 90kDa protein band was detected together with a 37kDa band. The 37kDa immunoreactive band has never been reported in Spz before. Both the 90kDa and 37kDa immunoreactive bands were absent following pre-adsorption (Fig. 7B-3).

1.2.2.3 Enzymatic activity

The HMG-CoA reductase activity tended to increase from 14 days to 42 days after birth and to slightly decrease with adulthood (Fig. 7C). The enzymatic activity ranged from 1.73e-7 ± 1.16e-8 (mean ±SEM) mol/min/μg protein (14 days) to 5.19e-7 ± 9.53e-8 mol/min/μg protein (42 days) (mean ±SEM). The largest increase in the enzymatic activity was observed in the 28 day-old mice (Fig. 7C). This time point corresponded to the time when the intensity of the 90kDa HMG-CoA reductase immunoreactive band was strongest and the mRNA levels were significantly increased.

1.2.3 Immunohistochemical localization in the testis

In the mouse, HMG-CoA reductase was detected in Sertoli cells in all age group studied (Fig. 8). HMG-CoA reductase was also found in elongating spermatids. HMG-CoA reductase was also detected in the interstitial tissue cells (Fig. 8).

2. HSL

2.1 Mink

2.1.1 Real time quantitative PCR, Western blot and enzymatic activity measurements in STf

2.1.1.1 mRNA

The mRNA expression of HSL was evaluated by real time quantitative PCR using the same cDNA as in HMG-CoA reductase measurements. A single 250bp product was amplified (Fig. 9). Quantification of the band during development and the annual reproductive cycle showed that the HSL mRNA levels significantly increased from 90 to 120 days after birth, then the levels slowly went down until 240 days, but HSL mRNA levels sharply and significantly increased by 270 days. During the seasonal cycle, the HSL mRNA levels showed a tendency to increase from September to October, but the changes were not statistically difference (Fig. 9).

2.1.1.2 Protein

Adsorption of anti-hHSL with human adipose tissue caused a major decrease in the intensity of the 90kDa immunoreactive bands in mink tissues (Kabbaj et al., 2003), demonstrating that the anti-hHSL antibody recognizes the enzyme in mink tissue. It has been reported that HSL gene in the testis encodes a protein which is identical to the adipocyte HSL (Mairal et al., 2002). We proposed that the 90kDa immunoreactive band detected in the testis is HSL. Considering the Western blot experiment in HSL knockout mice, only the 90kDa band was not detected, demonstrating that the 90kDa immunoreactive band corresponds to HSL. Representative Western blots are shown in Figure 10. The levels of the 90kDa HSL immunoreactive band were significantly increased from 150 to 180 days and again from 210 to 240 days after birth. The levels decreased slightly afterwards. During the annual reproductive cycle, the protein levels significantly increased from December to January, and then decreased from March to April and remained low in the following months (Fig. 10). HSL protein expression (Fig. 10) was not coincident with its mRNA expression (Fig. 9).

2.1.1.3 Enzymatic activity

At 90 days, HSL enzymatic activity was 30.56 nM/min/μg protein. HSL activity was increased by 8% in 120 days in mink STf compared to 90 days and again from days 180 to 210 when the spermatocytes differentiate from the preleptotene to prepuberal pachytene stages. In 210 days the HSL activity reached 35.61 nM/min/μg protein. During the annual reproductive cycle, HSL enzymatic activity increased by November on the onset of meiosis but the increase was not significantly different. However, activity levels peaked

in February and significantly decreased from February to March, from 40.88 ± 0.08 nM/min/μg protein to 34.59 ± 0.16 nM/min/μg protein. The increase of HSL activity is accompanied with the completion of spermatogenesis during development and in the adult during the active phase of the annual reproductive cycle. The enzymatic activity decreased more rapidly than the protein levels during the annual reproductive cycle (Fig. 11).

2.1.2 Immunohistochemical localization in the testis

In our lab, Kabbaj et al have reported that HSL immunoreactivity was detected in all ages of the seminiferous epithelium (Kabbaj et al., 2003). This enzyme was localized to Sertoli cell cytoplasmic processes surrounding germ cells throughout puberty and also was detected in elongating spermatids. HSL was also expressed in the epididymal spermatozoa (Kabbaj et al., 2003).

2.2 Mouse

2.2.1 Real time quantitative PCR, Western blot analyses in ITf

2.2.1.1 mRNA

The mRNA expression of HSL in mouse ITf was evaluated by real time quantitative PCR using the same cDNA as in HMG CoA reductase measurements. A single 113bp product was amplified (Fig. 12A). Quantification of this band showed that HSL mRNA levels significantly increased from 21 to 28 days after birth, they significantly decreased from 35 days onwards.

2.2.1.2 Protein

Identification of the 90kDa band as being the HSL immunoreactive band was performed using HSL knockout mice ITf (see figure 20B). A representative Western blot of the 90kDa HSL immunoreactive band is shown in Figure 12B. HSL protein levels tended to slightly increase from 28 to 35 days after birth, and then the protein content leveled high from 35 to adulthood and this was associated with the significant decrease of HSL mRNA levels (Fig. 12B).

2.2.2 Real time quantitative PCR, Western blot and enzymatic activity measurements in STf

2.2.2.1 mRNA

A single 113bp product was amplified by real time PCR with mouse HSL gene (Fig. 13A). Quantification of this band showed that HSL mRNA levels were significantly increased from 14 to 21 days, from 21 to 28 days and from 28 to 35 days after birth, then the levels remained high (Fig. 13A).

2.2.2.2 Protein

A representative Western blot of the 90kDa HSL immunoreactive band is shown in Figure 13B. The 90 kDa HSL protein levels were increased steadily with spermatogenic activity reaching maximal values with adulthood (Fig. 13B). The 90kDa protein level profiles paralleled the HSL mRNA levels.

2.2.2.3 Enzymatic activity

HSL enzymatic activity was significantly increased with the onset of puberty from 14 to 21days after birth, from 10.90 ± 0.38 nM/min/μg protein to 14.61 ± 0.84 nM/min/μg protein. The activity levels increased until days 42, but significantly decreased in the adult, where the averaged value was 9.61 ± 1.73 nM/min/μg protein (Fig. 13C). The decrease of HSL activity in the adult was coincident with an increase in both HSL mRNA (Fig. 13A) and protein expression (Fig. 13B).

3. ACAT-1 and ACAT-2

3.1 Mink

3.1.1 Real time quantitative PCR, Western blot and enzymatic activity measurements in STf

3.1.1.1 mRNA

Up to now, ACAT has been studied mainly in the gut and liver (Chang et al., 1993) but never in the testis. Moreover, the role of individual ACAT isoforms of the enzyme in the maintenance of cholesterol homeostasis in the gonads has never been addressed.

The presence of transcripts for ACAT-1 and ACAT-2 genes was evaluated by PCR using specific primers respectively. The amplified sequences between ACAT-1 and ACAT-2 showed no homology in BLAST analyses. One single 185bp sized product of ACAT-1 and one 70bp ACAT-2 product were amplified (Fig. 14A). The specificity of real time PCR

product of ACAT-2 was evaluated by restriction enzymes. Alu I, cleaves the recognition site (AG^CT). This sequence was only present in the ACAT-2. Two small DNA fragments of 20bp and 50bp respectively were obtained in a 3.5% agarose gel (Fig. 14B).

ACAT-1 mRNA expression differed greatly from ACAT-2 mRNA expression in mink STf during development and the annual reproductive cycle. During mink development, ACAT-1 mRNA levels significantly increased from 90 to 120 days and from 240 to 270 days (Fig. 14C). During the annual reproductive cycle, ACAT-1 mRNA levels significantly increased from September to October then significantly decreased from November to December before significantly increasing again from April to May and significantly decreasing in July (Fig. 14C). On the other hand, ACAT-2 mRNA levels significantly rose from 180 to 210 days but decreased significantly from 210 to 240 days during development (Fig. 14C). The mRNA levels were significantly elevated from December to January and from April to May but they significantly decreased from June to July during the annual reproductive cycle (Fig.14C).

3.1.1.2 Protein

Western blots performed with anti-ACAT-1 and ACAT-2 antibodies revealed a 50kDa and a 46kDa band respectively (Fig. 15).

Although ACAT-1 and ACAT-2 mRNA expression varied differently during development (Fig. 15), both ACAT-1 and ACAT-2 protein levels tended to increase and reached the highest levels with adulthood (270 days) (Fig. 15). Similarly, during the annual reproductive cycle ACAT-1 protein levels increased steadily during the period when spermatogenesis was completed in January, February and March and decreased gradually

during the periods when spermatogenesis was arrested. In contrast, ACAT-2 levels significantly rose from December to January and were maintained high from January to March before significantly dropping from March to April (Fig. 15).

3.1.1.3 Enzymatic activity

Here, we are the first to apply the novel selective ACAT-1 inhibitor, K-604, to the measurement of individual ACAT-1 and ACAT-2 enzymatic activity (Chen L., 2008). K-604 potently and selectively inhibited ACAT1 much more than ACAT2 with IC_{50} values of 100 and 1000 μM respectively (Fig. 16A), and the proper inhibitor concentration (100μM) that inhibits the activity of ACAT-1 but not the activity of ACAT-2 was selected (Fig. 16A).

ACAT-1 and ACAT-2 activity was evaluated by the quantification of the reaction product (cholesteryl oleate), which is separated from other unspecific products by TLC. The weak enzymatic activity or extremely different values between groups obtained could be due to an important loss of products during the necessary TLC manipulation (spotting and recovery) since the samples used and the method of quantification (evaluation of radioactive reaction product) were the same. Therefore, only a representative enzymatic activity measurement of ACAT-1 and ACAT-2 is shown in Figure 16 although the enzymatic activities were measured in three independent experiments. All experiments showed a similar trend.

Figure 16B shows representative histograms of ACAT-1 and ACAT-2 enzymatic activities in mink STf during development and the annual reproductive cycle. ACAT-1 enzymatic activity showed a steady decrease with development (range from 3140.00

CPMB/200μg protein to 43.00 CPMB/200μg protein) (CPMB = scintillated radioactivity), reaching minimal values by 270 days after birth. During the reproductive cycle, the levels of ACAT-1 enzymatic activity were reduced by 94% during the period when spermatogenesis was completed in January (January versus to August) and were increase to 265% during the regression of spermatogenesis in May (May to January) (Fig. 16B). In contrast, ACAT-2 enzymatic activity remained relatively constant during early development and was increased 2.4-fold of the value after day 240 (161.00 CPMB/200μg protein to 388.00 CPMB/200μg protein), and was maintained at this elevated level for up to day 270 (388.00 CPMB/200μg protein to 1190.00 CPMB/200μg protein). During the seasonal cycle, ACAT-2 enzymatic activity sharply increased from December to January remaining high from January to March but decreasing afterwards (Fig. 16B). Compared to the protein expression of each ACAT isoform, ACAT-1 enzymatic activities was opposite to its protein expression, whereas ACAT-2 enzymatic activity paralleled tois coincident with its protein levels.

3.1.2 Immunohistochemical localization in the testis

We are the first to immunolabel ACAT-1 and ACAT-2 in mink testis (Fig. 17). The ACAT-1 was detected only in germ cells of the tubules; it was localized in spermatocytes, elongating spermatids and in the acrosome of mature spermatids. ACAT-1 was also labeled the interstitial cells. In contrast, the ACAT-2 was only localized to Sertoli cell in the seminiferous tubules, and widely distributed in the interstitial cells; ACAT-2 labeled the endothelial cells lining blood vessels within the interstitial tissue (Fig. 17).

3.2 Mouse

3.2.1 Real time quantitative PCR, Western blot analyses in ITf

3.2.1.1 mRNA

We designed the pertinent primers to ACAT-1 and ACAT-2 genes respectively. No homologous sequences were found between ACAT-1 and ACAT-2 using BLAST analyses. mRNA expression of ACAT isoforms were measured separately by real time quantitative PCR. One single 126bp sized product of ACAT-1 and one 101bp sized product of ACAT-2 were amplified (Fig. 18A). In order to examine the amplified product of ACAT-2, the amplified PCR fragments were digested by restriction enzymes, EcoR II, which cut the two recognition sites (^CCWGG) in the ACAT-2 sequence (Fig. 18B). Three small DNA fragments of 49bp, 42bp and 10bp sized products were detected in a 3.5% agarose gel (Fig. 18B).

The amplified products of ACAT-1 and ACAT-2 are shown in Figure 18A. ACAT-1 mRNA level profiles differ from those of ACAT-2 during development. ACAT-1 mRNA levels significantly increased from 21 to 28 days after birth and from 35 to 42 days and tended to decrease from 42 days to adulthood. On the other hand, ACAT-2 mRNA levels showed no significant changes (Fig. 18A).

3.2.1.2 Protein

Western blot analyses revealed a 50kDa ACAT-1 immunoreactive band and a 46kDa ACAT-2 immunoreactive band (Fig. 18C). The changes in ACAT-1 protein levels were opposite to its mRNA levels. ACAT-1 protein levels were reduced with development and significantly from 42 to >60 days after birth. However, ACAT-2 protein levels remained virtually constant throughout development (Fig. 18C).

3.2.2 Real time quantitative PCR, Western blot and enzymatic activity measurements in STf

3.2.2.1 mRNA

Amplified product of ACAT-1 and ACAT-2 are shown in Figure 19A. One single 126bp sized product of ACAT-1 and one 101bp sized product of ACAT-2 were amplified. In contrast to what we found in the ITf, in the STf, ACAT-1 mRNA levels tended to decrease during development whereas ACAT-2 mRNA levels were increased significantly from 35 to 42 days after birth (Fig. 19A).

3.2.2.2 Protein

50kDa ACAT-1 and 46 kDa ACAT-2 immunoreactive bands were detected in STf (Fig. 19B). Moreover, the ACAT-1 immunoreactive band was also detected in epididymal Spz; however, no ACAT-2 immunoreactive band was detected even in overexposed membranes (Fig. 19B).

ACAT-1 protein expression (Fig. 19B) was similar as its mRNA profiles (Fig. 19A); the protein levels were markedly reduced with development. In contrast, ACAT-2 protein levels were sharply and significantly increased from 21to 28 days after birth, and then decreased from 42 to >60 days after birth (Fig. 19B). ACAT-2 protein expression is not coincident with its mRNA level changes (Fig. 19A).

3.2.2.3 Enzymatic activity

The same technique we have developed and used for mink was used for measuring individual ACAT isoform activities in mouse STf. The inhibitor concentration of K-604 was determined by the dose-dependent inhibition curve (Fig. 19C). One hundred μM of K-604 was the concentration selected (Fig. 19C). ACAT-1 enzymatic activity and protein levels profiles were similar; both decreased with development. The activity values ranged from 2776.00 CPMB/200μg protein to 713.00 CPMB/200μg protein. However, ACAT-2 enzymatic activity increased up to 42 days after birth (ranged from 620.00 CPMB/200μg protein to 2173.00 CPMB/200μg protein), and then substantially decreased with adulthood. ACAT-1 and ACAT-2 enzymatic activities showed complementary profiles in mouse STf during development and reached similar levels by adulthood (Fig. 19D).

3.2.3 Immunohistochemical localization in the testis

Immunohistochemistry studies revealed that ACAT-1 and ACAT-2 were both present in mouse testis (Fig. 20). In the seminiferous tubules, ACAT-1 only labeled germ cells including spermatogonia, spermatocytes and the acrosome of spermatids. In addition, ACAT-1 labeled the interstitial cells. Instead, ACAT-2 was only localized to Sertoli cell in

the tubules but showed no labeling in the interstitial tissue (Fig. 20). Considering detectable but low amount of ACAT-2 protein in interstitial tissue demonstrated by Western blot, we think immnunohistochemistry is not a sensitive enough to localize ACAT-2.

4. HMG-CoA reductase, ACAT-1, ACAT-2 in HSL knockout mice

4.1 Validation of HSL knockout mice

Firstly, real time PCR experiments revealed that STf and ITf from HSL -/- mice lack a wild type (wt) transcript with HSL mRNA which codes all forms of the protein (Fig. 21A). Secondly, Western blot analyses were performed to determine the expression of mouse HSL in the testis of wt and HSL-/- mice (Fig. 21B). Epididymal fat was used as control. An antibody directed against all forms of HSL recognized multiple protein bands between 25 to 150 kDa in fat, STf and ITf of wt mice (Fig. 21B). The 90kDa band, which corresponds to the 88 kDa band in human and to the 84 kDa band in rat (Langin et al., 1993), was detected in the testicular fat pad, STf and ITf in the wt mice but not in the HSL-/- mice, indicating that the 90kDa band is the HSL immunoreactive band. Although the 120kDa band was detected in the wt ITf and STf and not in the fat pad, this decreased band in the HSL-/- mice was still detectable. Thus, the 120kDa band was not considered as HSL immunoreactive band. In addition, the 120kDa protein, named HSL_{tes} (Blaise et al., 2001), is encoded by the 3.9kb HSL mRNA in rodent (Holst et al., 1996) and was reported to mainly be expressed in haploid germ cells (Osuga et al., 2000). Therefore, our studies on

HSL protein expression in STf and ITf will not focus on the 120kDa protein, while the 90kDa band has been considered in the Western blot analyses.

4.2 HMG-CoA reductase, ACAT-1 and ACAT-2 in HSL knockout mice

4.2.1 HMG-CoA reductase mRNA levels and enzymatic activity

4.2.1.1 ITf

To determine whether HSL deficiency changes the expression of HMG-CoA reductase, the essential enzyme in the cholesterol biosynthesis pathway, mRNA levels of the enzyme were measured in ITf of the wilde type (wt) and HSL deficient mice. HMG-CoA reductase mRNA levels mice significantly decreased by 30% in HSL-/- compared to wt mice ITf (Fig. 22A).

4.2.1.2 STf

The down-regulation of HMG-CoA reductase mRNA expression in HSL-/- mice was also detected in STf (Fig. 22B). HMG-CoA reductase mRNA levels decreased significantly by 57% in HSL-/- compared to wt mice. Furthermore, [^{14}C]- mevalonolactone product was measured in both wt and -/- mice STf microsomes to evaluate the enzymatic activity of HMG-CoA reducase. HMG-CoA reductase activity in the HSL-/- mice was dramatically reduced with respect to wt mice (Fig. 22C).

4.2.2 ACAT-1 and ACAT-2 mRNA levels and the enzymatic activity

In order to elucidate whether knocking out the HSL gene cause the changes of cholesterol esterification, two isoenzymes involved in this process were analyzed; specifically ACAT-1 and ACAT-2 mRNA expression and enzymatic activities were measured in wt and HSL-/- mouse ITf and STf.

4.2.2.1 ITf

HSL deficient mice down regulated ACAT-1 and ACAT-2 mRNA expression (Fig. 23A) and the decrease was statistically significant.

4.2.2.2 STf

Contrary to the mRNA expression of ACAT isoforms in ITf, ACAT-1 and ACAT-2 mRNA levels significantly increased in HSL-/- mice by 1.5-fold and 5.2-fold compared to wt mice, respectively (Fig. 23B). The enzymatic activities of ACAT-1 and ACAT-2 increased by 25% and by 200% respectively when the HSL gene was knockout. The enzymatic activity of ACAT-1 averaged 1150.00 CPMB/200 μg protein and that of ACAT-2 averaged 1276.00 CPMB/200 μg protein in HSL-/- mice STf (Fig. 23C).

5. HMG-CoA reductase, HSL, ACAT-1 and ACAT-2 in SR-BI and CD36 knockout mice

SR-BI and CD36 are selective cholesterol transporter genes. SR-BI and CD36 knockout mice were used as animal models in which SR-BI- or CD36-mediated cholesterol influx or efflux was blocked. Real time PCR experiments revealed that STf and ITf from SR-BI -/- mice or CD36-/- mice lack the wild type (wt) transcript with SR-BI or CD36 mRNA expression (data not shown).

5.1 HMG-CoA reductase mRNA levels and enzymatic activity in SR-BI knockout mice and in CD36 knockout mice.

5.1.1 SR-BI knockout mice

5.1.1.1 ITf

To determine the changes of HMG-CoA reductase if disrupting SR-BI-mediated flux of free cholesterol and HDL, the mRNA expression of the enzyme was measured in SR-BI wt and -/- mice ITf. HMG-CoA reductase mRNA levels were decreased by 44% in SR-BI-/- mice compared with wt mice (Fig. 24A).

5.1.1.2 STf

HMG-CoA reductase mRNA levels were 45% lower in SR-BI-/- compared to wt mice (Fig. 24B). The enzymatic activity of HMG-CoA reductase was also decreased in the SR-BI -/- mice STf (Fig. 24C). The enzymatic activity of HMG-CoA reductase averaged

3.19×10^{-7} mol/min/μg protein for SR-BI-/- mice and 6.94×10^{-7} mol/min/μg protein for wt mice. However, the decrease of HMG-CoA reductase activity was not significant.

5.1.2 CD36 knockout mice

To determine whether genetically blocking CD36, another scavenger receptor responsible for the uptake of oxidized LDL (oxLDL), causes changes in HMG-CoA reductase, the mRNA expression and the activity of the enzyme were measured in CD36 wt and knockout mouse testicular fractions.

5.1.2.1 ITf

In CD36-/- mice ITf, HMG CoA reductase mRNA levels were significantly decreased (Fig. 24D), and the down-regulation was decreased by 64% compared to wt mice ITf.

5.1.2.2 STf

HMG-CoA reductase mRNA levels were significantly decreased by 84% in CD36-/- mice STf compared to wt mice (Fig. 24E). HMG-CoA reductase enzymatic activity also tended to decrease in the CD36-/- mice STf, the decrease was not statistically significant (Fig. 24 F). The enzymatic activity averaged from 3.5550e-7 ± 1.5750e-7 mol/min/μg protein for wt mice to 1.3550e-7 ± 5.9500e-8 mol/min/μg protein for CD36-/- mice.

5.2 HSL mRNA levels and enzymatic activity in SR-BI knockout and in CD36 knockout mice

5.2.1 SR-BI knockout mice

To determine the changes of HSL if knocking out the SR-BI gene, the major enzyme for hydrolyzing cholesteryl esters, the mRNA expression and enzymatic activity of the enzyme were measured in wt and SR-BI wt and knockout mouse ITf.

5.2.1.1 ITf

After knocking out the SR-BI gene, the mRNA levels of HSL were significantly increased compared to those mRNA levels in the wt mice (Fig. 25A).

5.2.1.2 STf

Similarly to what we found in ITf, the mRNA levels of the enzyme were significantly increased in SR-BI-/- mouse STf, reaching 2.4-fold the value recorded in wt mouse STf (Fig. 25B). Coincidently with the increase in the mRNA expression, HSL activity was 18.14 nM/min/μg protein for SR-BI -/- mice which represents a 70% increase when compared to the activity in SR-BI wt mice (10.69 nM/min/μg protein). However, the increase was not statiscally significant.

5.2.2 CD36 knockout mice

To determine the changes of HSL if genetically blocking CD36, the mRNA expression and enzymatic activity of the enzyme were measured in CD36 wt and -/-mouse ITf.

5.2.2.1 ITf

In CD36 deficient mouse ITf, HSL mRNA levels were significantly increased compared to wt mice ITf (Fig. 25D).

5.2.2.2 STf

However, HSL mRNA levels in STf were decreased by 30% in CD36-/- mice compared to wt mice (Fig. 25E). The discrepancy of transcriptional regulation of HSL between ITf and STf show a distinct feedback mechanism in each compartment following genetically induced CD36 deficiency. Consistent with the slight reduction of mRNA levels in STf, the HSL activity was reduced to 13.23 nM/min/μg protein in CD36-/- mice, which is 73% of the value recorded in wt mice (Fig. 25F).

5.3 ACAT-1 and ACAT-2 mRNA levels and enzymatic activity in SR-BI knockout mice and in CD36 knockout mice

5.3.1 SR-BI knockout mice

To evaluate the impact of the disruption of SR-BI gene on ACAT-1 and ACAT-2, the important enzymes in the esterification of free cholesterol, the mRNA expression and enzymatic activity of the two isoforms were measured individually in SR-BI wt and -/- mice.

5.3.1.1 ITf

SR-BI deficient mice significantly down regulated ACAT-1 and ACAT-2 (Fig. 26A). The mRNA levels of ACAT-1 averaged 0.62 in SR-BI-/- mice compared to wt (1 fold). On the other hand, ACAT-2 mRNA levels were 0.65 in SR-BI-/- mice compared to wt (1 fold).

5.3.1.2 STf

SR-BI deficient mice significantly down regulated ACAT-1 and ACAT-2 mRNA expression. The mRNA levels of ACAT-1 and ACAT-2 decreased by 41% and 51% in SR-BI-/- compared to wt mice, respectively. ACAT-1 activity is correlated with its mRNA expression and decreased from 807.00 CPMB/200 μg protein for SR-BI-/- mice to 341.00 CPMB/200 μg protein for wt mice (Fig. 26C). However, ACAT-2 activity showed no

significant differences in SR-BI-/- compared to wt mice (Fig. 26C), suggesting that ACAT-2 enzymatic activity may not be regulated at the transcriptional levels.

5.3.2 CD36 knockout mice

To evaluate the effect on ACAT-1 and ACAT-2 if disrupting of CD36 gene, the mRNA expression and enzymatic activity of the isoforms of the enzyme were measured individually in CD36 wt and -/- mice.

5.3.2.1 ITf

Both ACAT-1 and ACAT-2 mRNA levels in CD36 knockout mice were significantly reduced, reaching half of the value recorded in wild type STf (Fig. 26D).

5.3.2.2 STf

In CD36 knockout mice STf however, there were no significant differences in ACAT-1 mRNA levels and enzymatic activity, indicating that ACAT-1 may not be affected by knocking out the CD36 gene (Fig. 26E and F). On the other hand, ACAT-2 mRNA levels were significantly decreased by 2.5-fold in CD36-/- mice. The proportional decrease of ACAT-2 activity is coincident with the diminution of mRNA expression in CD36-/- mice and reached to 257 CPMB/200 μg protein (Fig. 26E and F).

Figure 1. Calendar of the germ cell population in mink testis.

The variation of cellular composition of the seminiferous epithelium during the annual reproductive cycle of adult mink is shown in this figure. The figure depicts the oldest generations of germ cells found in the seminiferous epithelium during the last week of every month throughout the twelve months of the year. The 12-month reproductive cycle of adult mink is divided into two spermatogenic phases: active and inactive. The active phase is characterized by an increase in the mitotic and meiotic activities leading to the production of more germ cells at various degrees of development. The inactive phase is characterized by a decrease in the mitotic and meiotic activities, spermatogenic arrest and fewer germ cells. A=type A spermatogonia; B=type B spermatogonia; PL=pre-leptotene spermatocyte; P=pachytene spermatocyte; 7=step 7 spermatid; 19=step 19 spermatid (taken from Pelletier 1986).

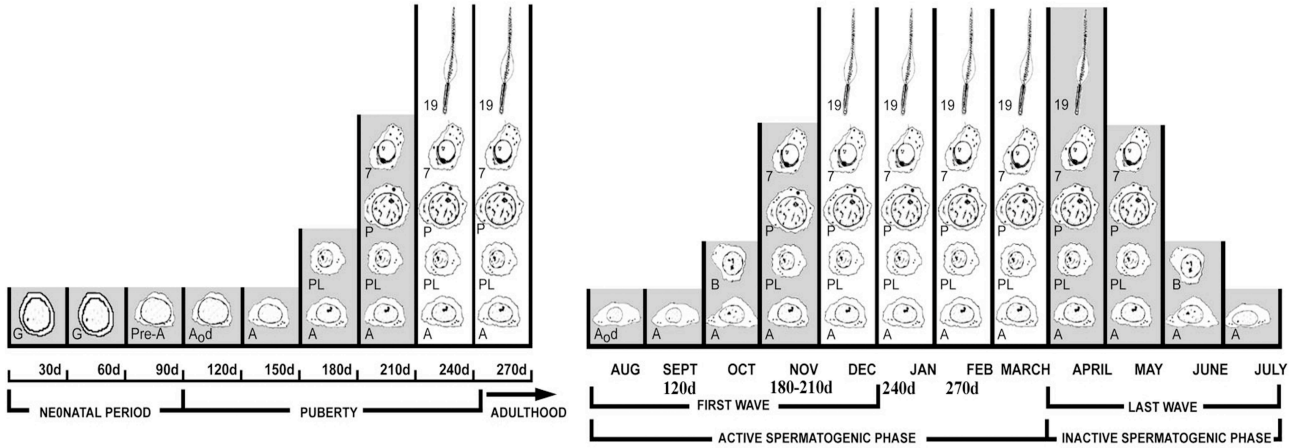

Figure 1 Calendar of the germ cell poplulation in mink testis

(Pelletier R.-M.,et al. 2009 AM. J. Physiol. Regul. Comp. Physiol.)

Figure 2. HMG-CoA reductase mRNA expression in mink STf during development and the annual reproductive cycle.

A. Total RNA was extracted from mink STf. After the reverse transcription, amplification was carried out with 0.5mM of mink HMG-CoA reductase primers (Table 1). Representative figures show the expression of HMG-CoA reductase mRNA and HPRT-1 mRNA in mink STf. A 105bp single product of HMG-CoA reductase and 93bp HPRT-1 product were detected.

B. All data were normalized to the internal reference HPRT-1 amounts and expressed as an *n-fold* increase relative to normalized calibrator value in each region. The results are representative of experiments done on three different STf sample preparations from three different animals. Data (mean ± SEM) are expressed relative to HMG-CoA reductase mRNA expression at 90 days (1 fold) during development or at August (1 fold) during annual reproductive cycle. The increase from 180 to 210 days (+ $P<0.05$) and from April to May (** $P<0.005$) and the decrease from 240 to 270 days (+ $P<0.05$) and June to July (+ $P<0.05$) were significant. d: days old. Neonatal period: day 90; puberty: 120d, 150d, 180d, 210d and 240d; adulthood 270d; the seasonal cycle: from August to July.

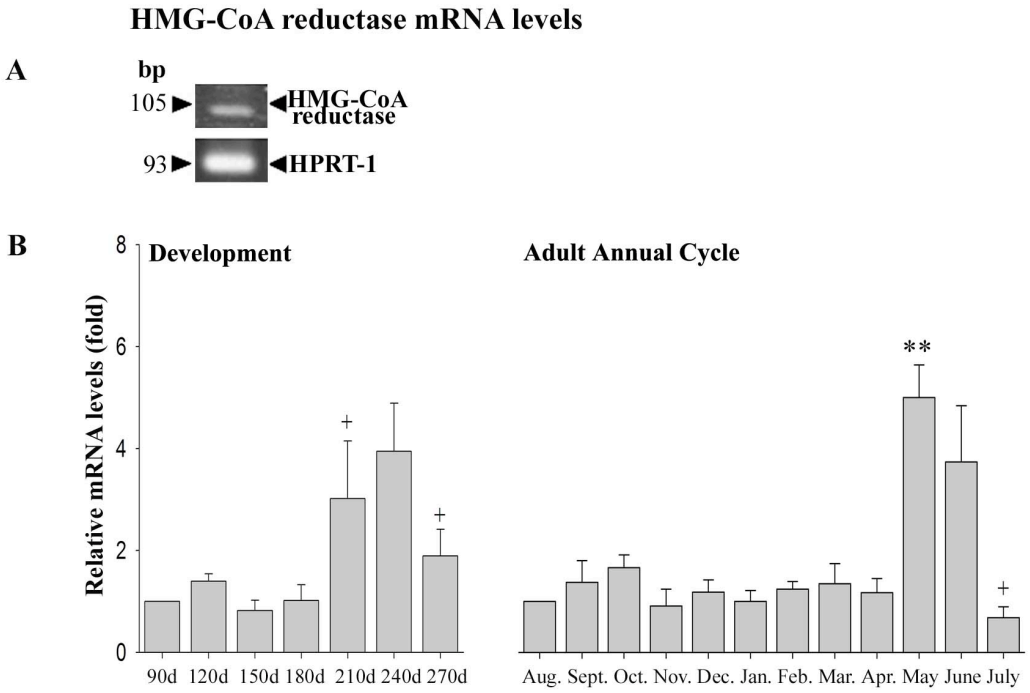

Figure 2 HMG-CoA reductase mRNA levels in mink STf during development and the annual reproductive cycle

Figure 3. HMG-CoA reductase protein expression in mink STf during development and the annual reproductive cycle.

Thirty μg of protein from STf were subjected to 10% of SDS PAGE and Western blot analyses were performed using anti-human HMG-CoA reductase antibody. HMG-CoA reductase peptide was used for the pre-adsorption. Ponseau S staining was performed before blocking to verify equal loading. The immunoreactive bands were scanned and their intensities were quantified using the Scion Image program. Data presented were obtained by quantifying the immunoreactive bands in at least three independent experiments.

A. Following adsorption of anti-HMG-CoA reductase with a HMG-CoA reductase peptide, the 90kDa immunoreactive band was no longer detected, whereas the 53kDa band decreased.

B. Representative Western blots of the 90kDa immunoreactive bands HMG-CoA reductase are shown. The bands were scanned. Data shown are the mean ± SEM and are expressed relative to HMG-CoA reductase protein levels at 90 days during development or at August during the annual reproductive cycle. The increase from 150 to 180 days after birth was significant (+ $P<0.05$) and the levels slightly decrease afterwards. The protein levels tended to decrease after February in the reproductive cycle.

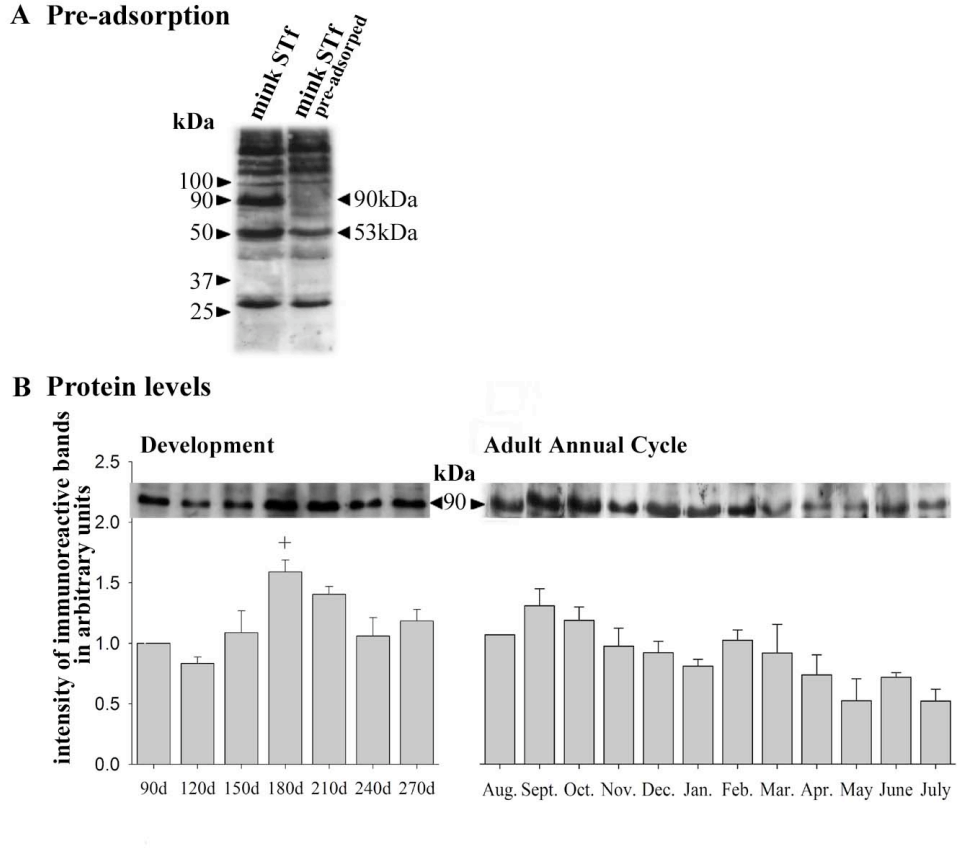

Figure 3 HMG-CoA reductase protein expression in mink STf during development and the annual reproductive cycle

Figure 4. HMG-CoA reductase enzymatic activity in mink STf during development and the annual reproductive cycle.

Two hundred μg of microsomes from STf were used for the enzymatic activity measurements. The final reaction mixture was filtered by silica gel SPE column to separate the polar (^{14}C-HMG-CoA) from non polar (^{14}C-MVL). The radioactivity in the fractions containing the radioactive reaction product (^{14}C-MVL) was evaluated with a β counter. All assays were evaluated in triplicates for three distinct microsome preparations obtained from three different mink for each age group. Data are expressed as mean ± SEM. The activity increased steadily with development except the decrease from 240 to 270 days. The increase from 150 to 180 days was significant (+ P<0.05), and from 210 to 240 days was significant (** P<0.005) and the decrease from 240 to 270 days was also significant (** P<0.005). During the annual reproductive cycle, the HMG-CoA reductase activity significantly increased from November to December (+ P<0.05), December to January (+ P<0.05) and again from January to February (+ P<0.05). The enzymatic activity of HMG-CoA reductase reached the maximal value at 1.21×10^{-6} mol/min/μg protein by February. The activity tended to decrease afterwards.

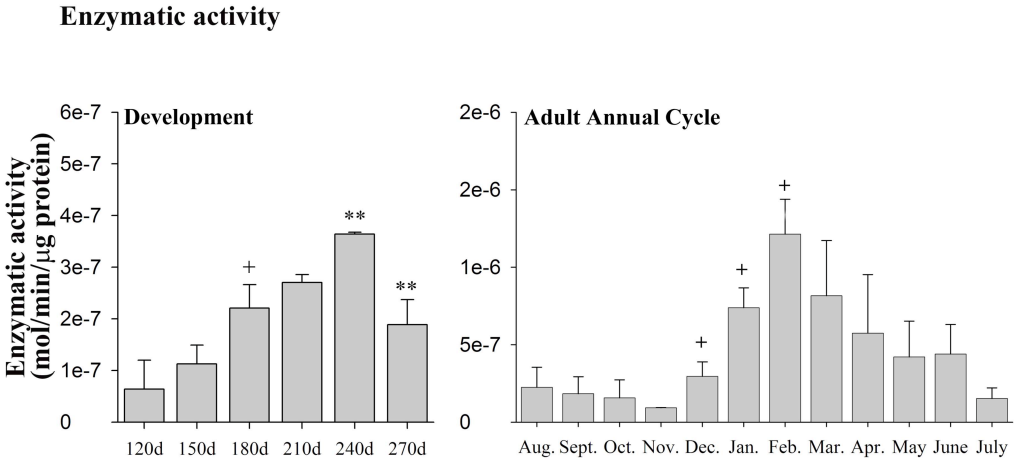

Figure 4 HMG-CoA reductase enzymatic activity in mink STf during development and the annual reproductive cycle

Figure 5. HMG-CoA reductase immunohistochemical localization in mink testis

The macrographs show the distribution of HMG-CoA reductase in mink testes taken from 200 days old and in the adult in March. HMG-CoA reductase localizes to Sertoli cells (thin arrows) and germ cells (wide arrow). HMG-CoA reductase also localized to interstitial cells (white arrow head). The scale bar equals to 50 μm.

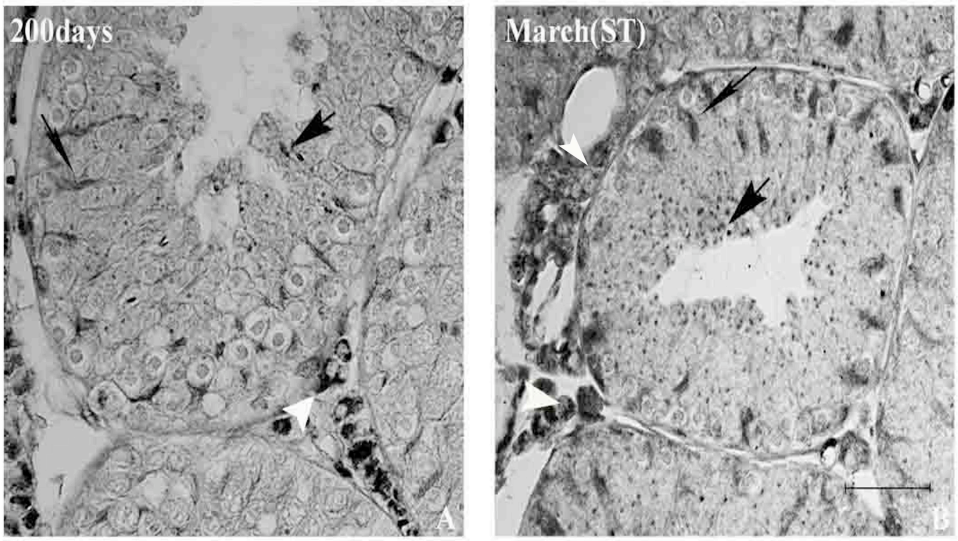

Figure 5 HMG-CoA reductase immunohistochemical localization in mink testis

Figure 6. HMG-CoA reductase mRNA and protein expression in mouse ITf during development.

A. Total RNA was extracted from mouse ITf. After the reverse transcription, amplification was carried out with 0.5mM of mouse HMG-CoA reductase primers (Table 1). mRNA HMG-CoA reductase and HPRT-1 expression in mouse ITf during development is shown in the inset. A 175bp single product of HMG-CoA reductase and a 93bp HPRT-1 product were detected. The relative fold induction was quantified in three independent experiments. Data shown are the mean ± SEM and are expressed relative to mRNA HMG-CoA reductase expression at 14 days (1 fold). A sharp and significant increase occurs from 21 to 28 days after birth (*** $P<0.001$); this is followed by a significant decrease from 28 to 35 days (+ $P<0.05$) and from 35 to 42 days (* $P<0.01$).

B-1. Pre-adsorption of anti-HMG-CoA reductase with a HMG-CoA reductase peptide, the 90kDa immunoreactive band in ITf disappeared.

B-2. Representative Western blots of the 90kDa HMG-CoA reductase and the histogram of the 90kDa HMG-CoA reductase protein expression are shown. Data shown are the mean ± SEM and are expressed relative to HMG-CoA reductase protein expression at 14 days (1 fold). The intensity of the 90kDa band showed no significant changes.

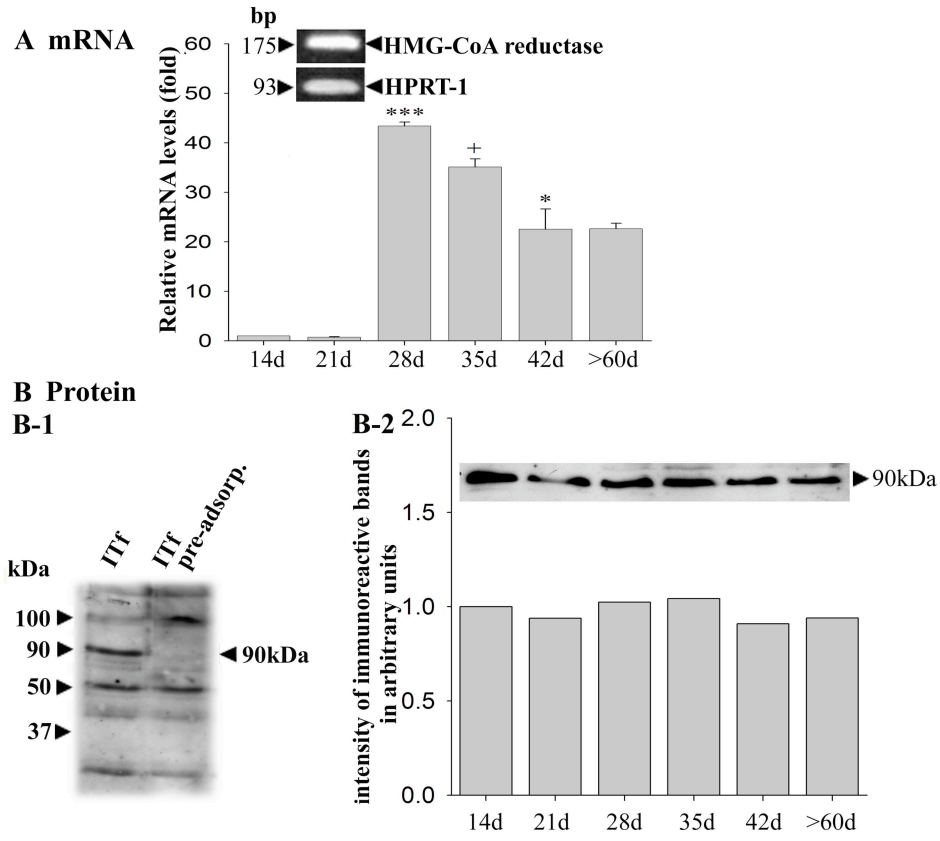

Figure 6 HMG-CoA reductase mRNA and protein expression in mouse ITf during development

Figure 7. HMG-CoA reductase mRNA, protein expression and enzymatic activity in mouse STf during development.

A. A two-step real time PCR performed on total RNA of mouse STf using specific primers for mouse HMG-CoA reductase gene shows the expression of HMG-CoA reductase and of the house keeper gene, HPRT-1. A 175bp single product of HMG-CoA reductase and a 93bp HPRT-1 product were detected. Experiments were done on three different STf sample preparations from testes of three different animals. Data shown are the mean ± SEM and are expressed relative to the mRNA HMG-CoA reductase levels at 14 days (1 fold). HMG-CoA reductase mRNA levels increased from 14 to 42 days. The increases from 14 to 21 days (*** $P<0.001$), from 21 to 28 days (*** $P<0.001$) and from 35 to 42 days (* $P<0.01$) were significant. The decrease from 42 to >60 days (** $P<0.005$) was also significant.

B-1. The 90kDa immunoreactive band in STf disappeared. Other immnunoreactive bands did not show noticeably decrease with the pre-adsorption experiments. Thus, the 90kDa immunoreactive band was the only band to be considered.

B-2. A representative Western blot of the 90kDa immunoreactive band of HMG-CoA reductase in STf is shown. The intensities of the bands from these independent experiments were scanned. Data shown are the mean ± SEM and are expressed relative to HMG-CoA reductase protein expression at 14 days (1 fold). HMG-CoA reductase protein levels increased from 14 to 35 days. The increases from 14 to 21 days (+ $P<0.05$), from 21 to 28 days (+ $P<0.05$) and the decrease from 35 to 42 days

were significant, and then the protein levels dropped to the levels similar to those in the 14 days old mice.

B-3. A representative Western blot showing the 90- and 37kDa immunoreactive bands in Spz. Pre-adsorption of anti-HMG-CoA reductase with a HMG-CoA reductase peptide shows that the 90- and 37kDa immunoreactive bands completely disappeared.

C. Two hundred microgram of microsomes from STf were used to perform HMG-CoA reductase enzymatic activity measurements. The enzymatic activity assay in this figure is representative of three independent experiments. Data are shown as mean ± SEM. The enzymatic activity of HMG-CoA reductase tended to increase from 14 to 42 days but not significantly. The increase from 21 to 28 days was significant (+ $P<0.05$). The activity levels decreased from 42 to >60days but not significantly.

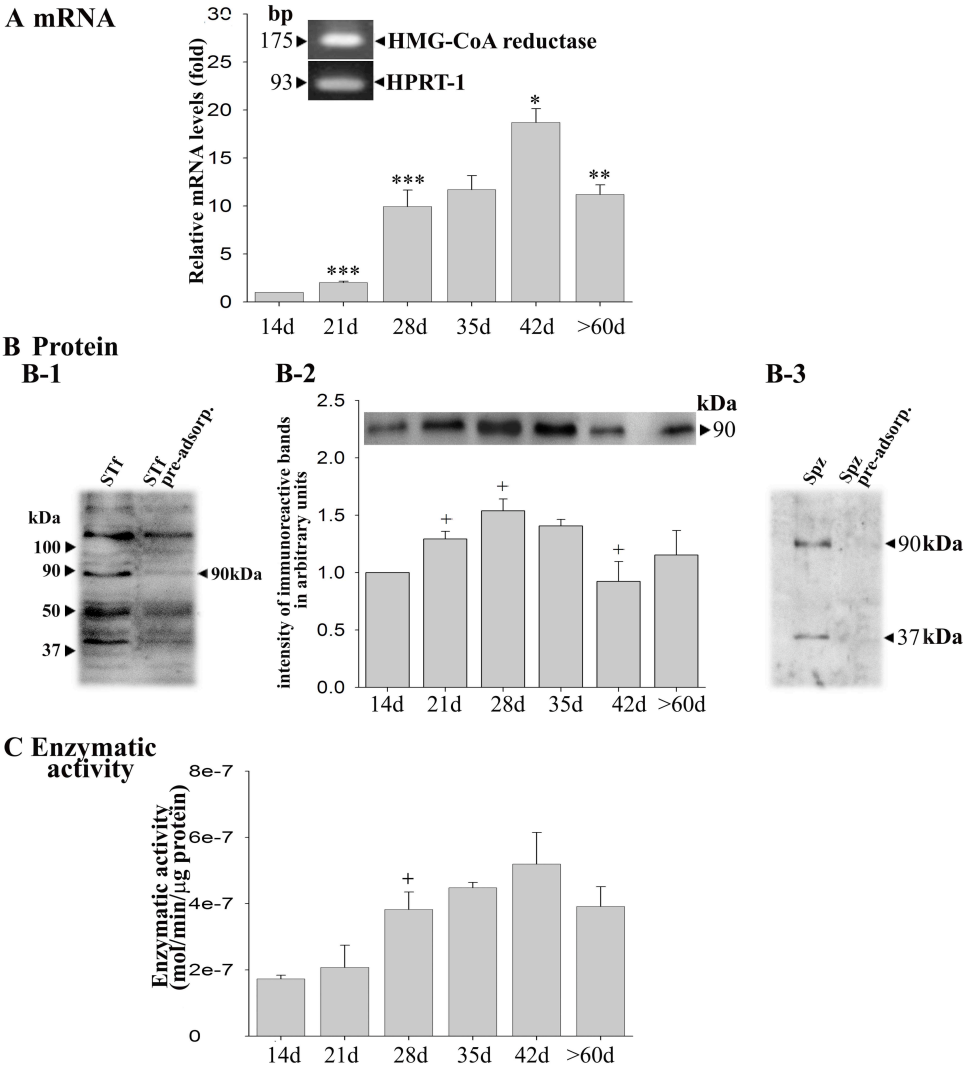

Figure 7 HMG-CoA reductase mRNA, protein expression and enzymatic activity in mouse STf during development

Figure 8. HMG-CoA reductase immunohistochemical localization in mouse testis.

Micrograph in A and B show the distribution of HMG-CoA reductase in the testes taken from adult mice. HMG-CoA reductase localizes to Sertoli cells (thin arrows) and germ cells (wide arrow). HMG-CoA reductase also localized to interstitial cells (white arrow head). The scale bar equals to 50 μm.

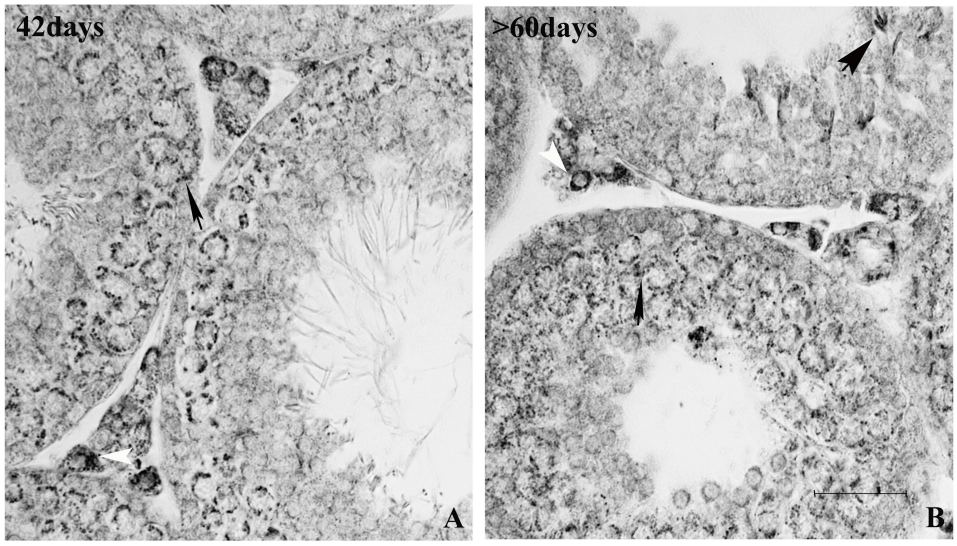

Figure 8 HMG-CoA reductase immunohistochemical localization in mice testis

Figure 9. HSL mRNA expression in mink STf during development and the annual reproductive cycle.

Real time PCR was performed on the same total RNA of mink STf using specific primers for HSL gene. A representative expression of HSL and house-keeper gene HPRT-1 is shown. A 250bp and a 93bp sized single product respectively were detected. Data shown are the mean ± SEM and are expressed relative to the mRNA HSL expression at 90 days (1 fold) or at August (1 fold). The results were obtained from three independent experiments. The increase from 90 to 120 days (** $P<0.005$) and from 240 to 270 days (*** $P<0.001$) were significant.

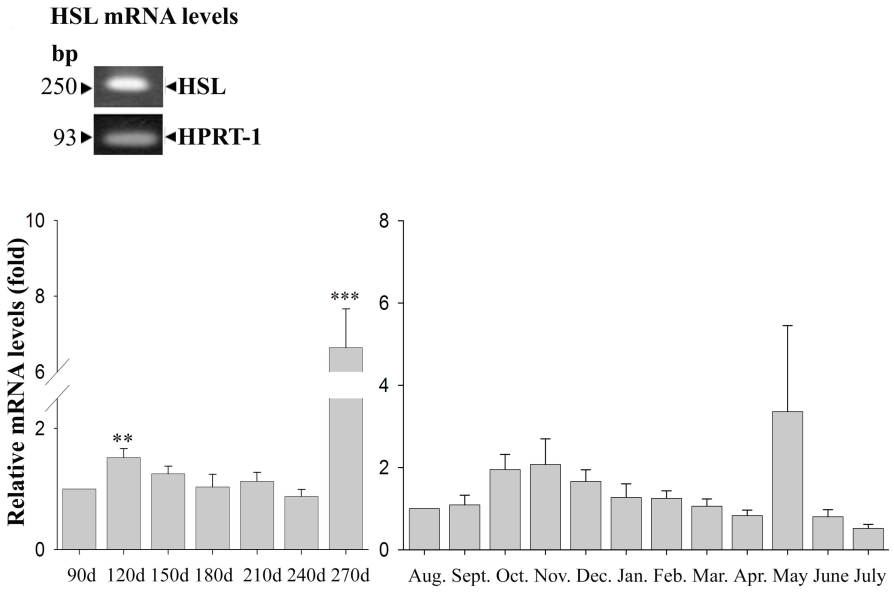

Figure 9 HSL mRNA expression in mink STf during development and the annual reproductive cycle

Figure 10. HSL protein expression in mink STf during development and the annual reproductive cycle.

Twenty μg of proteins from mink STf were subjected to 10% of SDS PAGE and Western blot analyses were performed using human HSL antibody. Two representative Western blot of the 90kDa immunoreactive band HSL are shown. Data shown are the mean ± SEM and are expressed relative to HSL protein expression at 90 days (1 fold) or at August (1 fold). The data present in this figure are representative of three independent experiments. The increase from 150 to 180 days (** $P<0.005$) and from 210 to 240 days (+ $P<0.05$) were significant. During the annual reproductive cycle, the increase from December to January (+ $P<0.05$) and the decrease from March to April (+ $P<0.05$) were significant.

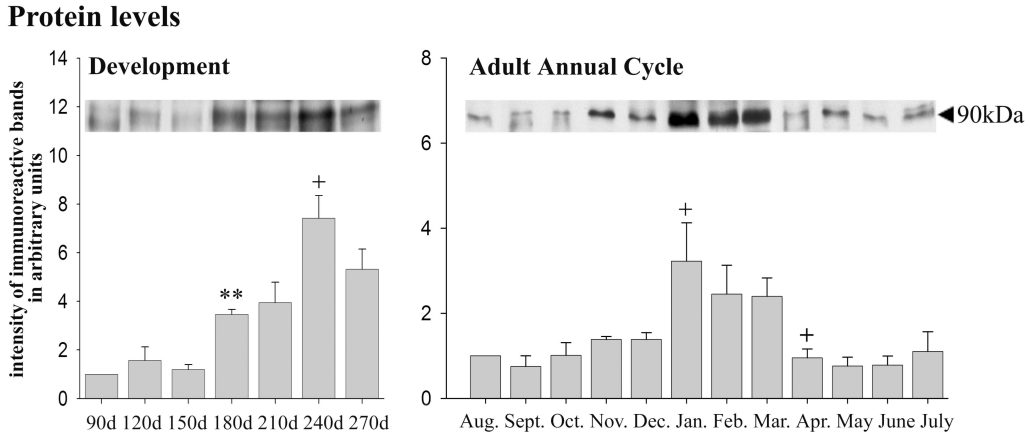

Figure 10 HSL protein expression in mink STf during development and the annual reproductive cycle

Figure 11. HSL enzymatic activity in mink STf during development and the annual reproductive cycle.

Twenty μg of total proteins from STf were subjected to the HSL enzymatic activity measurement. The enzymatic activity is expressed in units; one unit being equivalent to the release of 1μmol of *p*-nitrophenol per minute. All assays were evaluated in triplicates for three distinct protein preparations from three different animals and HSL activity was related to the total protein concentration of the sample. Data are expressed as mean ± SEM. The activity averaged from 30.56 ± 0.52 nM/min/μg protein to 36.20 ± 1.12 nM/min/μg protein during development and from 29.51 ± 3.36 nM/min/μg protein to 40.88 ± 0.08 nM/min/μg protein in the adult. The increase from the 90 to 120 days (+ $P<0.05$) was significant. The noticeable increases occurred from 180 to 210 days during development but it was not significantly different. During the annual reproductive cycle, HSL enzymatic activity increased noticeably from October to November but showed no significance. The enzymatic activity of HSL peaked in February (*** $P<0.001$), and then it decreased significantly from February to March (*** $P<0.001$).

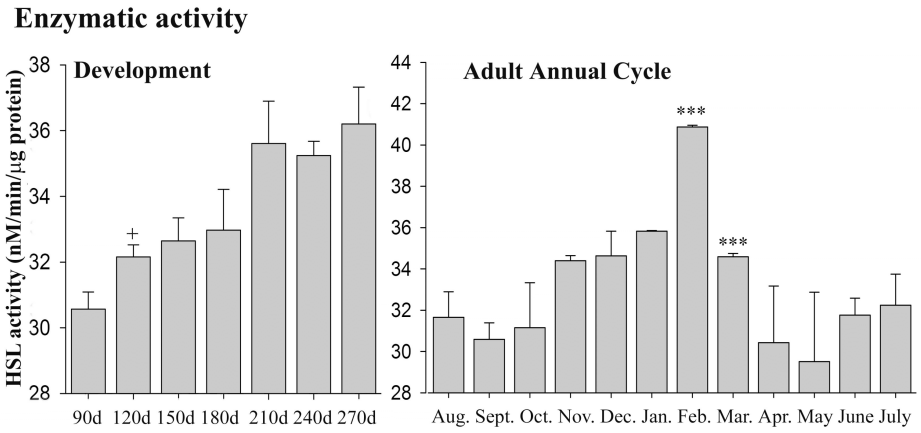

Figure 11 HSL enzymatic activity in mink STf during development and the annual reproductive cycle

Figure 12. HSL mRNA, protein expression in mouse ITf during development.

A. Real time PCR was performed using specific primers for mouse HSL gene. A representative HSL expression in mouse ITf during development is shown. An 113bp sized product was amplified. Quantitative analyses present the data as relative HSL expression ± SEM compared to 14 days (1 fold). The HSL mRNA levels increased significantly from 21 to 28 days (+ $P<0.05$), and then the mRNA levels dropped significantly from days 35 to 42 after birth (+ $P<0.05$).

B. Western blot analyses were performed using anti-mouse HSL antibody. A representative Western blot of 90kDa immunoreactive band is shown. Due to the limited numbers of the tissues, the assay was evaluated in one group of protein preparations. Data shown are expressed relative to HSL protein expression at 14 days (1 fold). The 90kDa HSL protein expression showed a slight increase from 28 to 35 days after birth and levels remained high afterwards.

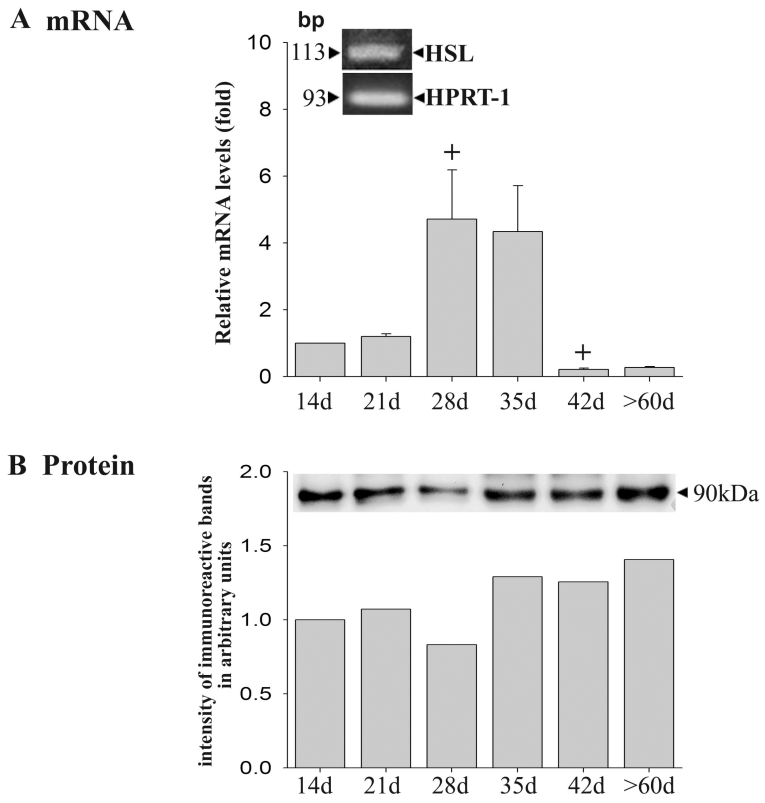

Figure 12 HSL mRNA, protein expression in mouse ITf during development

Figure 13. HSL mRNA, protein expression and enzymatic activity in mouse STf during development.

A. Real time PCR was performed using the specific primers for mouse HSL gene. A 113bp (HSL) and a 93bp (HPRT-1) sized products were amplified. Data shown are the mean ± SEM and are expressed relative to the mRNA HSL expression at 14 days (1 fold). The experiments were done on three different STf sample preparations from the testes of three different mice for each age group. The increase from 14 to 21 days (*** $P<0.001$) and from 21 to 28 days (* $P<0.01$) and from 28 to 35 days (+ $P<0.05$) were statistically significant.

B. Western blot analyses were performed using an anti-mouse HSL antibody. A representative Western blot of 90kDa immunoreactive band is shown. Data shown are the mean ± SEM and are expressed relative to HSL protein expression at 14 days (1 fold). Data were obtained from three independent experiments. The 90kDa HSL protein expression gradually increased throughout development.

C. The enzymatic activity was expressed in units where one unit is equivalent to the release of 1 μmol of p-nitrophenol/min. Data are expressed as mean ± SEM. The data are the results of three independent experiments. The increase from 14 to 21 days (+ $P<0.05$) and the decrease from 42 to adulthood (+ $P<0.05$) were statistically significant.

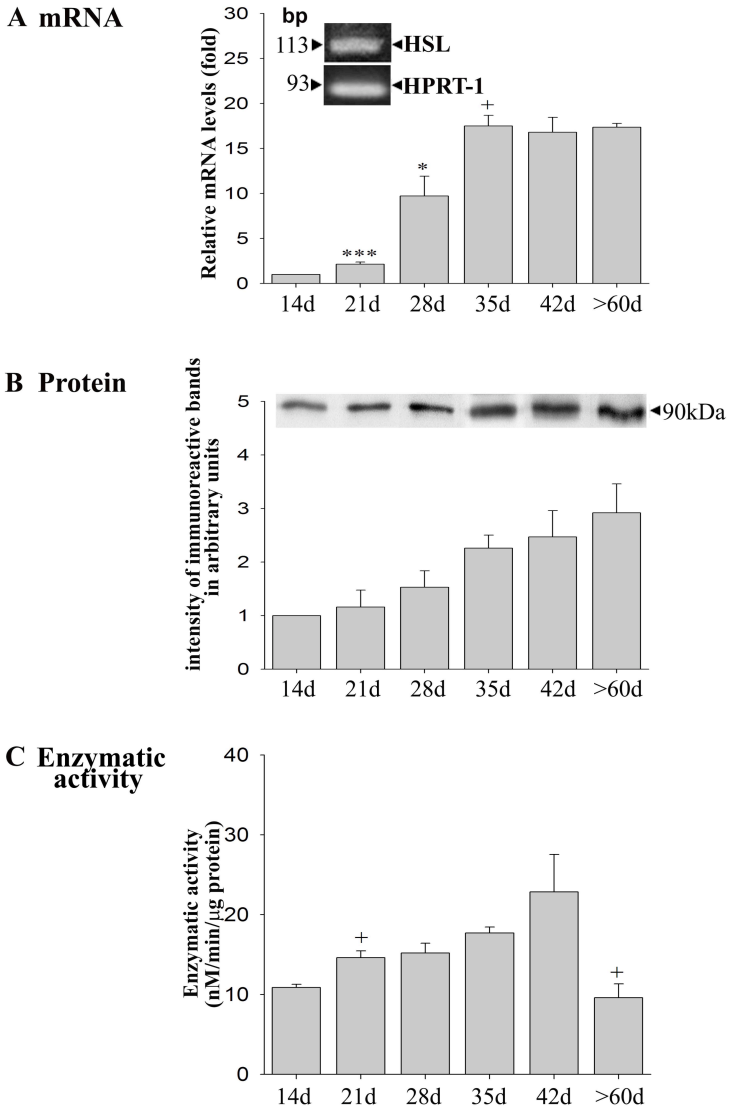

Figure 13 HSL mRNA, protein expression and enzymatic activity in mouse STf during development

Figure 14. ACAT-1 and ACAT-2 mRNA expression in mink STf during development and the annual reproductive cycle.

A. Two-step real time PCR was performed in mink STf using primers for ACAT-1 and ACAT-2 gene respectively. A representative expression of ACAT-1, ACAT-2 mRNA during development and the annual reproductive cycle is shown in the Figure. A 185bp sized single product of ACAT-1, a 70bp sized ACAT-2 product and a 93bp HPRT-1 product were detected.

B. The specificity of ACAT-2 amplicons amplified in real time PCR were evaluated by restriction enzymes, Alu I. Alu I cleaved the recognition site (AG^CT) which was only present in mink ACAT-2 PCR product and released a 20bp and a 50 bp DNA fragments. Amplicons with or without restriction enzymes digestion were visualized by electrophoresis in a 3.5% agarose gel, stained with ethidium bromide and photographed under a UV transilluminator.

C. All data were normalized to the internal reference HPRT-1 amounts and expressed as an *n-fold* increase relative to normalized calibrator value in each region. Data shown are the mean ± SEM and are expressed relative to mRNA ACAT-1 or ACAT-2 at 90 days (1 fold) or at August (1 fold). Results were obtained from experiments done on three different STf samples prepared from three distinct animals per age group. ACAT-1 and ACAT-2 mRNA expression differed during development and the annual reproductive cycle. The increase of ACAT-1 from 90 to 120 days (*** $P<0.001$), from 240 to 270 days (** $P<0.005$), from September to October (+ $P<0.05$) and from April to May (+ $P<0.05$) as well as the decrease from November to December and June to July (+ $P<0.05$) were significant. The increase of

ACAT-2 from 180 to 210 days (+ $P<0.05$) and December to January (+ $P<0.05$) were significant; the decrease of ACAT-2 from 210 to 240 days (+ $P<0.05$) and from June to July (+ $P<0.05$) were also significant.

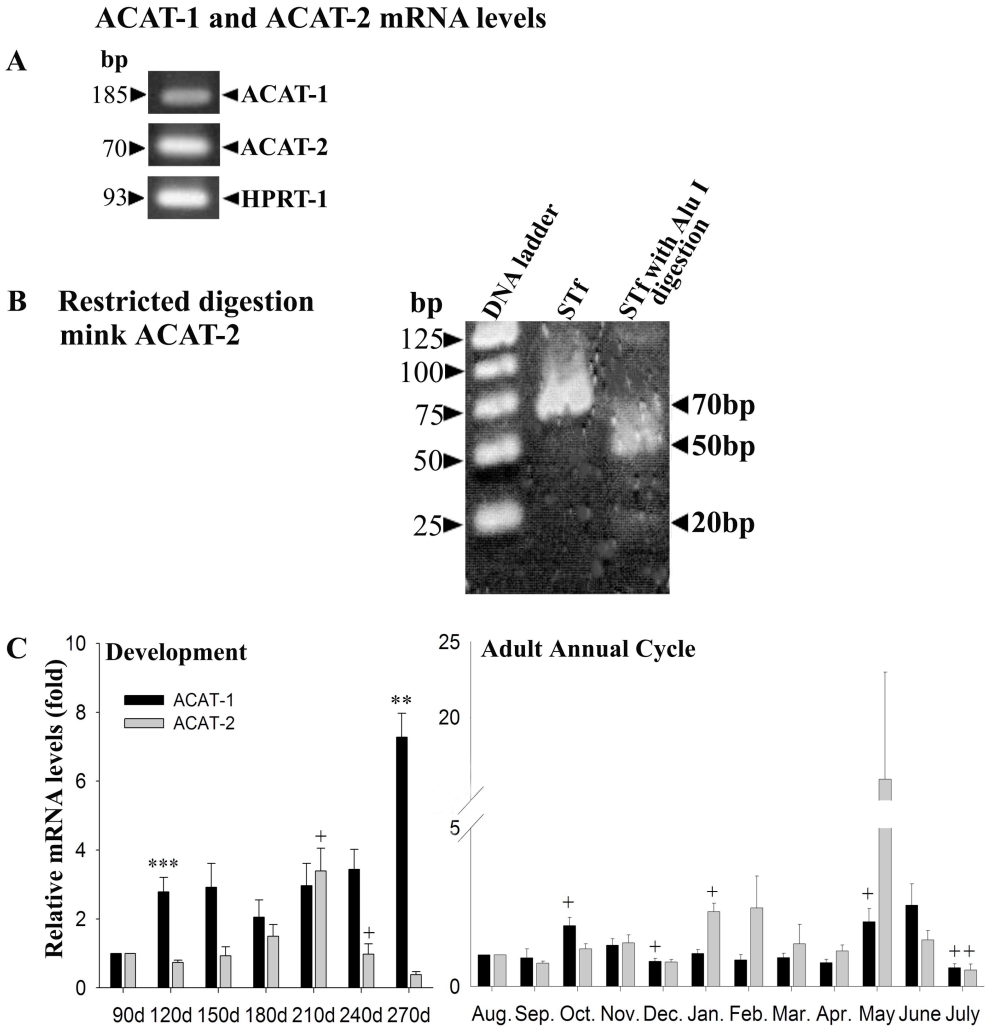

Figure 14 ACAT-1 and ACAT-2 mRNA expression in mink STf during development and the annual reproductive cycle

Figure 15. ACAT-1 and ACAT-2 protein expression in mink STf during development and the annual reproductive cycle.

Representative Western blots of ACAT-1 and ACAT-2 are shown. A 50kDa ACAT-1 and a 46kDa ACAT-2 immunoreactive band were detected. The intensity of the immunoreactive bands was quantified. Data shown are the mean ± SEM and are expressed relative to ACAT-1 or ACAT-2 protein expression at 90 days (1 fold) or at August (1 fold). Results were obtained from experiments done on three different STf sample preparations from three different animals per age group. ACAT-1 and ACAT-2 protein expressionh increased steadily with development. During the reproductive cycle, ACAT-1 tended to increase and to reach maximal values until January, and then to decrease gradually afterwards. However, the variations were not significant. The increase of ACAT-2 from December to January (+ $P<0.05$) and the decrease from March to April (+ $P<0.05$) were significant.

Protein levels

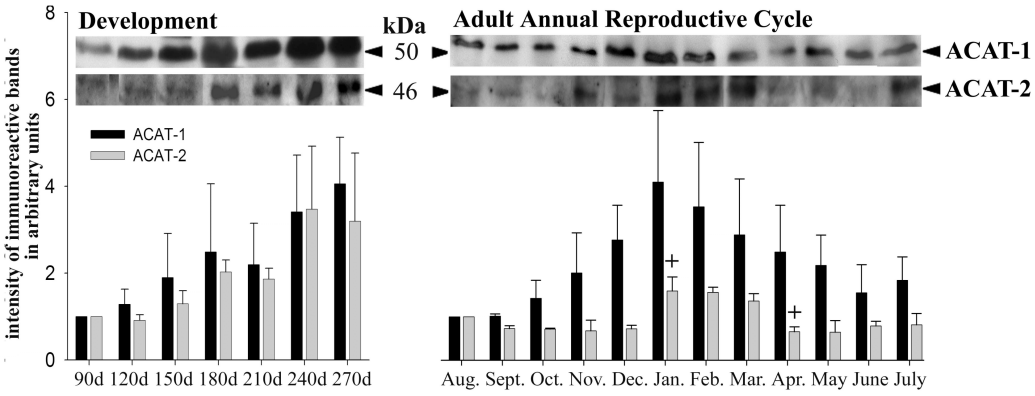

Figure 15 ACAT-1 and ACAT-2 protein expression in mink STf during development and the annual reproductive cycle

Figure 16. ACAT-1 and ACAT-2 enzymatic activity in mink STf during development and the annual reproductive cycle.

A. Dose-dependent inhibition curve (0-1000μM). A sharp decrease of total ACAT enzymatic activity was detected with the addition of 100μM inhibitor, and then total ACAT enzymatic activity decreased again with 200μM or more inhibitor. Thus the100μM inhibitor concentration was found to inhibit the activity of ACAT-1 but not the activity of ACAT-2 and this concentration was used to perform the enzymatic measurements.

B. All assays for ACAT-1 and ACAT-2 enzymatic activities were evaluated in triplicates using three distinct microsome preparations obtained from three distinct animals for each age group. Representative histograms of the enzymatic activities are shown. The enzymatic activities in different group have the same tendency. The enzymatic activity is expressed as CPMB per 200μg protein. The activity of ACAT-1 ranged from 5436.00 CPMB/200μg protein to 958.00 CPMB/200μg protein in the adult. ACAT-1 activity decreased from 180 to 210 days and from December to January but increased from April to May. ACAT-1 activity almost disappeared by 270 days compared to 90 days. On the other hand, the activity of ACAT-2 ranged from 280.00 CPMB/200μg protein to 2643.00 CPMB/200μg protein in the adult. The increase of ACAT-2 from 210 to 240 days and 240 to 270 days and from December to January were noticeable as well as the decrease from March to April.

A Dose-dependent inhibition curve of K-604 in mink STf (January)

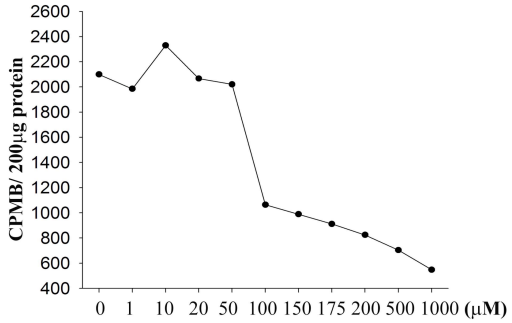

B Enzymatic activity of ACAT-1 and ACAT-2

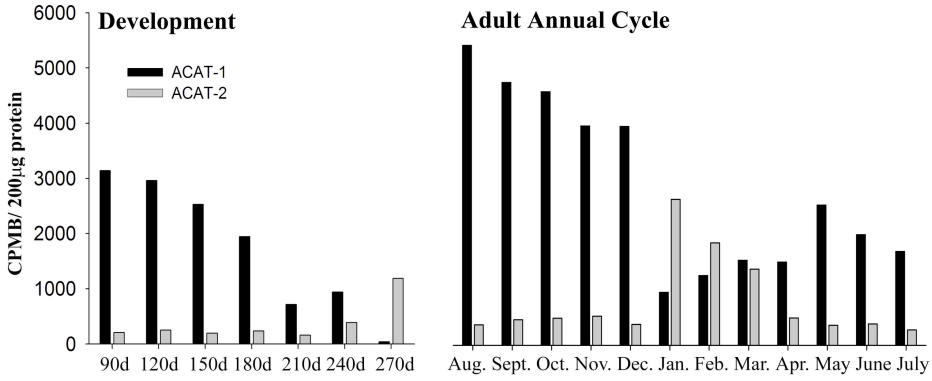

Figure 16 ACAT-1 and ACAT-2 enzymatic activity in mink STf during development and the annual reproductive cycle

Figure 17. ACAT-1 and ACAT-2 immunohistochemical localization in mink testis.

Micrographs show the distribution of ACAT-1 and ACAT-2 in mink testes taken from 150 day-old, 210 day-old mink and from adult mink killed in January and March. ACAT-1 was detected only in germ cell (wide arrow) and some interstitial cells (thin arrows), whereas ACAT-2 was found only in Sertoli cell (white arrowhead) and the endothelial cells of capillaries and interstitial cells (thin arrows). The bar is equal to 50 μm.

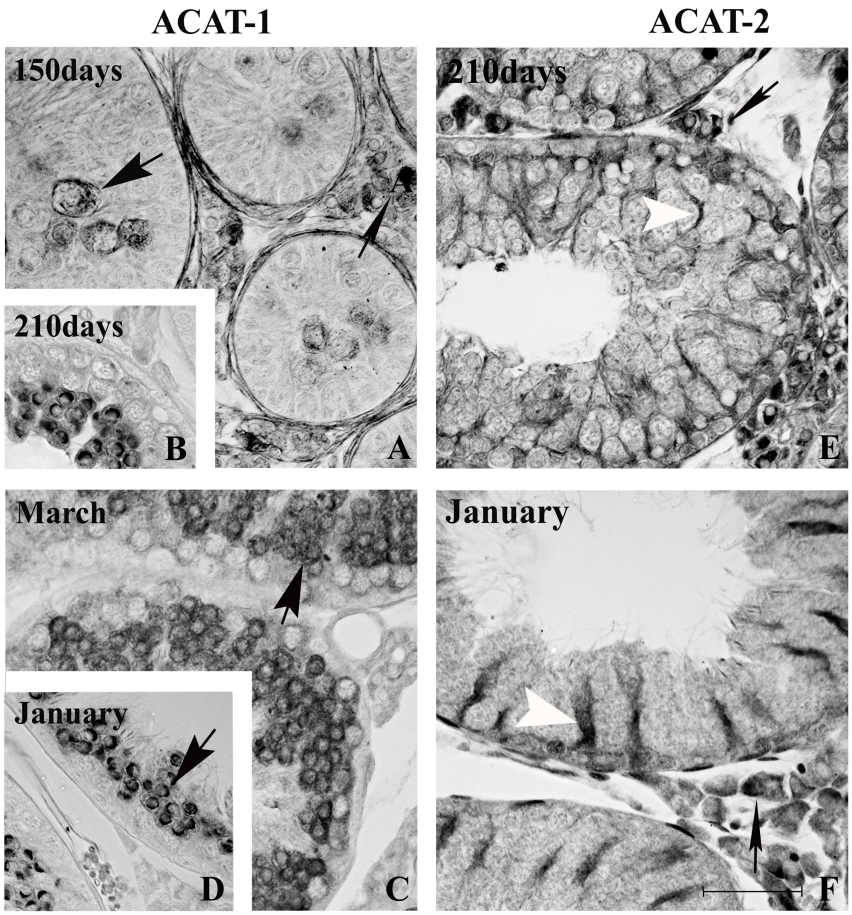

Figure 17 ACAT-1 and ACAT-2 imunohistochemical localization in mink testis

Figure 18. ACAT-1 and ACAT-2 mRNA, protein expression in mouse ITf during development.

A. Real time PCR was performed using specific ACAT-1 and ACAT-2 primers for mouse ACAT-1 and ACAT-2 gene respectively. ACAT-1 and ACAT-2 and HPRT-1 showed a 126bp, a 101bp and a 93bp sized single product. All data were normalized to the internal reference HPRT-1 amounts and expressed as an *n-fold* increase relative to normalized calibrator value in each region. Data shown are the mean ± SEM and are expressed relative to ACAT-1 and ACAT-2 mRNA expression at 14 days (1 fold). The experiments were done on three different ITf sample preparations from three different animals for each age group. The increase of ACAT-1 from 21 to 28 days (+ $P<0.05$) was significant but not that of ACAT-2 mRNA.

B. The specificity of ACAT-2 amplicons amplified in real time PCR were evaluated by restriction enzymes, EcoR II for mouse. EcoR II cut the recognition site (^CCWGG) which was only expressed in mouse ACAT-2 PCR product and released a 49bp, a 42bp and a 10bp DNA fragments. Amplicons with or without restriction enzymes digestion were visualized by electrophoresis in a 3.5% agarose gel, stained with ethidium bromide and photographed under a UV transilluminator.

C. Representative Western blots of the 50kDa ACAT-1 and the 46kDa ACAT-2 immunoreactive bands are shown. The immunoreactive bands were scanned and their intensities were quantified. Data shown are the mean ± SEM and are expressed relative to ACAT-1 or ACAT-2 protein levels at 14 days (1 fold). Experiments were done on three different ITf sample preparations from three different animals for each age group. ACAT-

1 protein levels decreased steadily with development and significantly from 42 to >60 days (+ $P<0.05$). ACAT-2 protein levels were constant.

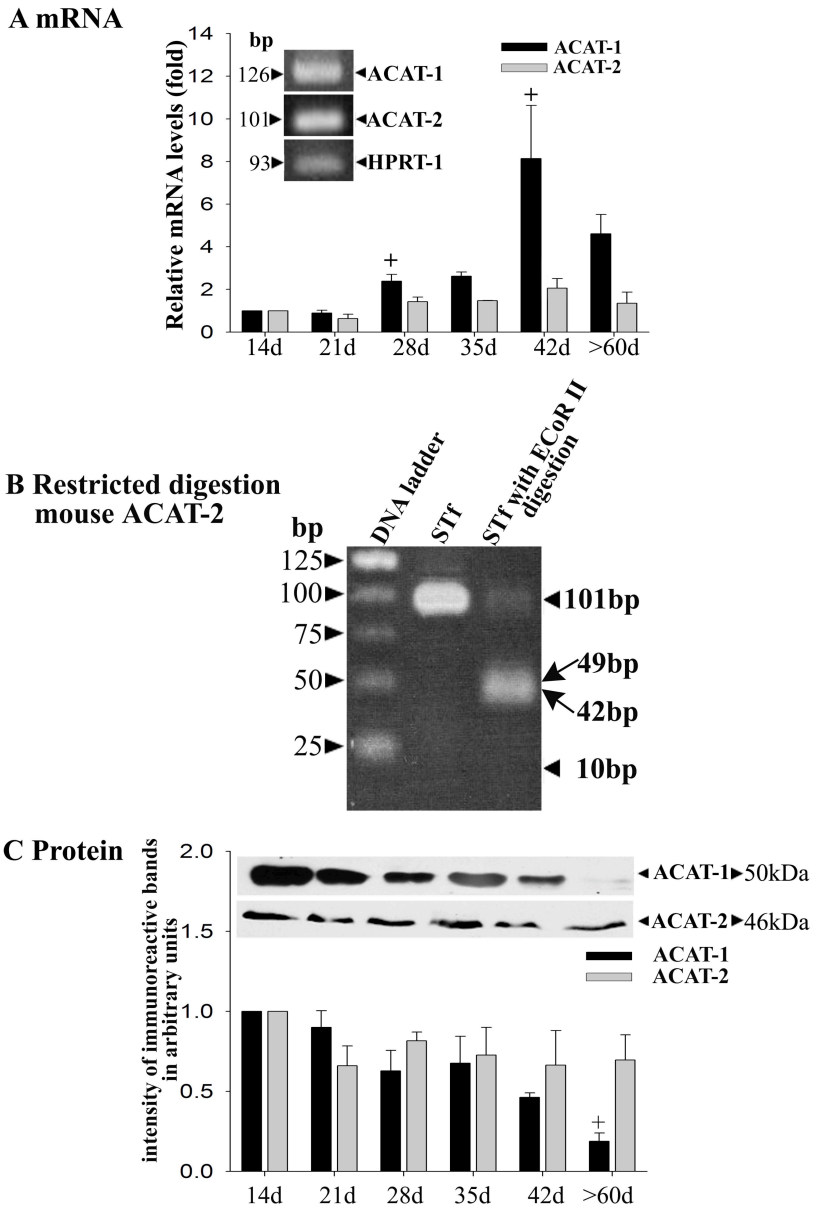

Figure 18 ACAT-1 and ACAT-2 mRNA, protein expression in mouse ITf during development

Figure 19. ACAT-1 and ACAT-2 mRNA, protein expression and enzymatic activity in mouse STf during development.

A. Real time PCR was performed for mouse ACAT-1 and ACAT-2 genes. A 126bp sized single product of ACAT-1 and a 101bp sized ACAT-2 product were detected in the STf. All data were normalized to the internal reference HPRT-1 amounts and expressed as an *n-fold* increase relative to normalized calibrator value in each region. Data shown are the mean ± SEM and are expressed relative to ACAT-1 or ACAT-2 mRNA levels at 14 days (1 fold). The data were obtained from three independent experiments for each age group. ACAT-1 mRNA levels tended to decrease with development but not significantly, whereas ACAT-2 levels significantly increase from 35 to 42 days (+ $P<0.05$) and were kept high in the adult.

B. Representative Western blots results showing that 50kDa ACAT-1 immunoreactive band was present in both the STf and Spz, and that the 46kDa ACAT-2 band was only detected in the STf. The bands were scanned and their intensities quantified. Data shown are the mean ± SEM and are expressed relative to ACAT-1 or ACAT-2 protein levels at 14 days (1 fold). Experiments were done on three different STf sample preparations from three different animals per age group. The ACAT-1 protein expression decreased with the development but not significantly. ACAT-2 protein levels increased significantly from 21 to 28 days (+ $P<0.05$), and the levels remained high until 42 days and then decreased from 42 to >60 days but not significantly.

C. The figure shows the concentration-enzymatic activity inhibition curve established from 0-1000μM K-604. A sharp decrease of total ACAT enzymatic activity was detected

with the addition of 100μM inhibitor (ACAT-1 activity is inhibited), and then total ACAT enzymatic activity decreased again with 200μM or more inhibitor. ACAT-1 and ACAT-2 enzymatic activities were blocked. Thus a 100μM inhibitor concentration was selected.

D. A representative histogram of the ACAT-1 and ACAT-2 enzymatic activities of the three experiments is shown. ACAT-1 activity gradually decreased from 14 to 42 days but increased from 42 to >60 days in contrast to ACAT-2 enzymatic activity which increased steady from 14 to 42days and decreased from 42 to >60 days. ACAT-1 and ACAT-2 activities varied complementarily.

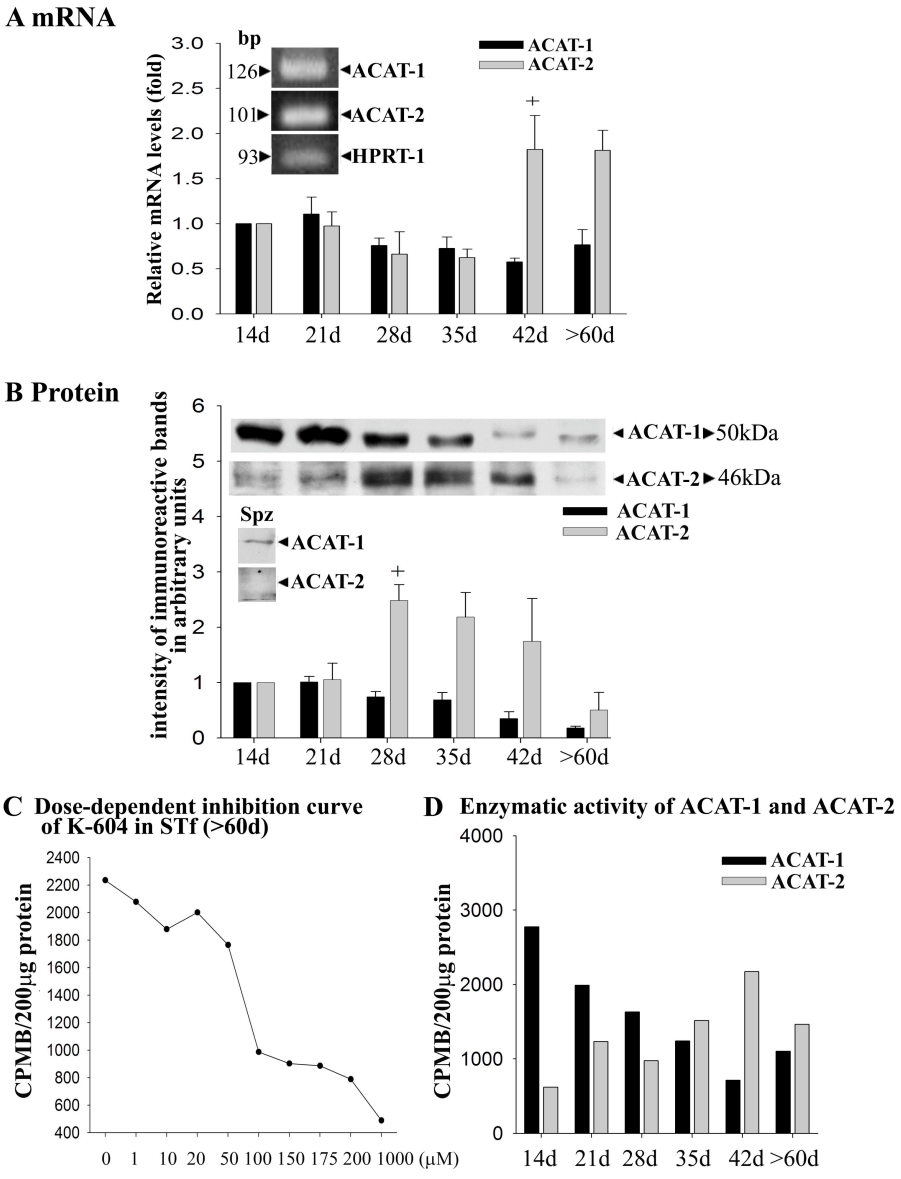

Figure 19 ACAT-1 and ACAT-2 mRNA, protein expression and enzymatic activity in mouse STf during development

Figure 20. ACAT-1 and ACAT-2 immunohistochemical localization in mice testis.

The micrographs show the distribution of ACAT-1 and ACAT-2 in mouse testes taken from 42 day-old and >60 day-old mice. ACAT-1 was detected only in germ cells within the seminiferous tubules (wide arrow), and ACAT-1 was plentiful in the interstitial cells (thin arrows), whereas ACAT-2 was found only in Sertoli cell (white arrowhead) in the tubule. The interstitial cells were not labeled. The bar is equal to 50 μm.

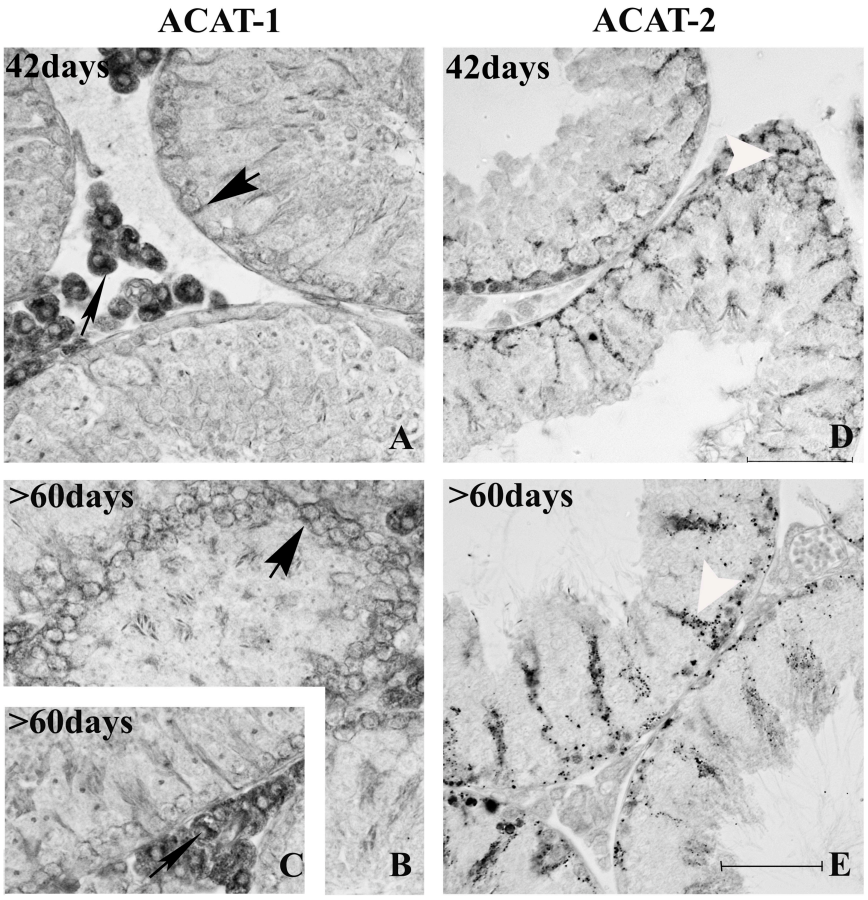

Figure 20 ACAT-1 and ACAT-2 immunohistochemical localization in mouse testis

Figure 21. Validation of HSL-/-mice.

A. A two-step real time PCR was performed on total RNA of HSL knockout mouse ITf and STf using specific primers targeted on HSL exons that existed in both testis and adipose tissue. HSL mRNA expression in fold induction is shown. Data shown are the mean ± SEM in HSL-/- mice and are expressed relative to HSL mRNA expression in wild type (wt) mice. The results were obtained from three independent experiments. The decrease in HSL-/- ITf compared to wt mice ITf (** $P<0.005$) and the one in HSL-/- STf compared to wt mice STf (*** $P<0.001$) were significant. HSL knockout mice lacked a wild type transcript.

B. Western blot analyses were performed in both HSL -/- and wt mice using anti-HSL antibody that recognized all forms of HSL. The testicular fat pad was used as control. The 90kDa band was intense in wt fat pad, less intense in ITf and STf, but was not detected in HSL-/- mice samples. The 120kDa band was only observed in the mice ITf and STf. The intensities were sharply decreased in HSL-/- mice but still detectable.

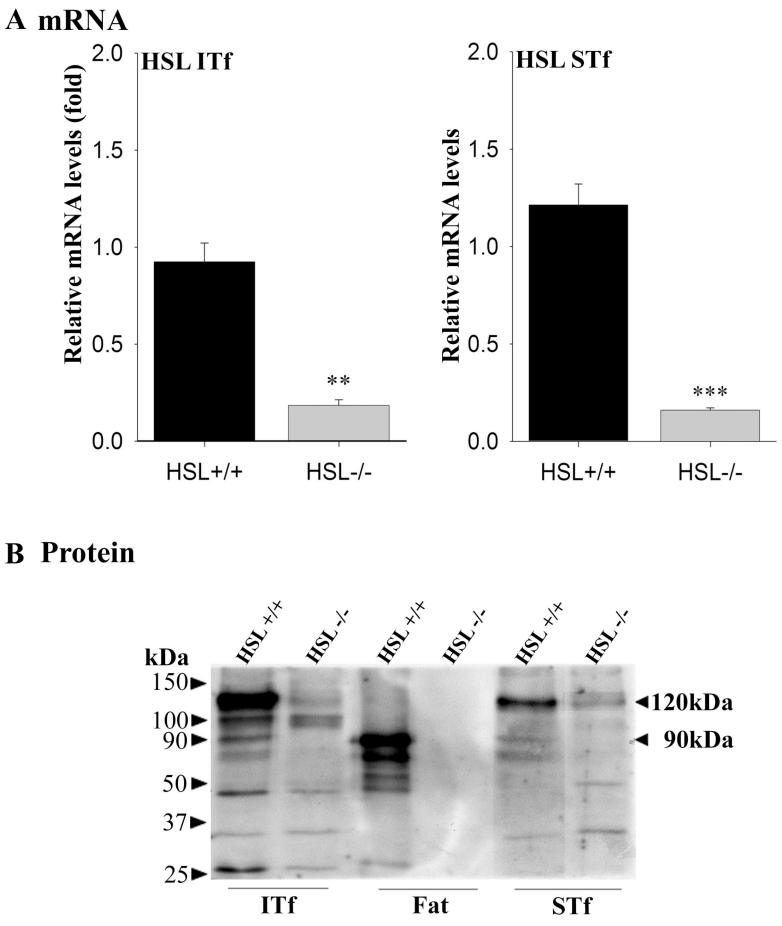

Figure 21 Validation of HSL-/- mice

Figure 22. HMG-CoA reductase mRNA expression and enzymatic activity in HSL-/- mice.

A and B. mRNA expression:

Real time PCR was performed on total RNA of HSL-/- mice ITf **(A)** and STf **(B)** using primers on HMG CoA reductase gene. HMG CoA reductase mRNA expression in fold induction is shown and the data are expressed as relative HMG- CoA reductase expression ± SEM. The data were obtained from three independent experiments. The decrease of HMG CoA reductase mRNA levels in HSL-/- ITf (** P<0.005) **(A)** and STf (** P<0.005) **(B)** compared to wt mice were significant.

C. Enzymatic activity:

Two hundred micrograms of total proteins from wt and HSL-/- mice STf were subjected to enzymatic activity measurements. A representative histogram of the HMG CoA reductase activity is shown. The HSL activity in the knockout animal was significantly reduced.

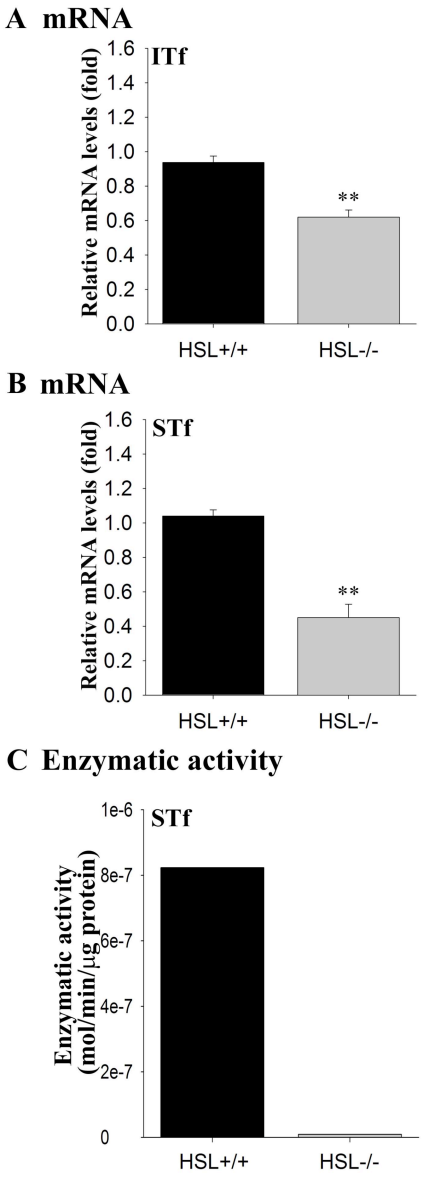

Figure 22 HMG-CoA reductase mRNA expression and enzymatic activity in HSL-/- mice

Figure 23. ACAT-1 and ACAT-2 mRNA expression and enzymatic activity in HSL-/- mice.

A and B. mRNA expression:

Real time PCR was performed on HSL-/- mice ITf **(A)** and STf **(B)** using primers on ACAT-1 and ACAT-2 genes. ACAT-1 and ACAT-2 mRNA expression in fold induction are shown, respectively. Data shown are the mean ± SEM in HSL-/- mice and are expressed relative to ACAT-1 and ACAT-2 mRNA expression in wt mice. All assays were evaluated in three independent experiments. ACAT-1 and ACAT-2 mRNA levels decreased in HSL-/- mice ITf (+ $P<0.05$) **(A)**. In contrast, the increase of ACAT-1 in HSL-/- mice STf (+ $P<0.05$) **(B)** compared to wt mice STf and the increase of ACAT-2 in HSL-/- STf (*** $P<0.001$) **(B)** compared to wt mice STf were significant.

C. Enzymatic activity:

A representative histogram of ACAT-1 and ACAT-2 enzymatic activities in HSL-/- mice STf is shown. ACAT-1 and ACAT-2 enzymatic activities were both increased in HSL-/- mice STf. The increasing of ACAT-2 activity was higher than ACAT-1 in HSL-/- mice STf.

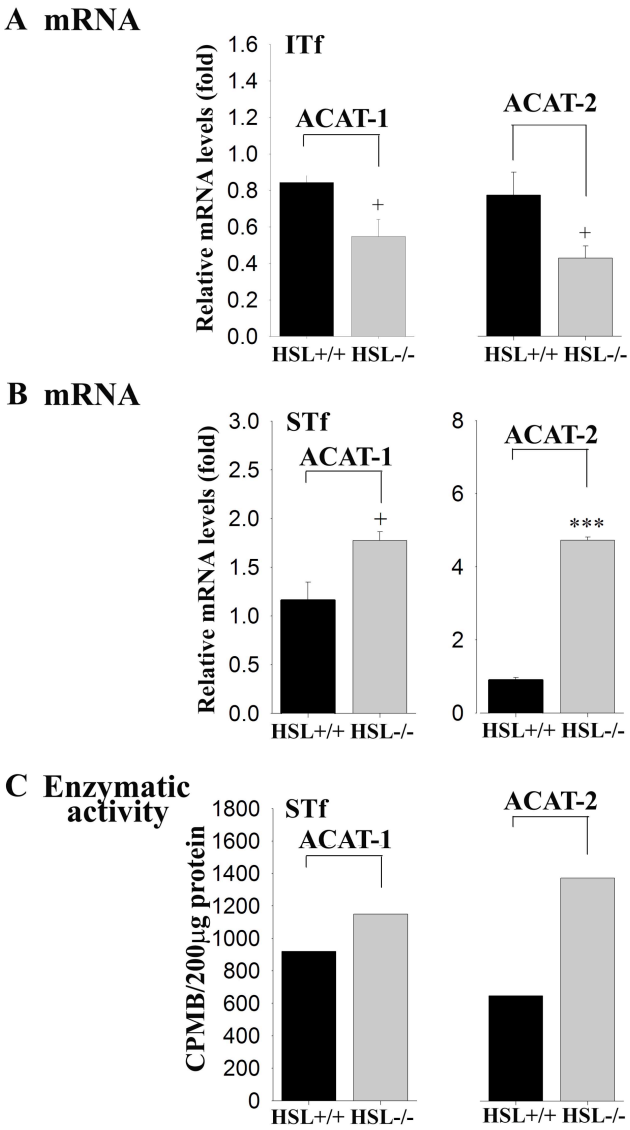

Figure 23 ACAT-1 and ACAT-2 mRNA expression and enzymatic activity in HSL-/- mice

Figure 24. HMG-CoA reductase mRNA expression and enzymatic activity in SR-BI and CD36 knockout mice.

A and B. mRNA expression:

Real time PCR was performed on total RNA of SR-BI knockout mice ITf **(A)** and STf **(B)** using primers on HMG CoA reductase gene. HMG CoA reductase mRNA expression in fold induction is shown. Data are expressed as relative HMG-CoA reductase expression ± S.E.M. in SRBI-/- compared to wt mice (1 fold). The fold induction of three independent experiments is shown. The decrease of HMG-CoA reductase in SR-BI-/- mice ITf (*** $P<0.001$) **(A)** and STf (* $P<0.01$) was significant **(B)**.

C. Enzymatic activity:

Two hundred micrograms of total proteins from mice STf were subjected to enzymatic activity measurements. Data are expressed as relative HMG-CoA reductase activity ± S.E.M. in SR-BI-/- compared to wt mice. HMG-CoA reductase enzymatic activity was reduced but not significantly in SR-BI knockout mice STf.

D and E. mRNA expression:

Real time PCR was performed on total RNA of CD36 knockout mice ITf **(D)** and STf **(E)** using primers on HMG-CoA reductase gene. HMG-CoA reductase mRNA expression in fold induction is shown. Data are expressed as relative HMG-CoA reductase expression ± SEM in CD36-/- compared to wt mice (1 fold). The fold induction of three independent experiments is present. The diminution of HMG-CoA reductase in CD36-/- ITf (*** $P<0.001$) **(D)** and STf (*** $P<0.001$) was significant **(E)**.

F. Enzymatic activity:

Two hundred micrograms of total proteins from mice STf were subjected to enzymatic activity measurements. Data are expressed as relative HMG-CoA reductase activity ± S.E.M. in CD36-/- compared to wt mice. HMG-CoA reductase enzymatic activity was reduced in CD36 knockout mice STf. The decrease showed no significance.

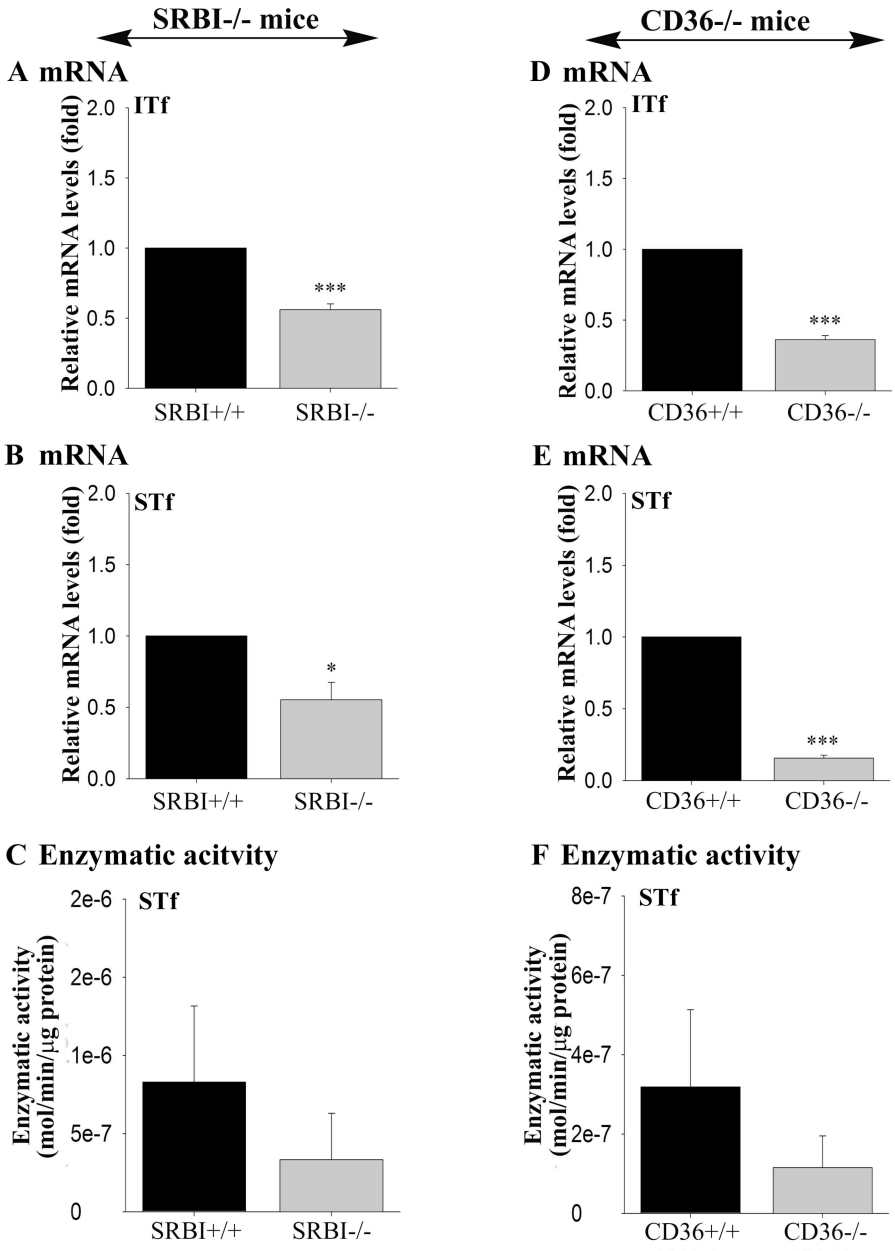

Figure 24 HMG-CoA reductase mRNA expression and enzymatic activity in SR-BI and CD36 knockout mice

Figure 25. HSL mRNA expression and enzymatic activity in SR-BI and CD36 knockout mice.

A and B. mRNA expression:

Real time PCR was performed on total RNA of SR-BI-/- mouse ITf **(A)** and STf **(B)** using primers on HSL gene. HSL mRNA is expressed in fold induction. Data are expressed as relative HSL expression ± SEM in SR-BI-/- compared to wt mice (1 fold). The data are representative of three independent experiments. The increase of HSL in SR-BI-/- (*** $P<0.001$) compared to wt mice ITf **(A)** and the increase in the enzyme in SR-BI-/- (** $P<0.005$) compared to wt mice STf **(B)** are significant.

C. Enzymatic activity:

Twenty micrograms of total proteins from SRBI knockout mice STf were subjected to the enzymatic activity measurements. Data are expressed as relative HSL expression ± S.E.M. The HSL enzymatic activity increased in SR-BI-/- mice STf but the increase was not significant.

D and E. mRNA expression:

Real time PCR was performed on total RNA of CD36-/- mice ITf **(D)** and STf **(E)** using primers on HSL gene. HSL mRNA is expressed in fold induction. Data are expressed as relative HSL expression ± SEM in CD36-/- compared to wt mice (1 fold). The data were obtained from three independent experiments. The increase of HSL in CD36-/- (** $P<0.005$) compared to wt mice ITf **(D)** is significant, whereas HSL mRNA levels decreased in CD36-/- compared to wt mice STf **(E)** but not significantly.

F. Enzymatic activity:

Twenty micrograms of total proteins from CD36 knockout mice STf were subjected to the enzymatic activity measurements. Data are expressed as relative HSL expression ± SEM. The HSL enzymatic activity decreased in CD36-/- mice STf but showed no significance.

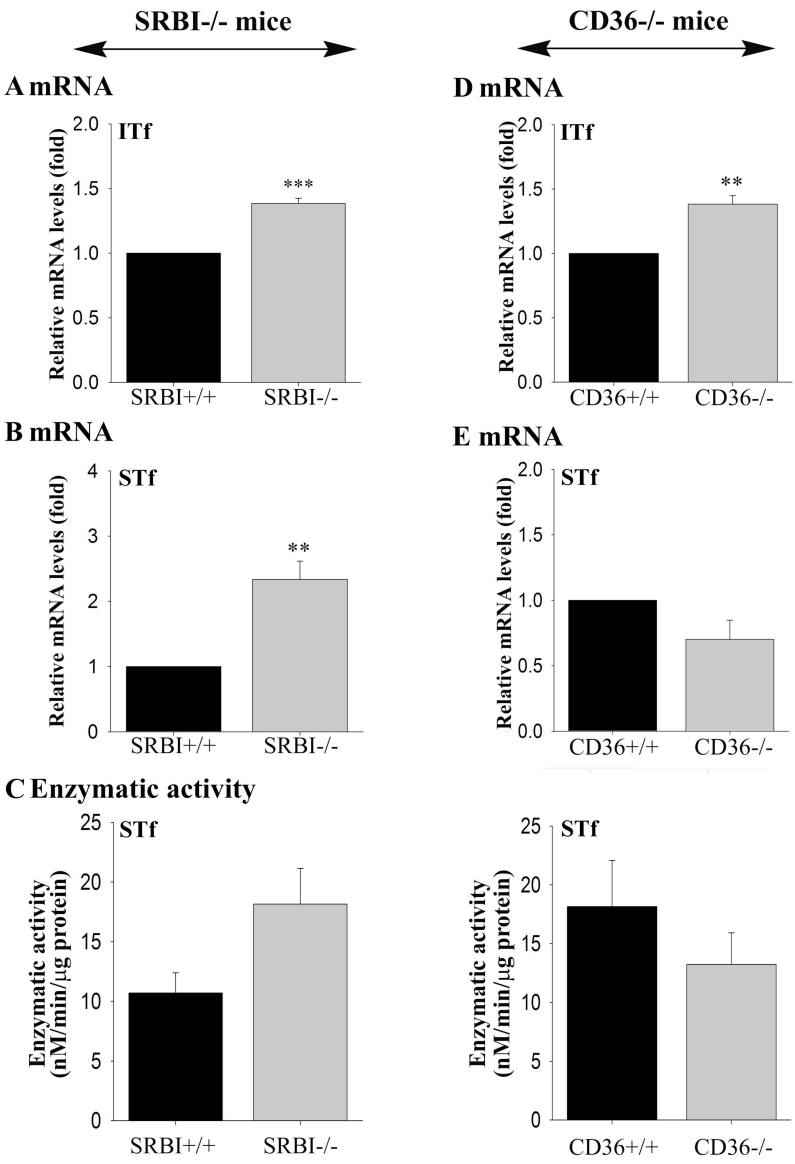

Figure 25 HSL mRNA expression and enzymatic activity in SR-BI and CD36 knockout mice

Figure 26. ACAT-1 and ACAT-2 mRNA expression and enzymatic activity in SR-BI and CD36 knockout mice.

A and B. mRNA expression:

Real time PCR was performed on total RNA of SR-BI-/- mice ITf **(A)** and STf **(B)** using primers on ACAT-1 or ACAT-2 gene. ACAT-1 or ACAT-2 mRNA is expressed in fold induction. Data shown are the mean ± SEM in SR-BI-/- mice and are expressed relative to ACAT-1 or ACAT-2 expression in wt mice (1 fold). The data are representative of three independent experiments. ACAT-1 mRNA levels (*** $P<0.001$) and ACAT-2 mRNA levels decreased (* $P<0.01$) significantly in SR-BI-/- mice ITf **(A)**. Similarly, ACAT-1 (* $P<0.01$) and ACAT-2 (*** $P<0.001$) decreased significantly in SR-BI-/- mice STf **(B)**.

C. Enzymatic activity:

Two hundred micrograms of total microsome proteins from SR-BI-/- mice STf were subjected to the enzymatic activity measurements. Two representative histograms of ACAT-1 and ACAT-2 activity in SR-BI-/- mice are shown. ACAT-1 activity decreased in SR-BI-/- mice STf, whereas ACAT-2 activity showed no change between wt and SR-BI-/- mice.

D and E. mRNA expression:

Real time PCR was performed on total RNA of CD36-/- mice ITf **(D)** and STf **(E)** using primers on ACAT-1 or ACAT-2 gene. ACAT-1 or ACAT-2 mRNA is expressed in fold induction. Data are expressed as relative ACAT-1 or ACAT-2 expression ± SEM in CD36-/- compared to wt mice (1 fold). The data were obtained from three

independent experiments. ACAT-1 mRNA levels decreased (** P<0.005) and ACAT-2 mRNA levels decreased (*** P<0.001) significantly in CD36-/- mice ITf **(D)**. In contrast, ACAT-1 mRNA levels showed no significance compared to wt mice STf. The decrease in ACAT-2 in CD36-/- mice STf (** P<0.005) compared to wt mice STf was significant **(E)**.

F. Enzymatic activity:

Two hundred micrograms of total microsome proteins from CD36-/- mice STf were subjected to the enzymatic activity measurements. Two representative histograms of ACAT-1 and ACAT-2 activity in SR-BI-/- mice are shown. ACAT-2 activity decreased in CD36-/- mice STf. Conversely, ACAT-1 activity in CD36-/- mice STf showed no significant changes.

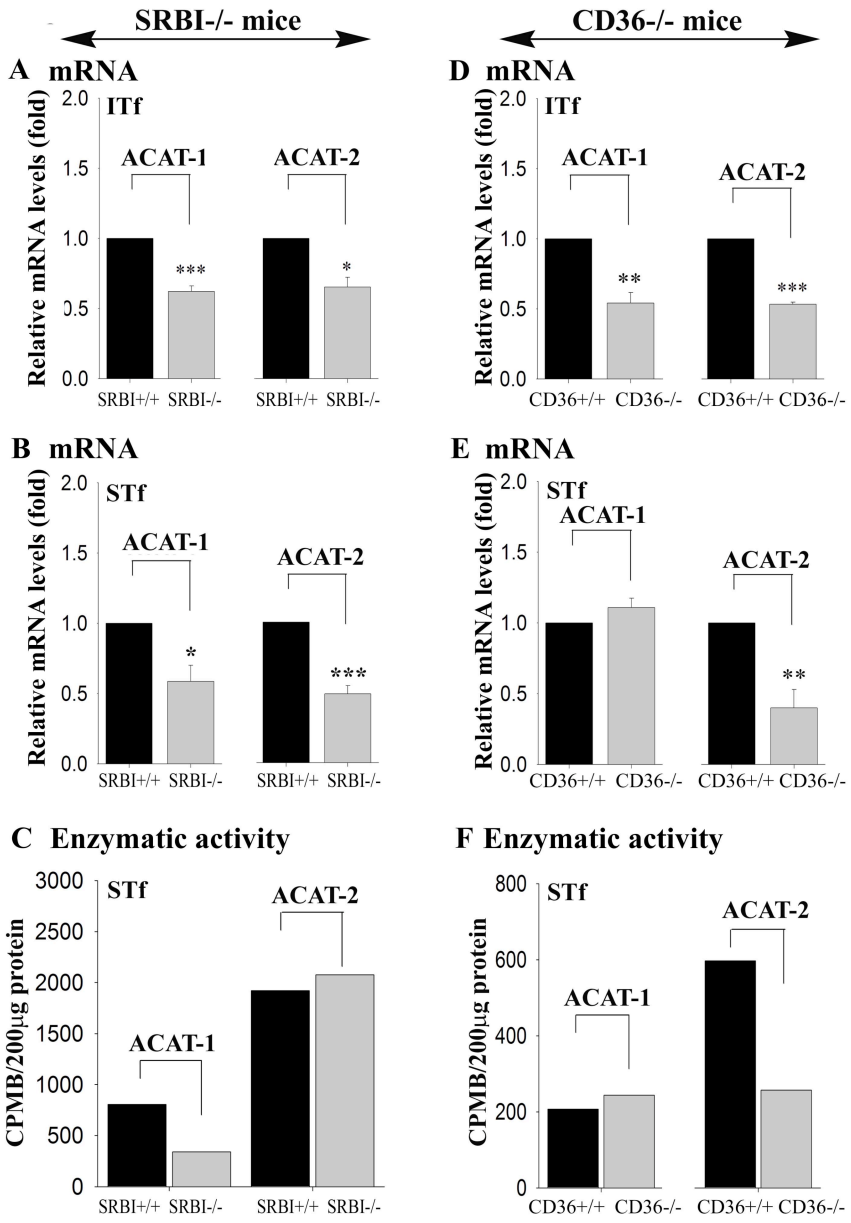

Figure 26 ACAT-1 and ACAT-2 mRNA expression and enzymatic activity in SR-BI and CD36 knockout mice

Discussion

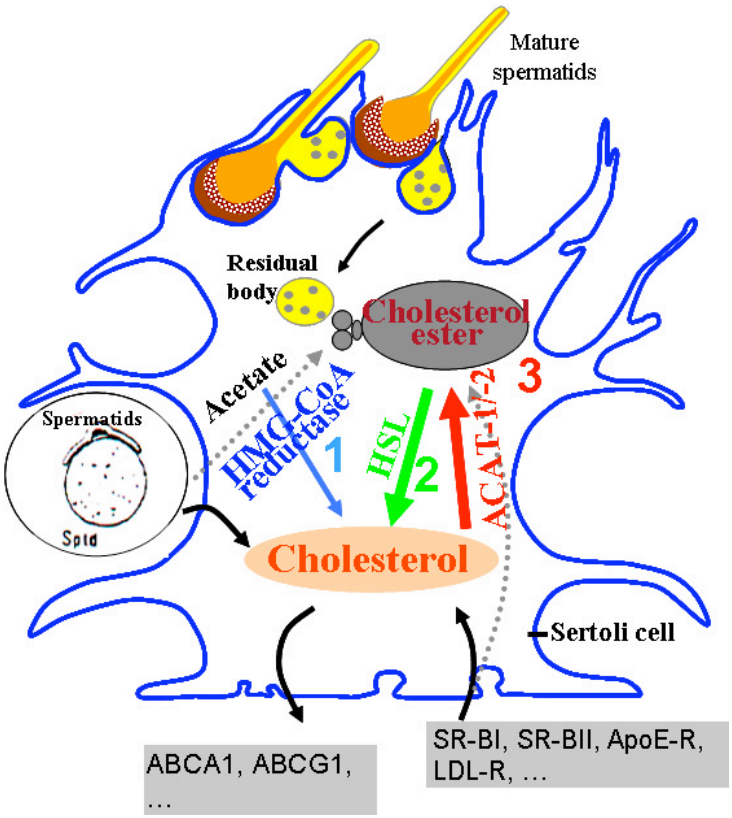

Schematic drawing of HMG-CoA reductase, HSL and ACAT in intracellular cholesterol metabolism during normal spermatogenesis.

Outline of Discussion

1. HMG-CoA reductase

1.1 Mink

1.1.1 HMG-CoA reductase mRNA, protein expression and enzymatic activity in the seminiferous tubules during development and annual reproductive cycle

1.2 Mouse

1.2.1 HMG-CoA reductase mRNA, protein expression in the interstitial tissue during development

1.2.2 HMG-CoA reductase mRNA, protein expression and enzymatic activity in the seminiferous tubules during development

2. HSL

2.1 Mink

2.1.1 HSL mRNA, protein expression and enzymatic activity in the seminiferous tubules during development and annual reproductive cycle

2.2 Mouse

2.2.1 HSL mRNA, protein expression in the interstitial tissue during development

2.2.2 HSL mRNA, protein expression and enzymatic activity in the seminiferous tubules during development

3. ACAT-1 and ACAT-2

3.1 Mink

3.1.1 ACAT-1 and ACAT-2 mRNA, protein expression and enzymatic activity in the seminiferous tubules during development and annual reproductive cycle

3.2 Mouse

3.2.1 ACAT-1 and ACAT-2 mRNA, protein expression in the interstitial tissue during development

3.2.2 ACAT-1 and ACAT-2 mRNA, protein expression and enzymatic activity in the seminiferous tubules during development

4. The mRNA expression and activities of HMG-CoA reductase, ACAT-1 and ACAT-2 in HSL-/- male mouse

4.1 ITf

4.2 STf

5. The mRNA expression and activities of HMG-CoA reductase, HSL, ACAT-1 and ACAT-2 in SRBI-/- and CD36-/- male mouse

5.1 SR-BI-/- mice

5.1.1 ITf

5.1.2 STf

5.2 CD36-/- mice

5.1.1 ITf

5.1.2 STf

6. Intracellular cholesterol homeostasis by the coordination of three key enzymes (HMG-CoA reductase, HSL and ACAT-1,2)

1. HMG-CoA reductase

Sertoli cells reportedly have the capacity to synthesize cholesterol from acetate *in vitro* (Wiebe & Tilbe, 1979). If this cholesterol synthesis capacity exists *in vivo*, then HMG-CoA reductase showed contribute to regulate the cholesterol biosynthesis pathway in respondse to the metabolic demands of the cyclic production of germ cells. HMG-CoA reductase activity was reported to undergo significant changes during testicular development in rats (Potter et al., 1981). The enzymatic activity was especially high at the prepubertal pachytene stage of spermatogenesis but the regulation of enzyme has not been studied. The present study addresses, to our knowledge for the first time, the physiological significance of HMG-CoA reductase in the seminiferous tubules. In addition, this is the first study of the testicular HMG-CoA reductase that is carried out in seasonal breeders. Moreover, this study provides a comprehensive and accurate account of the impact of HMG-CoA reductase on testicular cholesterol metabolism by taking measurements every 30 days, rather than only sporadically as done in most studies that used seasonal breeders as their animal model. Furthermore, this study provides new and more precise insights into the role and the dynamics of the enzyme in individual cellular compartments of the testis by performing measurements in individual seminiferous tubule-enriched fractions and interstitial tissue-enriched fractions rather than whole-testis extracts as it is widely done.

1.1 mink

1.1.1 HMG-CoA reductase mRNA, protein expression and enzymatic activity in the seminiferous tubules during development and the annual reproductive cycle

Contrary to earlier observations that HMG-CoA reductase mRNA levels in rat testes remained constant during development (Ness & Nazian, 1992), we demonstrated that HMG-CoA reductase mRNA levels in mink STf during development significantly but transiently increased by day 210-240 before decreasing by 270 day in the adult. The mRNA levels at 270 day were not significantly different from those were orded in the 90-180 day old mink. Moreover, HMG-CoA reductase mRNA levels remained relatively constant during the annual reproductive cycle, except in May-June where the mRNA levels nearly

tripled before significantly decreasing 3-fold in July. The increase in HMG-CoA reductase mRNA expression during mink development suggests that transcription may be a significant mean of enzyme regulation at the completion of spermatogenesis. However, the transcpritionally regulatory mechanism cannot alone explain the observation of the transient increase in the mRNA levels in May. Additional regulatory mechanism may be involved.

Western blot analyses performed with anti-HMG-CoA reductase antibody revealed several bands in mink STf during development and the annual reproductive cycle. Adsorption of anti-HMG-CoA reductase with an HMG-CoA reductase peptide caused the disappearance of the 90kDa immunoreactive band and a decrease in the 53kDa band. Because the 53kDa band did not completely disappear with the pre-adsorption, the 90kDa

was considered the HMG-CoA reductase immunoreactive band. The 90kDa HMG-CoA reductase immunoreactive band corresponds to the native monomeric form of the enzyme reported as a 97 kDa protein in the rat liver (Istvan et al., 2000). We demonstrated that the 90kDa HMG-CoA reductase protein levels significantly increased by 180 days after birth. The increase in the 90kDa protein levels occured one month prior that in the mRNA levels. We speculate that HMG-CoA reductase may have unique regulatory pathway to accumulate protein. Previous study in the yeast confirmed that the cell can immediately start with proteins translation concerning the proteins that are quickly required in response to a stimulus (Beyer et al., 2004). In such situations the usual order of events, with transcription and subsequent translation, may be too slow for an appropriate hysiological reaction. Instead, the cell might keep a constant level of reservoir mRNA but quick protein accumulation. Thus, a remarkably increasing HMG-CoA reductase protein expression by 180 days after birth may be due to the necessity for relatively fast responses to the demand on cholesterol. Moreover, an earlier study in rats reported that the liver, which may have sudden demands for large amounts of cholesterol, may use phosphorylation-dephosphorylation to maintain a reservoir of inactive HMG-CoA reductase that can be quickly activated (Ness & Chambers, 2000). Whether phosphorylation-dephosphorylation mechanism occurs during the spermatogenic activity in the testis remains to be elucidated.

In addition, the protein levels of 90kDa HMG-CoA reductase tended to decrease from 240-270 days after birth; the 90kDa protein levels decreased from April-July in the adult during the seasonal cycle, while in May-June HMG-CoA reductase mRNA expression peaked, suggesting that the post-transcriptional regulation is crucial for HMG-CoA

reductase expression. It is well documented that post-transcriptional regulation determines the fate of the RNAs, including their subcellular localization, stability, and translation efficiency (Ross,1995). Thus, post-transcriptional regulation of the enzyme may provide a more elaborate regulation of the activity. It has been reported that the monomeric form of HMG-CoA reductase protein could be cleaved by proteolysis and the two-third of the enzyme COOH- terminal be released into the cytosol while the enzymatic activity increases (Jingami et al., 1987). Therefore, it is possible that cleaved HMG-CoA reductase isoform may be expressed in STf. A precise measurement of multiple forms of HMG-CoA reductase is necessary in followup studies.

Our enzymatic activity measuements show that the increase in enzymatic activity recorded at 180 days was coincident with an increase in the protein levels of the 90kDa band. Previous findings reported that the rate of [^{14} C] acetate incorporation into cholesterol was increased 4- to 5-folds as spermatocytes went from preleptotene to pachytene (Hou et al., 1990). We show a relationship between the activity of this enzyme and the initiation of meiosis as if cholesterol would be required during this phase.

We found that HMG-CoA reductase activity significantly increased again from 180 to 240 days, and peaked from December to February. Other studies showed that the rate of acetate incorporation into cholesterol decreased and remained low at the end of meiosis, and was low in mature spermatozoa (Potter et al., 1981). Our laboratory reported that free cholesterol levels in STf were lowered from December to March (Akpovi et al., 2006). It would seem unlikely that the high HMG-CoA reductase activity would be responsible for the production of the relatively large amounts of mevalonate used for cholesterol synthesis.

We speculate that the elevated activity of HMG-CoA reductase may have a yet unknown physiological role in these special periods. A recent study has indicated that HMG-CoA reductase may contribute in the production of high concentration of cholesterol intermediates in mature spermatozoa (Tacer et al., 2002). Their observations showed that rat male germ cells lack a coordinate transcriptional control over the cholesterol biosynthetic pathway (Tacer et al., 2002). These authors reported that high expression of HMG-CoA reductase gene was correlated to the low expression of post meiosis-activating sterol (MAS) genes in the cholesterol biosynthesis pathway, causing the accumulation of the meiosis signaling sterol testis-MAS (T-MAS) during the maturation of male germ cells (Tacer et al., 2002). The high concentration of T-MAS in spermatozoa may contribute to completion of the second meiotic division of the oocyte (Byskov et al., 1999). Accordingly, we suggest that the role of HMG-CoA reductase may be not only to synthesize cholesterol but in addition, to produce the intermediate molecule, T-MAS, in the cholesterol biosynthetic pathway.

1.2 Mouse

1.2.1 HMG-CoA reductase mRNA, protein expression in the interstitial tissues during development

Our observations demonstrated that HMG-CoA reductase mRNA levels were significantly increased by 28 days after birth but decreased steadily after until adulthood in the ITf. Between days 28 and 35, a major increase in the number of Leydig cells per testis

has been reported (Vergouwen et al.,1993). Since Leydig cells are the major cells being involved in the biosynthesis of cholesterol and testosterone (Ewing et al.,1981), one would expect that the more Leydig cells, the more cholesterol and testosterone. This would lead to the conclusion that HMG-CoA reductase may contribute in the modulation of the biosynthesis of the cholesterol to be used for testosterone production by the Leydig cells.

Earlier immunocytochemical studies located HMG-CoA reductase protein not only in Leydig cells (Hegardt, 1999; Royo et al., 1993) but also in macrophages (Chen et al., 2002). It has been documented that testicular macrophages can convert cholesterol into 25-hydroxycholesterol which strongly stimulates Leydig cell testosterone production (Chen et al., 2002). Moreover, the number of macrophages in the testicular interstitium has been shown to increase significantly throughout puberty (Hutson,1990; Vergouwen et al.,1991). Therefore, our finding of an increase of HMG-CoA reductase mRNA level during puberty is compatible with the contribution of the enzyme to testosterone production. However, the enzyme protein expression remained more or less constant throughout development, contrary to the mRNA levels that decreased, the precise mechanism of HMG-CoA reductase is participated in testosterone synthesis will require additional investigation, such as to elucidate whether the phosphorylation-dephosphorylation mechanism occurs during the spermatogenic activity.

1.2.2 HMG-CoA reductase mRNA, protein expression and enzymatic activity in the seminiferous tubules during development

Contrary to HMG-CoA reductase expression pattern in the interstitial tissue, we show that HMG-CoA reductase mRNA and 90 kDa protein expression profiles increased simultaneously from 14 to 28 days in the seminiferous tubules. However, HMG-CoA reductase mRNA levels peaked by 42 days before decreasing while the protein levels tended to decrease steadily. Here, we show that the increase in HMG-CoA reductase mRNA and protein levels and activity in mouse STf was coincided with the apprearance of round spermatids in the tubules, suggesting a role of HMG-CoA reductase in the meiosis. However, previous studies showed that the rate of acetate incorporation into cholesterol decreased and remained low at the end of meiosis, and was low in mature spermatozoa (Potter et al., 1981). It is possible that HMG-CoA reductase have an unique physiological function besides synthesizing cholesterol. In addition, the 90kDa HMG-CoA reductase protein levels decreased significantly by 42 days after birth, which is in contrast to the enzyme mRNA expression. Since the enzymatic activity levels reached maximal values by 42 days, coincidentally with a peak in the mRNA levels, we speculate that post-transcriptional regulatory mechanism of the enzyme may exist during this period. The spermatozoa were present in the tubules by 42 days, and significantly we found that a 37kDa HMG-CoA reductase immunoreactive band was expressed in spermatozoa in addition to the 90kDa immunoreactive band. Whether the 37kDa band is the product of post-transcriptional modulation and whether it would be involved in the regulation of HMG-CoA reductase activity requires additional investigation.

2. HSL

An earlier report showed that seminiferours tubules could not contribute the majority of the cholesterol required for spermatogenesis through the biosynthesis pathway *in vitro* (Wiebe & Tilbe, 1979). Thus, other enzymes besides HMG-CoA reductase should regulate cholesterol to levels that are consistent with the production of viable and fertile male germ cells in the tubules. Previous reports showed that HSL activity was positively correlated with free cholesterol to esterified cholesterol ratios in the seminiferous tubules (Kabbaj et al., 2003). Furthermore, the physiological significance of HSL in testis is highlighted by the report that HSL knockout male mice are sterile due to the toxicity effect caused by the over-accumulation of esterified cholesterol (Osuga et al., 2000). The present study addresses the physiological significance of HSL in each compartment of mink and mouse testis. Our studies confirm previous findings by showing that HSL protein levels and HSL activity increased in parallel in STf until 240 days. We are the first to detect that HSL activity in STf was modulated at the transcriptional levels during mouse development. In addition, we demonstrated that 90 kDa HSL protein levels tended to increase from 35 days to adulthood, while HSL mRNA expression significantly decreased in mouse interstitial tissue. Because HSL is assumed to hydrolyze esterified cholesterol and to provide available free cholesterol to fullfil the needs of cells (Holm et al., 2000), HSL high expression and activity in the developemental tubules and interstitum is likely responsible for regulating cholesterol concentration.

2.1 Mink

2.1.1 HSL mRNA, protein expression and enzymatic activity in the seminiferous tubules during development and annual reproductive cycle

This study demonstrated that HSL mRNA levels in mink STf during development significantly increased once by day 120 and again by 270, but not during the annual reproductive cycle. The increase of HSL mRNA expression during mink development suggests that transcription may be a significant means of enzyme regulation at the initiation of spermatogenesis. However, the transcriptionally regulatory mechanism can not alone explain the observation of low HSL protein level at 120 day or decreased HSL protein expression by 270 days after birth. Earlier study showed that post-transcriptional regulation determines the fate of the RNAs and modulates the translation efficiency (Ross,1995). Therefore, post-transcriptional regulation of HSL may provide a more elaborate regulation of the enzymatic activity. However, this remains to be determined.

Adsorption of anti-hHSL with human adipose tissue caused a major decrease in the intensity of the 90kDa immunoreactive bands in mink tissues (Kabbaj et al., 2003), demonstrating that the anti-hHSL antibodies recongnizes the enzyme in mink tissue. In the present study, the detection of a mink tubular HSL with larger molecular mass (120 kDa) and another smaller form of HSL (90kDa), is in agreement with the results of studies in other species (Kabbaj et al., 2001; Mairal et al., 2002; Vallet-Erdtmann et al., 2004). Except the “well recognized” testicular HSL isoform (120 kDa) which is only expressed in postmeiotic germ cells, the 90 kDa HSL isoform was studied in our study. This specific

HSL isoform was reported in interstitial and tubular Sertoli cells as well as premeiotic germ cells, but not in postmeiotic germ cells (Mairal et al., 2002). Thus, the measurement of 90kDa HSL protein expression in STf provides new insights into the study of HSL in the particular phases of testicular development. The present study recorded one increase of 90kDa HSL protein expression by day 180- and a second increase by 240 days as well as in January, which is independent of the enzyme mRNA expression. Therefore, HSL may have regulatory pathway to accumulate protein rather than transcriptional regulation. Earlier studies showed that the yeast cells could immediately started with protein translation if the corresponding protein is rapidly needed (Beyer et al., 2004). In such situation the mRNA abundance may not need to change much more drastically to achieve a significant change of protein concentrations. Therefore, the 90kDa HSL protein increases which are anterior to the mRNA level increase may be due to the necessity for relatively fast responses to the cholesterol demand. In addition, it has been documented that lipolytic and anti-lipolytic hormones regulate HSL activity in adipose tissue via reversible HSL protein phosphorylation mediated by protein kinase A (PKA) (Yeaman, 1990). HSL activity in STf may be influenced via reversible HSL phosphorylation of serine residues mediated by PKA. It would be interesting to identify changes in phosphorylation sites of the HSL protein that could account for putative changes in HSL activity in STf.

The enzymatic activity in this study using PNPB as the substrate reflects the activity of HSL in STf. The results showed that HSL activities gradually increased duing development and the period from August to February. HSL activity peaked in the adult and in February but it significantly decreasd from March-May. The current study substantiates

previous reports that HSL activity varied in STf and reached maximal values in the adult during the period of maximal spermatogenic activity (Kabbaj et al., 2003). Combining the earlier finding of a strong correlation of the free cholesterol/esterified cholesterol ratios with HSL activity in the tubules, we support the notion that HSL may be the cholesterol esterase, which maintains the cholesterol homeostasis in the tubules. To be noted, the increase of HSL activity followed the 90kDa HSL protein accumulation by180-, 240- days after birth as well as January in the seasonal cycle, suggesting that 90 kDa HSL protein accumulations could be the crucial mechanism in the regulation of HSL activity. Additionally, the present study recorded the elevation in HSL activity in STf, which is independent of the enzyme mRNA and protein expression. The finding entails distinct cholesterol regulatory mechanism in the seminiferous tubules.

2.2 Mouse

2.2.1 HSL in the interstitial tissue (ITf)

The present study recorded a sharp increase of HSL mRNA expression by 28 days after birth followed by a significant decrease by 42 days in mouse ITf. The observation agrees with the earlier report that HSL mRNA level is 25-fold increased in rat testis during puberty (Kraemer et al.,1991). It has been documented that 90kDa HSL is expressed in interstitial tissue (Mairal et al., 2002); and the enzyme is localized in the macrophages of interstitial tissue (Kabbaj et al.,2003). Since the number of macrophages/units area increased significantly during puberty (Hutson,1990; Vergouwen et al.,1991), we put

forward the view that macrophage HSL may free cholesterol from esterified cholesterol to be converted into 25-hydrocholesterol taken up by Leydig cells to synthesize testosterone during spermatogenesis. The present study further suggests that the modulation of HSL activity in ITf is at the transcriptional level.

The current study first reported the variation of 90kDa HSL protein expression in mouse ITf during development. The results showed that the 90kDa HSL protein level tended to increase from 35 days onwards. The observation is in agreement with other reports that a delay between mRNA and protein appearance is characteristic of many genes expression in the testis (Blaise et al.,1999; Blaise et al.,2001). The finding of an increased HSL mRNA level and 90kDa HSL protein expression is compatible with the contribution of testosterone production. Combining the fact that the increase of HSL expression corresponded to a decrease in esterified cholesterol levels in ITf (Akpovi et al, unpublished data), we suggest that HSL is involved in the cholesterol metabolism while contributing to testosterone production in the interstitial tissue. Remarkably, HSL mRNA levels decreased in adulthood, while its protein levels increased. The results suggest a regulation of HSL protein expression in ITf during adulthood different from that during development.

2.2.2. HSL mRNA, protein expression and enzymatic activity in the seminiferous tubules during development

Our observations showed three successive significant increases in HSL mRNA levels in STf one by 21, then by 28, and again by 35 days. The HSL mRNA expression

pattern was accompanied by a steady elevation of HSL protein expression throughout development. The finding of a different HSL mRNA and protein expression in the seminiferous tubules and interstitial tissue entails distinct cholesterol regulatory mechanisms in individual compartment of the testis. Such elevation seems to be testis-specific and species-specific since this change was not observed in the adipose tissue and HSL mRNA levels remained constant in rat testis during development (Kraemer et al., 1991).

The present study demonstrated that HSL activity as well as the enzyme expression was increased in parallel in STf throughout development, except in the STf of the adult, in which a significant decrease of HSL activity is associated with an increase of HSL mRNA and protein level. The results suggest HSL activity is regulated on the transcriptional level during development. They also suggest a regulation of HSL activity during adulthood was different from that during development. In addition, the current finding recorded a significant increase in HSL activity in STf that coincided with period (i.e., the 21-day-old) characterized by numerous pachytene spermatocytes in the tubules, reflecting intense meiotic activity. Moreover, the present study showed an increased HSL activity during the period when the spermatognesis was completed during development. Combining with the previous finding in Guinea pig that HSL accumulated near the base of Sertoli cells in stages following the release of spermatids (Kabbaj et al., 2003), we suggest a role of HSL in the processing of lipids borne by residual bodies.

3. ACAT-1 and ACAT-2

ACAT reduces cholesterol solubility in the cell membrane and promotes storage of cholesterol ester in the lipid droplets within the cytoplasm by esterifying cholesterol (Suckling & Stange,1985). Thus, normal ACAT activity prevents potential accumulation of excess free cholesterol which might jeopardize vital cellular functions (Warner et al.,1995). Two distinct isoforms of ACAT have been documented: ACAT-1 and ACAT-2. ACAT-1 converts cholesterol into cholesteryl ester in response to cholesterol abundance inside the cells (Chang et al., 1993); and ACAT-2 appears to provide cholesteryl esters for transport in lipoproteins (Buhman et al., 2000; Cases et al., 1998a). The contribution of individual ACAT isoforms to cholesterol homeostasis in the male gonads has never been reported. The current study, for the first time, demonstrated that ACAT-1 and ACAT-2 are both expressed in the interstitial tissue and seminiferous tubules, and showed that the ACAT-1 enzymatic activity is complementary to ACAT-2 in the seminiferous tubules.

3.1 mink

3.1.1 ACAT-1 and ACAT-2 mRNA, protein expression and enzymatic activity in the seminiferous tubules (STf) during development

ACAT-1 has been well documented in the steroid hormone-producing Leydig cells and macrophages of testis, while ACAT-2 was claimed to be absent from testis (Dove et al., 2006; Dove et al., 2005; Lee et al., 2000; Rudel et al., 2001). Our observation argued with this report by showing that not only ACAT-1 but also ACAT-2 was present in mink testis. The present immunohistochemistry studies showed for the first time that ACAT-1 and ACAT-2 both localized in the mink seminiferous tubules: ACAT-1 to the germ cells,

ACAT-2 to the Sertoli cells. These differences in the cellular localization of ACAT-1 and ACAT-2 suggest different functions of the two isoforms. Previous studies demonstrated that ACAT-1 maintains free cholesterol equilibrium in by storing excess of cholesterol as cholesterol esters (Chang et al., 1997). ACAT-2 is thought to provide cholesterol esters for very low density lipoprotein (VLDL) assembly in specific tissues (Cases et al., 1998a; Joyce et al., 1999). Thus, we attempted to address the hypothesis that, ACAT-1 may be associated with the cholesterol esterification and store the lipid droplet content in the seminiferous tubules, whereas ACAT-2 may participate in the removal of excessive cholesterol from the tubules. Our data provided the besis in support of this view.

Our results showed the presence of transcripts and protein expression of ACAT-1 and ACAT-2 in mink seminiferous tubules, and confirmed the specificity of the PCR products by the restriction enzyme, Alu I. We found that ACAT-1 mRNA expression levels followed a profile similar to that of its protein levels during development but not during the seasonal reproductive cycle. Conversely, ACAT-2 mRNA expression levels followed protein levels during the annual reproductive cycle but not the end of development. ACAT-2 mRNA expression was high while its protein levels were low in the 240 and 270 days samples. This indicates that different regulatory mechanisms are involved in these two ACAT isoforms despite their structural and functional similarities. Evidence shows that post-transcriptional regulation is crucial for gene expression in all organisms (Ross,1995). The post-transcriptional regulation determines the fate of the RNAs, including their subcellular localization, stability, and translation efficiency (Ross,1995). Thus, ACAT isoforms during distinct period of spermatogenesis could be regulated at post-transcriptional level, which

might provide a more elaborate regulation of ACAT-1 or ACAT-2 activity for cellular cholesterol homeostasis.

Our results showed that ACAT-1 mRNA levels were significantly increased during early development when numerous type A_0 spermatogonia were seen arising apparently from divisions of spermatogonia stem cells (by 120 days after birth) or in October; and (by 270 days) with the appearance of the mature spermatids, suggesting an active participation of ACAT-1 in germ cells during mitosis and spermiogenesis. We recorded another increase in ACAT-1 mRNA expression in May when meiosis was arrested and elongated spermatids have left and great amount of lipid droplets were present in the tubules (Pelletier & Vitale, 1994). This association of ACAT-1 mRNA expression with the lipid content in the tubules suggests that ACAT-1 participates in the cholesterol esterification and in the increase in cholesterol ester contents in the tubules. On the other hand, the increased ACAT-2 mRNA levels by 210 days and in January following the release of mature spermatids and the accumulation of residual bodies, suggest a contribution of ACAT-2 in Sertoli cells and an active participation of Sertoli cells in the removal of residual body-borne lipids.

The enzymatic activities of both ACAT-1 and ACAT-2 in the testis were never reported and the physiological significance of having two ACAT isoforms in different cells of seminiferous tubules remains elusive. The experimental inhibition of individual ACAT enzymes was believed to be a useful strategy to identify ACAT-1 and ACAT-2 respective activity. However, most ACAT inhibitors inhibit both ACAT-1 and ACAT-2. After the ACAT genes were identified, investigators began to develop ACAT isotype-selective inhibitors (Cho et al., 2003; Ikenoya et al., 2007; Lee et al., 2004). Manassantin B, which

has been isolated from the methanol extracts of *Saururus chinensis* root, exhibited significant human ACAT (hACAT) inhibitory activity (Lee et al., 2004). However, Manassantin B mainly inhibited hACAT-1 but not hACAT-2 (Lee et al., 2004). Pyripyropene A is another ACAT inhibitor that selectively inhibits ACAT-2 in insect cells transfected with either ACAT-1 or ACAT-2, while pyripyropene A inhibited only the hACAT-2 but not hACAT-1(Cho et al., 2003). K-604, a novel ACAT inhibitor highly selective for ACAT-1 (Ikenoya et al., 2007), was reported to inhibit cholesterol esterification in human macrophages and to suppress the formation of macrophage-enriched fatty streak in fat-fed hamsters (Ikenoya et al., 2007). The present study provides a novel technical approach for individual ACAT-1 and ACAT-2 enzymatic activity measurements in the STf based on the use of K-604. K-604 potently and selectively inhibited ACAT1 activity with IC50 values of 100μM. With the increase of IC50 to 1000 μM, both ACAT 1 and 2 activities were inhibited. Thus, we used 100μM K-604 selectively inhibit ACAT-1 activity and measure ACAT-2 enzymatic activity directly. Thereafter, we calculate ACAT-1 activity by substracting ACAT-2 activity from total ACAT activity. We have detected dramatic alterations of ACAT-1 and ACAT-2 activities during mink development and the annual reproductive cycle. The present studies showed high ACAT-1 activity while ACAT-2 activity was low. Conversely, at times when mature spermatids were present and the residual bodies released and phagocytosed by Sertoli cells, ACAT-2 activity increased, while ACAT-1 activity decreased. Considering the distinct individual localization of ACAT-1 and ACAT-2 in the seminiferous epithelium, we speculate that ACAT-1 may be involved in modulation of cholesterol delicate equilibrium in the tubules. On the other hand,

ACAT-2 was related to cholesterol metabolized by the Sertoli cells following phagocytosis of residual bodies and apoptotic cells.

This study showed that ACAT-1 activity in mink was not coincident with its mRNA and protein expression. The phenomenon was reported previously in other tissues. In Nagase hypoalbuminemic rat liver-ACAT-1 mRNA and protein contents did not change but the enzymatic activity was mildly elevated (Roberts et al., 2004). Lee also demonstrated that rat hepatic ACAT-1 activity was increased with a high diet in fat, which was not paralleled by the alterations seen in ACAT-1 mRNA and protein (Lee & Carr, 2004). Together, these results support the concept that ACAT-1 activity may not be regulated on transcriptional or translational levels. In fact, a recent study showed that unlike other enzymes or proteins involved in the cellular cholesterol metabolism, ACAT-1 expression is not regulated by the transcription factor sterol regulatory element binding protein (SREBP) (Chang et al., 2000; Liu et al., 2005). The authors concluded this after the sterol-regulatory element could not be identified within the ACAT-1 promoter (Li et al., 1999). Instead, the enzyme is regulated by cholesterol via an allosteric activation mechanism (Chang et al., 2000). The activation of the enzyme is not due to an increase in ACAT-1 protein content, but in part to an increase in cholesterol content in the endoplasmic reticulum of human macrophages where ACAT-1 resides (Liu et al., 2005). Therefore, the down-regulation of ACAT-1 activity in the STf reflects the decreased cholesterol concentration in the germ cells with the degree of spermatogenic activity.

Our findings showed that ACAT-2 enzymatic activity as well as its protein level were high when large numbers of mature spermatids were present in the seminiferous

tubules. During this period, spermatozoa are released into the lumen and residual bodies are phagocytosed by the Sertoli cells. Our observations are suggestive that ACAT-2 may be involved in storing excessive cholesterol and in recycling of the cholesterol contained in the residual bodies. Previous studies revealed that ACAT-2 may not only participate in forming cholesteryl ester lipid droplet, but be mainly involved in supplying the cholesteyl ester for lipoprotein (i.e. VLDL) assembly in human hepatocytes and intestinal enterocytes (Chang et al., 2001b). If ACAT-2 has similar capacity in the testis then, Sertoli cells could express lipoprotein receptors such as VLDL receptor that could uptake the lipoproteins assembled in the lumen of endoplasmic reticulum of Sertoli cells. Evidence shows that a novel lipoprotein receptor designated apolipoprotein E receptor 2 (apoE-2), consists of five functional domains resembling the VLDL receptor, and is highly expressed in rabbit Sertoli cells (Kim et al., 1996). Other receptors could also be expressed in the testis that could favor removal of cholesteryl ester from the Sertoli cells. The report of a significant decrease in the esterified cholesterol levels from December to March in adult tubules (Akpovi et al., 2006) reinforces the notion that ACAT-2 is activated to protect against toxicity resulting from excessive cholesterol levels. The most striking finding in the current study was that the increase of ACAT-2 enzymatic activity was correlated with the decrease of ACAT-1 enzymatic activity during mink development. In this regard, we suggest that ACAT-1 and ACAT-2 isoforms are functioning complementarily so as to complete the translocation of cholesterol in excess from mature germ cells to Sertoli cells. This could be tested by elucidating the contribution of ACAT isoforms in testicular cholesterol homeostasis in mouse where individual ACAT-1 or ACAT-2 would be genetically impeded.

3.2 Mouse

Before this study, identification of ACAT-2 as one of the principal ACAT enzymes in mouse testis had not been reported. Additionally, the expression of both ACAT-1 and ACAT-2 in the seminiferous tubules or interstitial tissue had not been addressed. We showed for the first time that the presence of ACAT isoforms transcripts and protein expression in mouse seminiferous tubules and interstitium, and the specificity of ACAT-2 transcripts were confirmed by restriction enzymes-ECoR II. Different ACAT-1 and ACAT-2 mRNA and protein expression pattern were detected in the seminiferous tubules and interstitial tissue. The immunohistochemistry studies demonstrated that ACAT-2 was located in Sertoli cells and ACAT-1 in germ cells.

3.2.1 ACAT-1 and ACAT-2 mRNA, protein expression in the interstitial tissue during development

Our observation showed that not only ACAT-1 but also ACAT-2 was present in mouse ITf. The differences in mRNA expression and protein levels of ACAT-2 were not significant during development in ITf. The existence of ACAT-2 and its enzymatic activity in ITf needs further investigation. Our results further demonstrated that ACAT-1 mRNA levels had a profile opposite that of the protein levels, increasing throughout development and peaking by 42 days. The mRNA expression pattern of ACAT-1 suggested that the post-transcriptional regulation is crucial for ACAT-1 expression. As already noted, post-transcriptional regulation determines the fate of the RNAs, including their subcellular localization, stability, and translation efficiency (Ross,1995). Thus, post-transcriptional

regulation of ACAT-1 might provide a more elaborate regulation of the enzymatic activity. The regulatory mechanism requires further investigation.

ACAT-1 was reportedly present in Leydig cells as well as macrophages (Sakashita et al.,2000). Our immunohistochemisty study confirmed that ACAT-1 was plentiful in the interstitial cells, suggesting a possible involvement of ACAT-1 in converting cholesterol into cholesteryl ester in response to cholesterol abundance inside the cells. It has been reported that the testicular macrophages contain HSL (Kabbaj et al.,2003), which contributes a 25-hydroxycholesterol for testosterone production in Leydig cells. Thus, the presence of both ACAT-1 and HSL in the interstitial cells suggests that ACAT-1 and HSL may regulate cholesterol homeostasis in complementary manners. Macrophage HSL frees cholesterol from the esterified form before converting it into 25- hydroxycholesterol which is then used by Leydig cells to synthesize testosterone. On the other hand, ACAT-1 esterifies excess cholesterol in macrophages or Leydig cells to maintain cholesterol homeostasis for testosterone production. Based on this information, a future area of interest is to identify whether ACAT-1 is present or active in the interstitial macrophages, and whether it participate to the removal of excessive cholesterol in these cells.

3.2.1 ACAT-1 and ACAT-2 mRNA, protein expression and enzymatic activity in the seminiferous tubules during development

ACAT-1 and ACAT-2 were also expressed in the seminiferous tubules. However, ACAT-1 mRNA expression pattern in mouse STf differed from that in the ITf. In fact, our

findings show that unlike the constant expression of ACAT-2 mRNA and protein in ITf, ACAT-2 mRNA levels were increasing throughout development in STf, which had an opposite profile that of the protein levels, suggesting another regulatory mechanism of the enzyme in STf. The significance of ACAT-2 expression pattern in STf remains to be determined. On the other hand, ACAT-1 mRNA and protein levels were both decreased throughout development. These results suggest ACAT-1 is regulated on the transcriptional levels in the tubules. Previous studies demonstrated that ACAT-1 and ACAT-2 genes are located on distinct chromosomes (Cases et al., 1998a; Li et al., 1999; Uelmen et al., 1995). Thus, the differences in the transcriptional regulation of ACAT-1 and ACAT-2 in STf may be caused by independent regulatory mechanism.

Previous reports found that sterol regulatory elements, present in the promoters of many cholesterol-regulated genes. However, the sterol regulatory elements have not been identified within the ACAT-1 or ACAT-2 (Chang et al., 2001b; Li et al., 1999). Thus, the main mode of sterol-dependent regulation of ACAT activity may not be at transcriptional but at translational levels. Change et al. (1997) reported that ACAT-1 and ACAT-2 are allosteric enzymes with two types of sterol-binding sites. One substrate site is able to accommodate a wide variety of sterols, while another activator site may only recognize cholesterol (Chang et al., 1997).

The present study also applied the novel selective ACAT-1 inhibitor, K-604, to the measurements of individual ACAT-1 and ACAT-2 enzymatic activity in mouse seminiferous tubules. K-604 potently and selectively inhibited adult mouse ACAT1 much more than ACAT2 with IC_{50} values of 100 and 1000 μM respectively. The proper inhibitor

concentration (100μM) that inhibits the activity of ACAT-1 but not the activity of ACAT-2 was selected, and applied to the measurement of ACAT-1 and ACAT-2 enzymatic activities in mouse seminiferous tubules. Dramatic alterations of ACAT-1 and ACAT-2 activities during mouse development were detected. Our observations showed that ACAT-1 enzymatic activity was high in new borns and decreased in adults, and that ACAT-2 activity was low in newborns but high in adults. Yet, the enzymatic activity of ACAT-1 and ACAT-2 reached comparable levels in the adult. Considering the distinct individual localization of ACAT-1 and ACAT-2 in the seminiferous tubules, we speculated that ACAT-1 may be involved in modulation of cholesterol delicate equilibrium in the developing germ cells. On the other hand, ACAT-2 was related with the removal of accumulated cholesterol in the Sertoli cells by phagocytosis of residual bodies and apoptotic cells.

Summary for HMG-CoA redcutase, HSL, ACAT-1 and ACAT-2: 1) HMG-CoA redcutase, HSL and ACAT-2 showed similar enzymatic activity profiles. They increased during development but decreased in adulthood, and their activities varied in parellel with development and germ cells development. These results suggest that all three enzymes work in synchrony and they may get involved in the spermatogenetic activity. 2) On the other hand, ACAT-1 activity showed an opposite tendency to the other enzymes. It is high in newborn, but decreased afterwards. ACAT-1 acitivity is complementary to ACAT-2.

4. The mRNA expression and activities of HMG-CoA reductase, ACAT-1 and ACAT-2 in HSL-/- male mouse

The most striking phenotype of HSL knockout mice is male sterility caused by oligospermia (Osuga et al., 2000). It has been demonstrated that the absence of HSL in the testis resulted in a 2.3-fold increase in testicular cholesterol ester (Osuga et al., 2000). Therefore, we questioned whether the disruption of HSL geen could effect on other enzymes (HMG-CoA redcutase, ACAT-1 and ACAT-2) mRNA and protein expression and enzymatic activity, and thus causing cholesteryl esters over-accumulated in the testis.

Real-time quantitative PCR analysis revealed that STf and ITf from HSL -/- testis lack a wild type (wt) transcript with HSL mRNA which codes all forms of the protein. Western blot analyses showed no 90kDa immunoreactive HSL protein in testis from HSL-/- mice. The 90kDa band, which corresponds to the 88 kDa band in human adipocyte and to the 84 kDa band in rat fat (Langin et al., 1993), is reported to be expressed in interstitial and tubular somatic cells as well as premeiotic germ cells (Blaise et al., 2001; Mairal et al., 2002). To test the hypothesis of a differential HSL-meidated modulation of cholesterol metabolism in Sertoli cells, germ cells and testicular macrophages, changes in protein expression of 90kDa HSL were measured in STf and ITf.

4.1 ITf

Previous study in testis supported the notion that interstitial macrophage HSL could free cholesterol from esterified cholesterol to be converted into 25-hydrocholesterol

taken up by Leydig cells to synthesize testosterone (Kabbaj et al., 2003). It is also reported that HSL overexpression in macropahges stimulates cholesterol ester hydrolase activities (Escary et al., 1998). Therefore, it appears HSL is responsible for cholesterol ester hydrolase activities in macropahges, and play crucial role in supporting steroidogenesis. Our findings in HSL knockout mice ITf demonstrated that HMG-CoA reductase mRNA levels were decreased in HSL knockout mice ITf as well as ACAT-1 and ACAT-2 mRNA levels, indicating that the disruption of the HSL gene in mice caused changes in the mRNA expression of several enzymes in ITf. However, these changes did not seem to affect the physiological function of the interstitial tissue due to the fact that HSL knockout mice have normal plasma levels of testosterone, follicle-stimulating hormone and luteinizing hormone (Osuga et al., 2000). The observations suggest that other lipases might be involved in the physiological events of the interstitial tissue, and could at least in part compensate for the lack of HSL. It is also possible that other sources of cholesterol come from the blood circulation. In this concern, the possible source of cholesterol from *de novo* cholesterol synthesis was reduced due to the suppression of HMG-CoA reductase mRNA expression. Since HMG-CoA reductase is an integral membrane proteins present in the endoplasmic reticulum (ER) (Ness & Nazian, 1992), Down-regulation of HMG-CoA reductase expression could cause the decrease of cholesterol pool in ER. It has been documented that cholesterol is the activator for ACAT isoforms in ER. Upon stimulation by low concentration of cholesterol, ACAT isoforms expression could be decreased.

4.2 STf

Because HSL knockout mice have normal plasma levels of testosterone, follicle-stimulating hormone, and luteinizing hormone (Osuga et al., 2000), thus oligospermia does not result from hypogonadism. Instead, the testes completely lost neutral cholesterol ester activities and included increased amounts of cholesterol ester (Osuga et al., 2000). Osuga et al. (2000) reported extensive vacuolation within the seminiferous epithelium of HSL knockout mice; and Oli Red O staining of tissue sections suggested that these vacules are actually filled with lipids (Haemmerle et al., 2003). The remarkable accumulation of cholesterol esters in the tubules leads to the question of whether mutations in the HSL gene may cause tubular cholesterol inquilibrium due to the interruption of the enzyme expression and activity. Our results in HSL-/- mice STf showed that HMG-CoA reductase mRNA levels as well as the enzymatic activity were decreased in HSL-/- mice STf. Conversely, ACAT-1 and ACAT-2 mRNA levels and their respective enzymatic activities were significantly increased. Thus, HSL deficiency caused a change in other enzymes (HMG-CoA redcutase, ACAT-1 and ACAT-2) expressions and activities in STf. Since numerous immature germ cells were present in the epididymis of the HSL knockout mice (Vallet-Erdtmann et al., 2004); Sertoli cells are involved in the phagocytosis of these apoptptic germ cells and accumulate stacks of cholesterol-rich cellular debris in lysosomes (Pelletier & Vitale, 1994), we believe that the increased ACAT-1 and ACAT-2 activities could contribute to the removal of accumulated cholesterol in cell debris-borne cholesterol. The excess cholesterol that comes from the cell debris-born-lipids could suppress the biosynthesis pathway and activity of the rate-limiting HMG-CoA reductase expression. Our

finding demonstrates that the variation of HMG-CoA reductase, ACAT-1 and ACAT-2 expression and activity are the consequence of the absence of corrected HSL transcription in testis. Further studies are needed to clarify the mechanism by which HSL deficiency causes abnormal spermatids development.

Summary of HSL-/- mice: HSL gene deletion caused a cascade of physiological responses on HMG-CoA reductase and ACAT isoforms, which could be the pivotal response that modifies cholesterol homeostasis in testis.

5. The mRNA expression and activities of HMG-CoA reductase, HSL, ACAT-1 and ACAT-2 in SR-BI and CD36 knockout mice

5.1 SR-BI-/- mice:

Scavenger receptor class B type I (SR-BI) mediates the selective uptake of HDL cholesterol (Kozarsky et al., 1997; Temel et al., 1997). In addition, SR-BI selectively removes cholesteryl esters from the HDL to which it binds (Kozarsky et al., 1997; Temel et al., 1997) and contributes to the HDL-mediated cellular cholesterol efflux (Ji et al., 1997). Experimetnal deficiency of SR-BI is accompanied by abnormal structure, composition, and abundance of lipoproteins because of defective cholesterol efflux from cells to lipoprotein particles (Miettinen et al., 2001). The SR-BI deficient male mice exhibit a reduction in their number of homozygous offspring relative to wild-type offspring from F1 heterozygous intercrosses although the mice were fertile (Rigotti et al., 1997). Therefore, abnormalities in cholesterol metabolism in SR-BI knockout male mice might cause the reduction of male offspring numbers. To assess how the enzymatic system in the regulation of cholesterol metabolism is affected by shutting SR-BI-dependent cellular flux, the mRNA expression and the activity of HMG-CoA reductase, HSL, ACAT-1 and ACAT-2 in individual compartments of SR-BI knockout mouse testis were measured.

SR-BI gene deficit caused a significant decrease in HMG-CoA reductase, ACAT-1 and ACAT-2 mRNA expression, while causing a remarkable increase of HSL mRNA level

in ITf and STf. Similarly, HMG-CoA reductase and ACAT-1 enzymatic activities were significantly reduced, while HSL activity was significantly elevated in SR-BI KO seminiferours tubules. These observations suggest at the absence of SR-BI receptor leads to the consequent functional changes of the major enzymes regulating cholesterol metabolism in testis, which is regulatd at the level of transcription. Given that SR-BI deficiency impaired the cholesterol efflux from the cells in the interstitial tissue or seminiferous tubules, this could cause an increased cholesterol level inside of cells. Excessive cholesterol may directly inhibit the transcription of one or more of the enzyzmes in the cholesterol biosynthetic pathway (i.e. HMG-CoA reductase) and decrease the enzymatic activity(s) in testis. Since HMG-CoA reductase is an integral membrane proteins present in the endoplasmic reticulum (ER) of the cells (Ness & Nazian, 1992), down-regulation of HMG-CoA reductase expression and activity will cause the decrease of the cholesterol pool in ER. It has been documented that cholesterol pool in ER is the activator for ACAT isoforms (Liu et al., 2005). Thus, low level of cholesterol could inhibit ACAT isoforms expression and activities. However, ACAT-2 activity was not decresed although its mRNA expression significantly reduced. These results suggest that ACAT-2 may have other regulatory mechanism in modulating the cholesterol esterification, and ACAT-2 may be the only esterase that converts of cholesterol to cholesterol ester in SR-BI KO male testis. In addition, since the origin of cholesterol from the biosynthesis pathway was reduced due to the decreased HMG-CoA reductase activity, the increasing HSL expression and activity could contribute cholesterol to ensure normal spermatogenesis.

.

5.2 CD36-/- mice:

CD36 belongs to the class B scavenger receptor family, which is responsible for the selective uptake of cholesterol esters (Febbraio et al., 2001). CD36, expressed in Sertoli cells, was claimed to be involved in the phagocytosis process of the residual bodies shed from spermatozoa lipid (Gillot et al., 2005). A null mutation in CD36 was not reported to affect the fertility of mutant animals but reveals crucial roles of CD36 in fatty acid and cholesterol metabolism (Febbraio et al., 1999; Febbraio et al., 2002). To assess how the enzymatic system in the regulation of intracellular cholesterol metabolism is affected by shutting CD36-dependent cholesterol uptake, the mRNA expression and the activity of HMG-CoA reductase, HSL, ACAT-1 and ACAT-2 in individual compartments of CD36 knockout mouse testis were measured.

This study showed, for the first time, a significant decrease of HMG-CoA reductase, ACAT-2 mRNA in the interstitial tissue and seminiferous tubules together with a decrease in HMG-CoA reductase and ACAT-2 activity but not in ACAT-1 in CD36 deficient mice testis in comparison to wild type. Conversely, CD36 gene deficit caused a significant increase of HSL mRNA expression, while causing a decrease of ACAT-1 mRNA expression in the interstitial tissue.

The results show that blocking the gene expression of CD36 leads to the consequent mRNA expression variation of the major enzymes regulating cholesterol metabolism in the interstitial tissue. It is hypothesized that this modification reflects in part the effect of CD36 on the transport of cholesterol to the Leydig cells. In the seminiferous tubules, it has been claimed that CD36 is expressed in Sertoli cells and that the protein localized in the residual

bodies shed from mature spermatids (Gillot et al., 2005). Thus, it is possible that CD36-mediated phagocytosis of residual bodies could be one of the processes involved in the cholesterol exchange between Sertoli cells and germ cells. Our results in CD36 deficient mice showed ACAT-2 mRNA expression and enzymatic activity significantly decreased in the CD36 null mice, suggesting that ACAT-2 may be closely related to the expression of CD36 in the tubules. Gillot et al. (2005) suggested that CD36 may be involved in lipid recycling from the residual bodies. Thus, ACAT-2 may participate in the removal of cholesterol stored in the residual bodies. Sertoli cells may function as a recycling centre, where lipid content in the residual bodies would be reused and thus providing the cholesterol required for normal spermatogenesis. However, ACAT-1 mRNA expression and enzymatic activity showed no significant changes in tubules of CD36 null mice. Considering the fact that ACAT-1 is localized in germ cells, while CD36 was said to be expressed in Sertoli cells (Gillot et al., 2005), it is possible that ACAT-1 may be not closely associated to the expression of CD36 in the tubules, thus may not be inflenced by blocking out CD36 gene. Given that CD36 deficiency impaired the removal of the residual bodies in Sertoli cells, this could cause the accumulation of cholesterol-rich, germ cell-born membranes, which might directly inhibit the transcription of one or more of the enzyzmes in the cholesterol biosynthetic pathway (i.e. HMG-CoA reductase) and decrease the enzymatic activity(s) in the tubules. On the other hand, HSL could play an important role in the regulation of CD36 expression (Chung et al., 2001). However, our results in CD36-deficient mice demonstrated that no significant changes of the HSL mRNA expression and enzymatic activity in the seminiferous tubules. It is possible that the remaining scavenger

receptors could account for CD36 deficiency, for instance, SR-BI may replace CD36 thus, preserving the function of HSL. It would be interesting to identify the changes of the enzymes in SR-BI and CD36 double knockout mice testes.

Summary of SR-BI-/- or CD36-/- mice: Genetically blocking SR-BI or CD36 affects the regulation of the enzymes (HMG-CoA reductase, HSL and ACAT-1 and ACAT-2) expression and activities.

6. Relationship of intracellular enzymes in the cholesterol metabolism in each compartment of testis

Cellular cholesterol homeostasis is a tightly regulated system in which the amount of unesterified cholesterol within the cells is controlled by the rate of cholesterol uptake, synthesis, esterification, and hydrolysis of cholesterol esters. Thus, a series of enzymatic factors are required in cholesterol metabolism to maintain the concentration of unesterified cholesterol within narrow physiological limits. Recent advances have mainly focused on the intracellular enzyme, HSL. These observations noted that HSL knockout mice were sterile (Hermo et al., 2008; Osuga et al., 2000; Vallet-Erdtmann et al., 2004). Alterations in the testis of HSL-deficient mice are associated with decreased sperm counts, motility, and fertility (Hermo et al., 2008). In this present study we build on the previous work, by discussing more detailed mechanisms of additional enzymes HMG-CoA reductase, ACAT-1 and ACAT-2 as well as HSL in cholesterol ester cycle; furthermore, we particularly emphasize the cooperation of these enzymes in achieving and maintaining cholesterol homeostasis in the individual compartments of the testis.

Under physiological conditions, the completion of spermatogenesis in seasonal breeders was associated with elevated HMG-CoA reductase mRNA levels and enzymatic activity, increased HSL protein expression and activity, up-regulated ACAT-2 mRNA levels and activity, but decreased ACAT-1 activity. These findings point to increased cholesterol biosynthesis and hydrolysis of cholesterol esters and recycling of lipids as well as impaired cholesterol esterification. This suggests that the main

enzymes act cooperatively in the regulation of intracellular cholesterol during the completion of spermatogenesis to maintain adequate cholesterol concentration. As demonstrated using a mouse model, the spermatogenetic activity is accompanied with increased HMG-CoA reductase, elevated HSL, and up-regulated ACAT-2 but impaired ACAT-1. These observations may reflect an increased hydrolysis and deesterification of intracellular cholesteryl esters and an elevated cholesterol biosynthesis. Thus, unesterified cholesterol would be produced when spermatogenesis is active. During the testicular regression period, all three enzyme's (HMG-CoA reductase, HSL and ACAT-2) activities were down-regulated, while ACAT-1 activity was increased. The findings may reflect the response to a decrease in free cholesterol. The results suggest that the three main enzymes control the cholesterol ester cycle and thereby, decrease the supply of cholesterol to tubules and remove excess cholesterol in lipid droplets.

Under pathological condition, interruption of the cholesteryl ester cycle by knocking out HSL, which causes a decrease in HMG-CoA reductase but an increase in ACAT-1 and ACAT-2, may result in the decrease of unesterified cholesterol and the accumulation of cholesterol ester-rich lipid droplets. In agreement with our findings, previous studies have shown a 2-fold elevation in the ratio of esterified to free cholesterol in testis (Wang et al., 2004). In addition, cholesteryl ester hydrolase activity was almost completely blocked in HSL-deficient testis (Vallet-Erdtmann et al., 2004). Moreover, the finding that HSL null male mice were spermatozoa-deficient (Osuga et al., 2000) demonstrates one level at which the HSL can affect the cascade of physiological responses. This finding, that the enzymes function in coordination in the

cholesterol ester cycle, may be the pivotal pathological response that destroys the cholesterol homeostasis in the tubules. On the other hand, in the absence of SR-BI or CD36, the increased HSL was accompanied by decreased ACAT isoforms and HMG-CoA reductase. Since SR-BI or CD36 deficient mice did not display interrupted fertility compared with wild-type male mice (Febbraio et al., 1999; Rigotti et al., 1997), and SR-BI or CD36 null mice did not affect the rate of cholesterol in testis (Akpovi et al., data not shown), we assume that either SR-BI or CD36 deficiencies respond to an up-regulation of extratubular cholesterol uptake by certain compensatory pathways. These results indicate that the main enzymes in cholesterol ester cycle not only function in coordination in the intratubular cholesterol metabolism and control the proper cholesterol distribution, but also response to the variation from extratubular cholesterol pool. The enzymes interconnect with the transporters, contributing to the preservation of the intratesticular cholesterol homeostasis.

Conclusion

Our results suggest:

1. This study showed that the three enzymes participate together in the regulation of cholesterol metabolism in testis.
2. Our results suggest that dysfunction in the action of individual enzymes or transporters affect the activities of remaining enzymes and their contribution to cholesterol homeostasis in tubules.

Our results suggest that this coordination in the action of enzymes may represent the basis of a system that helps to maintain constant cholesterol levels in the testis.

References

Akpovi C. D., Yoon S. R., Vitale M. L., & Pelletier R. M. (2006) The predominance of one of the SR-BI isoforms is associated with increased esterified cholesterol levels not apoptosis in mink testis. *J Lipid Res* **47:** 2233-2247.

An S., Cho K. H., Lee W. S., Lee J. O., Paik Y. K., & Jeong T. S. (2006) A critical role for the histidine residues in the catalytic function of acyl-CoA:cholesterol acyltransferase catalysis: evidence for catalytic difference between ACAT1 and ACAT2. *FEBS Lett* **580:** 2741-2749.

Anderson R. A., Joyce C., Davis M., Reagan J. W., Clark M., Shelness G. S., & Rudel L. L. (1998) Identification of a form of acyl-CoA:cholesterol acyltransferase specific to liver and intestine in nonhuman primates. *J Biol Chem* **273:** 26747-26754.

Anthonsen M. W., Ronnstrand L., Wernstedt C., Degerman E., & Holm C. (1998) Identification of novel phosphorylation sites in hormone-sensitive lipase that are phosphorylated in response to isoproterenol and govern activation properties in vitro. *J Biol Chem* **273:** 215-221.

Aoki A., & Massa E. M. (1975) Subcellular compartmentation of free and esterified cholesterol in the interstitial cells of the mouse testis. *Cell Tissue Res* **165:** 49-62.

Arenas M. I., Lobo M. V., Caso E., Huerta L., Paniagua R., & Martin-Hidalgo M. A. (2004) Normal and pathological human testes express hormone-sensitive lipase and the lipid receptors CLA-1/SR-BI and CD36. *Hum Pathol* **35:** 34-42.

Armstrong D. T. (1970) Reproduction. *Annu Rev Physiol* **32:** 439-470.

Bartke A., Musto N., Caldwell B. V., & Behrman H. R. (1973) Effects of a cholesterol esterase inhibitor and of prostaglandin F2alpha on testis cholesterol and on plasma testosterone in mice. *Prostaglandins* **3:** 97-104.

Bataineh H. N., & Nusier M. K. (2005) Effect of cholesterol diet on reproductive function in male albino rats. *Saudi Med J* **26:** 398-404.

Bearer E. L., & Friend D. S. (1982) Modifications of anionic-lipid domains preceding membrane fusion in guinea pig sperm. *J Cell Biol* **92:** 604-615.

Beg Z. H., Allmann D. W., & Gibson D. M. (1973) Modulation of 3-hydroxy-3-methylglutaryl coenzyme A reductase activity with cAMP and wth protein fractions of rat liver cytosol. *Biochem Biophys Res Commun* **54:** 1362-1369.

Bell J. B., Vinson G. P., & Lacy D. (1971) Studies on the structure and function of the mammalian testis. 3. In vitro steroidogenesis by the seminiferous tubules of rat testis. *Proc R Soc Lond B Biol Sci* **176:** 433-443.

Beyer A., Hollunder J., Nasheuer H. P., & Wilhelm T. (2004) Post-transcriptional expression regulation in the yeast Saccharomyces cerevisiae on a genomic scale. *Mol Cell Proteomics* **3:** 1083-1092.

Bittman R., Kasireddy C. R., Mattjus P., & Slotte J. P. (1994) Interaction of cholesterol with sphingomyelin in monolayers and vesicles. *Biochemistry* **33:** 11776-11781.

Blaise R., Grober J., Rouet P., Tavernier G., Daegelen D., & Langin D. (1999) Testis expression of hormone-sensitive lipase is conferred by a specific promoter that contains four regions binding testicular nuclear proteins. *J Biol Chem* **274:** 9327-9334.

Blaise R., Guillaudeux T., Tavernier G., Daegelen D., Evrard B., Mairal A., Holm C., Jegou B., & Langin D. (2001) Testis hormone-sensitive lipase expression in spermatids is governed by a short promoter in transgenic mice. *J Biol Chem* **276:** 5109-5115.

Boggs J. M. (1987) Lipid intermolecular hydrogen bonding: influence on structural organization and membrane function. *Biochim Biophys Acta* **906:** 353-404.

Bradford M. M. (1976) A rapid and sensitive method for the quantitation of microgram quantities of protein utilizing the principle of protein-dye binding. *Anal Biochem* **72:** 248-254.

Brown A. J. (2007) Cholesterol, statins and cancer. *Clin Exp Pharmacol Physiol* **34:** 135-141.

Brown M. S., & Goldstein J. L. (1980) Multivalent feedback regulation of HMG CoA reductase, a control mechanism coordinating isoprenoid synthesis and cell growth. *J Lipid Res* **21:** 505-517.

Brown M. S., & Goldstein J. L. (1986) A receptor-mediated pathway for cholesterol homeostasis. *Science* **232:** 34-47.

Brown M. S., & Goldstein J. L. (1997) The SREBP pathway: regulation of cholesterol metabolism by proteolysis of a membrane-bound transcription factor. *Cell* **89:** 331-340.

Buhman K. F., Accad M., & Farese R. V. (2000) Mammalian acyl-CoA:cholesterol acyltransferases. *Biochim Biophys Acta* **1529:** 142-154.

Byskov A. G., Andersen C. Y., Leonardsen L., & Baltsen M. (1999) Meiosis activating sterols (MAS) and fertility in mammals and man. *J Exp Zool* **285:** 237-242.

Carmen G. Y., & Victor S. M. (2006) Signalling mechanisms regulating lipolysis. *Cell Signal* **18:** 401-408.

Cases S., Novak S., Zheng Y. W., Myers H. M., Lear S. R., Sande E., Welch C. B., Lusis A. J., Spencer T. A., Krause B. R., Erickson S. K., & Farese R. V., Jr. (1998a) ACAT-2, a second mammalian acyl-CoA:cholesterol acyltransferase. Its cloning, expression, and characterization. *J Biol Chem* **273:** 26755-26764.

Cases S., Smith S. J., Zheng Y. W., Myers H. M., Lear S. R., Sande E., Novak S., Collins C., Welch C. B., Lusis A. J., Erickson S. K., & Farese R. V., Jr. (1998b) Identification of a gene encoding an acyl CoA:diacylglycerol acyltransferase, a key enzyme in triacylglycerol synthesis. *Proc Natl Acad Sci U S A* **95:** 13018-13023.

Cavicchia J. C., & Miranda J. C. (1988) The blood-testis barrier in lizards during the annual spermatogenic cycle. *Microsc Electron Biol Celular* **12:** 73-87.

Cavicchia J. C., & Sacerdote F. L. (1991) Correlation between blood-testis barrier development and onset of the first spermatogenic wave in normal and in busulfan-treated rats: a lanthanum and freeze-fracture study. *Anat Rec* **230:** 361-368.

Cerolini S., Kelso K. A., Noble R. C., Speake B. K., Pizzi F., & Cavalchini L. G. (1997) Relationship between spermatozoan lipid composition and fertility during aging of chickens. *Biol Reprod* **57:** 976-980.

Chambers C. M., & Ness G. C. (1998) Dietary cholesterol regulates hepatic 3-hydroxy-3-methylglutaryl coenzyme A reductase gene expression in rats primarily at the level of translation. *Arch Biochem Biophys* **354:** 317-322.

Chang C. C., Huh H. Y., Cadigan K. M., & Chang T. Y. (1993) Molecular cloning and functional expression of human acyl-coenzyme A:cholesterol acyltransferase cDNA in mutant Chinese hamster ovary cells. *J Biol Chem* **268:** 20747-20755.

Chang C. C., Lee C. Y., Chang E. T., Cruz J. C., Levesque M. C., & Chang T. Y. (1998) Recombinant acyl-CoA:cholesterol acyltransferase-1 (ACAT-1) purified to essential homogeneity utilizes cholesterol in mixed micelles or in vesicles in a highly cooperative manner. *J Biol Chem* **273:** 35132-35141.

Chang C. C., Noll W. W., Nutile-McMenemy N., Lindsay E. A., Baldini A., Chang W., & Chang T. Y. (1994) Localization of acyl coenzyme A:cholesterol acyltransferase gene to human chromosome 1q25. *Somat Cell Mol Genet* **20:** 71-74.

Chang C. C., Sakashita N., Ornvold K., Lee O., Chang E. T., Dong R., Lin S., Lee C. Y., Strom S. C., Kashyap R., Fung J. J., Farese R. V., Jr., Patoiseau J. F., Delhon A., & Chang T. Y. (2000) Immunological quantitation and localization of ACAT-1 and ACAT-2 in human liver and small intestine. *J Biol Chem* **275:** 28083-28092.

Chang T. Y., Chang C. C., & Cheng D. (1997) Acyl-coenzyme A:cholesterol acyltransferase. *Annu Rev Biochem* **66:** 613-638.

Chang T. Y., Chang C. C., Lin S., Yu C., Li B. L., & Miyazaki A. (2001a) Roles of acyl-coenzyme A:cholesterol acyltransferase-1 and -2. *Curr Opin Lipidol* **12:** 289-296.

Chang T. Y., Chang C. C., Lu X., & Lin S. (2001b) Catalysis of ACAT may be completed within the plane of the membrane: a working hypothesis. *J Lipid Res* **42:** 1933-1938.

Chen J. J., Lukyanenko Y., & Hutson J. C. (2002) 25-hydroxycholesterol is produced by testicular macrophages during the early postnatal period and influences differentiation of Leydig cells in vitro. *Biol Reprod* **66:** 1336-1341.

Chen L., Lafond J., Pelletier R.M. (2009) A novel technical approach for the measurement of individual ACAT-1 and ACAT-2 enzymatic activity in the testis. In: Human embryogenesis: Methods and protocols. Julie Lafond & Cathy Vaillancourt. (eds) The Humana Press Inc. Press Totowa NJ

Chin D. J., Gil G., Russell D. W., Liscum L., Luskey K. L., Basu S. K., Okayama H., Berg P., Goldstein J. L., & Brown M. S. (1984) Nucleotide sequence of 3-hydroxy-3-methyl-glutaryl coenzyme A reductase, a glycoprotein of endoplasmic reticulum. *Nature* **308:** 613-617.

Cho K. H., An S., Lee W. S., Paik Y. K., Kim Y. K., & Jeong T. S. (2003) Mass-production of human ACAT-1 and ACAT-2 to screen isoform-specific inhibitor: a different substrate specificity and inhibitory regulation. *Biochem Biophys Res Commun* **309:** 864-872.

Chung S., Wang S. P., Pan L., Mitchell G., Trasler J., & Hermo L. (2001) Infertility and testicular defects in hormone-sensitive lipase-deficient mice. *Endocrinology* **142:** 4272-4281.

Clarke C. F., Fogelman A. M., & Edwards P. A. (1984) Diurnal rhythm of rat liver mRNAs encoding 3-hydroxy-3-methylglutaryl coenzyme A reductase. Correlation of functional and total mRNA levels with enzyme activity and protein. *J Biol Chem* **259:** 10439-10447.

Clegg E. J. (1963) Studies on Artificial Cryptorchidism: Degenerative and Regenerative Changes in the Germinal Epithelium of the Rat Testis. *J Endocrinol* **27:** 241-251.

Clermont Y. (1972) Kinetics of spermatogenesis in mammals: seminiferous epithelium cycle and spermatogonial renewal. *Physiol Rev* **52:** 198-236.

Contreras J. A. (2002) Hormone-sensitive lipase is not required for cholesteryl ester hydrolysis in macrophages. *Biochem Biophys Res Commun* **292:** 900-903.

Cook K. G., Yeaman S. J., Stralfors P., Fredrikson G., & Belfrage P. (1982) Direct evidence that cholesterol ester hydrolase from adrenal cortex is the same enzyme as hormone-sensitive lipase from adipose tissue. *Eur J Biochem* **125:** 245-249.

Corton J. M., & Hardie D. G. (1992) Evidence against a role for phosphorylation/dephosphorylation in the regulation of acyl-CoA:cholesterol acyl transferase. *Eur J Biochem* **204:** 203-208.

Davignon J. (2004) Beneficial cardiovascular pleiotropic effects of statins. *Circulation* **109:** III39-43.

De Rooij D. G., Van Dissel-Emiliani F. M., & Van Pelt A. M. (1989) Regulation of spermatogonial proliferation. *Ann N Y Acad Sci* **564:** 140-153.

DeBose-Boyd R. A. (2008) Feedback regulation of cholesterol synthesis: sterol-accelerated ubiquitination and degradation of HMG CoA reductase. *Cell Res* **18:** 609-621.

Delmas V., van der Hoorn F., Mellstrom B., Jegou B., & Sassone-Corsi P. (1993) Induction of CREM activator proteins in spermatids: down-stream targets and implications for haploid germ cell differentiation. *Mol Endocrinol* **7:** 1502-1514.

Djakoure C., Guibourdenche J., Porquet D., Pagesy P., Peillon F., Li J. Y., & Evain-Brion D. (1996) Vitamin A and retinoic acid stimulate within minutes cAMP release and growth hormone secretion in human pituitary cells. *J Clin Endocrinol Metab* **81:** 3123-3126.

Dove D. E., Su Y. R., Swift L. L., Linton M. F., & Fazio S. (2006) ACAT1 deficiency increases cholesterol synthesis in mouse peritoneal macrophages. *Atherosclerosis* **186:** 267-274.

Dove D. E., Su Y. R., Zhang W., Jerome W. G., Swift L. L., Linton M. F., & Fazio S. (2005) ACAT1 deficiency disrupts cholesterol efflux and alters cellular morphology in macrophages. *Arterioscler Thromb Vasc Biol* **25:** 128-134.

Duncan R. E., El-Sohemy A., & Archer M. C. (2005) Dietary factors and the regulation of 3-hydroxy-3-methylglutaryl coenzyme A reductase: implications for breast cancer and development. *Mol Nutr Food Res* **49:** 93-100.

Dym M., & Cavicchia J. C. (1977) Further observations on the blood-testis barrier in monkeys. *Biol Reprod* **17:** 390-403.

Dym M., & Cavicchia J. C. (1978) Functional morphology of the testis. *Biol Reprod* **18:** 1-15.

Easom R. A., & Zammit V. A. (1987) Acute effects of starvation and treatment of rats with anti-insulin serum, glucagon and catecholamines on the state of phosphorylation of hepatic 3-hydroxy-3-methylglutaryl-CoA reductase in vivo. *Biochem J* **241:** 183-188.

Eberle D., Hegarty B., Bossard P., Ferre P., & Foufelle F. (2004) SREBP transcription factors: master regulators of lipid homeostasis. *Biochimie* **86:** 839-848.

Einarsson K., Benthin L., Ewerth S., Hellers G., Stahlberg D., & Angelin B. (1989) Studies on acyl-coenzyme A: cholesterol acyltransferase activity in human liver microsomes. *J Lipid Res* **30:** 739-746.

Erickson S. K., Shrewsbury M. A., Brooks C., & Meyer D. J. (1980) Rat liver acyl-coenzyme A:cholesterol acyltransferase: its regulation in vivo and some of its properties in vitro. *J Lipid Res* **21:** 930-941.

Escary J. L., Choy H. A., Reue K., & Schotz M. C. (1998) Hormone-sensitive lipase overexpression increases cholesteryl ester hydrolysis in macrophage foam cells. *Arterioscler Thromb Vasc Biol* **18:** 991-998.

Fawcett D. W., Neaves W. B., & Flores M. N. (1973) Comparative observations on intertubular lymphatics and the organization of the interstitial tissue of the mammalian testis. *Biol Reprod* **9:** 500-532.

Fazio S., Major A. S., Swift L. L., Gleaves L. A., Accad M., Linton M. F., & Farese R. V., Jr. (2001) Increased atherosclerosis in LDL receptor-null mice lacking ACAT1 in macrophages. *J Clin Invest* **107:** 163-171.

Febbraio M., Abumrad N. A., Hajjar D. P., Sharma K., Cheng W., Pearce S. F., & Silverstein R. L. (1999) A null mutation in murine CD36 reveals an important role in fatty acid and lipoprotein metabolism. *J Biol Chem* **274:** 19055-19062.

Febbraio M., Guy E., Coburn C., Knapp F. F., Jr., Beets A. L., Abumrad N. A., & Silverstein R. L. (2002) The impact of overexpression and deficiency of fatty acid translocase (FAT)/CD36. *Mol Cell Biochem* **239:** 193-197.

Febbraio M., Hajjar D. P., & Silverstein R. L. (2001) CD36: a class B scavenger receptor involved in angiogenesis, atherosclerosis, inflammation, and lipid metabolism. *J Clin Invest* **108:** 785-791.

Field F. J., Erickson S. K., Shrewsbury M. A., & Cooper A. D. (1982) 3-hydroxy-3-methylglutaryl coenzyme A reductase from rat intestine: subcellular localization and in vitro regulation. *J Lipid Res* **23:** 105-113.

Fon Tacer K., Kalanj-Bognar S., Waterman M. R., & Rozman D. (2003) Lanosterol metabolism and sterol regulatory element binding protein (SREBP) expression in male germ cell maturation. *J Steroid Biochem Mol Biol* **85:** 429-438.

Foulkes N. S., Mellstrom B., Benusiglio E., & Sassone-Corsi P. (1992) Developmental switch of CREM function during spermatogenesis: from antagonist to activator. *Nature* **355:** 80-84.

Garton A. J., Campbell D. G., Carling D., Hardie D. G., Colbran R. J., & Yeaman S. J. (1989) Phosphorylation of bovine hormone-sensitive lipase by the AMP-activated protein kinase. A possible antilipolytic mechanism. *Eur J Biochem* **179:** 249-254.

Garton A. J., & Yeaman S. J. (1990) Identification and role of the basal phosphorylation site on hormone-sensitive lipase. *Eur J Biochem* **191:** 245-250.

Gibbons G. F., Pullinger C. R., Chen H. W., Cavenee W. K., & Kandutsch A. A. (1980) Regulation of cholesterol biosynthesis in cultured cells by probable natural precursor sterols. *J Biol Chem* **255:** 395-400.

Gibson D., & Parker R. (1986) Control of HMG CoA reductase by reversible phosphorylation. In: The enzyme: Enzyme control by phosphorylation Krebs EG (eds), Academic Press, New York., . pp.235-257.

Gil G., Goldstein J. L., Slaughter C. A., & Brown M. S. (1986) Cytoplasmic 3-hydroxy-3-methylglutaryl coenzyme A synthase from the hamster. I. Isolation and sequencing of a full-length cDNA. *J Biol Chem* **261:** 3710-3716.

Gillot I., Jehl-Pietri C., Gounon P., Luquet S., Rassoulzadegan M., Grimaldi P., & Vidal F. (2005) Germ cells and fatty acids induce translocation of CD36 scavenger receptor to the plasma membrane of Sertoli cells. *J Cell Sci* **118:** 3027-3035.

Goldstein J. L., & Brown M. S. (1990) Regulation of the mevalonate pathway. *Nature* **343:** 425-430.

Goldstein J. L., Rawson R. B., & Brown M. S. (2002) Mutant mammalian cells as tools to delineate the sterol regulatory element-binding protein pathway for feedback regulation of lipid synthesis. *Arch Biochem Biophys* **397:** 139-148.

Goodman D. S., Deykin D., & Shiratori T. (1964) The Formation of Cholesterol Esters with Rat Liver Enzymes. *J Biol Chem* **239:** 1335-1345.

Graaf M. R., Richel D. J., van Noorden C. J., & Guchelaar H. J. (2004) Effects of statins and farnesyltransferase inhibitors on the development and progression of cancer. *Cancer Treat Rev* **30:** 609-641.

Greenberg A. S., Shen W. J., Muliro K., Patel S., Souza S. C., Roth R. A., & Kraemer F. B. (2001) Stimulation of lipolysis and hormone-sensitive lipase via the extracellular signal-regulated kinase pathway. *J Biol Chem* **276:** 45456-45461.

Griswold M. D., Bishop P. D., Kim K. H., Ping R., Siiteri J. E., & Morales C. (1989) Function of vitamin A in normal and synchronized seminiferous tubules. *Ann N Y Acad Sci* **564:** 154-172.

Grober J., Laurell H., Blaise R., Fabry B., Schaak S., Holm C., & Langin D. (1997) Characterization of the promoter of human adipocyte hormone-sensitive lipase. *Biochem J* **328 (Pt 2):** 453-461.

Grober J., Lucas S., Sorhede-Winzell M., Zaghini I., Mairal A., Contreras J. A., Besnard P., Holm C., & Langin D. (2003) Hormone-sensitive lipase is a cholesterol esterase of the intestinal mucosa. *J Biol Chem* **278:** 6510-6515.

Guo Z. Y., Lin S., Heinen J. A., Chang C. C., & Chang T. Y. (2005) The active site His-460 of human acyl-coenzyme A:cholesterol acyltransferase 1 resides in a hitherto undisclosed transmembrane domain. *J Biol Chem* **280:** 37814-37826.

Haemmerle G., Zimmermann R., Hayn M., Theussl C., Waeg G., Wagner E., Sattler W., Magin T. M., Wagner E. F., & Zechner R. (2002) Hormone-sensitive lipase deficiency in mice causes diglyceride accumulation in adipose tissue, muscle, and testis. *J Biol Chem* **277:** 4806-4815.

Haemmerle G., Zimmermann R., & Zechner R. (2003) Letting lipids go: hormone-sensitive lipase. *Curr Opin Lipidol* **14:** 289-297.

Hamilton J. J., Auestad N., & Innis S. M. (1994) A comparative study of hepatic HMG CoA reductase activity and LDL receptor relative mass in suckling and adult guinea pigs. *Biol Neonate* **65:** 317-325.

Hampton R. Y. (2002) ER-associated degradation in protein quality control and cellular regulation. *Curr Opin Cell Biol* **14:** 476-482.

Hardeman E. C., Jenke H. S., & Simoni R. D. (1983) Overproduction of a Mr 92,000 protomer of 3-hydroxy-3-methylglutaryl-coenzyme A reductase in compactin-resistant C100 cells. *Proc Natl Acad Sci U S A* **80:** 1516-1520.

Harries L. W., Ellard S., Jones R. W., Hattersley A. T., & Bingham C. (2004) Abnormal splicing of hepatocyte nuclear factor-1 beta in the renal cysts and diabetes syndrome. *Diabetologia* **47:** 937-942.

Hegardt F. G. (1999) Mitochondrial 3-hydroxy-3-methylglutaryl-CoA synthase: a control enzyme in ketogenesis. *Biochem J* **338 (Pt 3):** 569-582.

Hermo L., Chung S., Gregory M., Smith C. E., Wang S. P., El-Alfy M., Cyr D. G., Mitchell G. A., & Trasler J. (2008) Alterations in the testis of hormone sensitive lipase-deficient mice is associated with decreased sperm counts, sperm motility, and fertility. *Mol Reprod Dev* **75:** 565-577.

Herrada G., & Wolgemuth D. J. (1997) The mouse transcription factor Stat4 is expressed in haploid male germ cells and is present in the perinuclear theca of spermatozoa. *J Cell Sci* **110 (Pt 14):** 1543-1553.

Higgins M., Kawachi T., & Rudney H. (1971) The mechanism of the diurnal variation of hepatic HMG-CoA reductase activity in the rat. *Biochem Biophys Res Commun* **45:** 138-144.

Hochereau-de Reviers M. T., & Lincoln G. A. (1978) Seasonal variation in the histology of the testis of the red deer, Cervus elaphus. *J Reprod Fertil* **54:** 209-213.

Hofmann K. (2000) A superfamily of membrane-bound O-acyltransferases with implications for wnt signaling. *Trends Biochem Sci* **25:** 111-112.

Holm C. (2003) Molecular mechanisms regulating hormone-sensitive lipase and lipolysis. *Biochem Soc Trans* **31:** 1120-1124.

Holm C., Belfrage P., & Fredrikson G. (1987) Immunological evidence for the presence of hormone-sensitive lipase in rat tissues other than adipose tissue. *Biochem Biophys Res Commun* **148:** 99-105.

Holm C., Kirchgessner T. G., Svenson K. L., Fredrikson G., Nilsson S., Miller C. G., Shively J. E., Heinzmann C., Sparkes R. S., Mohandas T., & et al. (1988) Hormone-sensitive lipase: sequence, expression, and chromosomal localization to 19 cent-q13.3. *Science* **241:** 1503-1506.

Holm C., & Osterlund T. (1999) Hormone-sensitive lipase and neutral cholesteryl ester lipase. *Methods Mol Biol* **109:** 109-121.

Holm C., Osterlund T., Laurell H., & Contreras J. A. (2000) Molecular mechanisms regulating hormone-sensitive lipase and lipolysis. *Annu Rev Nutr* **20:** 365-393.

Holst L. S., Hoffmann A. M., Mulder H., Sundler F., Holm C., Bergh A., & Fredrikson G. (1994) Localization of hormone-sensitive lipase to rat Sertoli cells and its expression in developing and degenerating testes. *FEBS Lett* **355:** 125-130.

Holst L. S., Langin D., Mulder H., Laurell H., Grober J., Bergh A., Mohrenweiser H. W., Edgren G., & Holm C. (1996) Molecular cloning, genomic organization, and expression of a testicular isoform of hormone-sensitive lipase. *Genomics* **35:** 441-447.

Horton J. D., Goldstein J. L., & Brown M. S. (2002) SREBPs: activators of the complete program of cholesterol and fatty acid synthesis in the liver. *J Clin Invest* **109:** 1125-1131.

Hoshi K., Aita T., Yanagida K., Yoshimatsu N., & Sato A. (1990) Variation in the cholesterol/phospholipid ratio in human spermatozoa and its relationship with capacitation. *Hum Reprod* **5:** 71-74.

Hou J. W., Collins D. C., & Schleicher R. L. (1990) Sources of cholesterol for testosterone biosynthesis in murine Leydig cells. *Endocrinology* **127:** 2047-2055.

Hutson J. C. (1992) Development of cytoplasmic digitations between Leydig cells and testicular macrophages of the rat. *Cell Tissue Res* **267:** 385-389.

Ichihara I. (1969) Cholesterol changes in developing testicular interstitial cells of the mouse: histochemical and biochemical study. *Anat Rec* **163:** 595-601.

Ikenoya M., Yoshinaka Y., Kobayashi H., Kawamine K., Shibuya K., Sato F., Sawanobori K., Watanabe T., & Miyazaki A. (2007) A selective ACAT-1 inhibitor, K-604, suppresses fatty streak lesions in fat-fed hamsters without affecting plasma cholesterol levels. *Atherosclerosis* **191:** 290-297.

Istvan E. S., Palnitkar M., Buchanan S. K., & Deisenhofer J. (2000) Crystal structure of the catalytic portion of human HMG-CoA reductase: insights into regulation of activity and catalysis. *Embo J* **19:** 819-830.

Jeong T. S., Kim S. U., Son K. H., Kwon B. M., Kim Y. K., Choi M. U., & Bok S. H. (1995) GERI-BP001 compounds, new inhibitors of acyl-CoA: cholesterol acyltransferase from Aspergillus fumigatus F37. I. Production, isolation, and physico-chemical and biological properties. *J Antibiot (Tokyo)* **48:** 751-756.

Ji Y., Jian B., Wang N., Sun Y., Moya M. L., Phillips M. C., Rothblat G. H., Swaney J. B., & Tall A. R. (1997) Scavenger receptor BI promotes high density lipoprotein-mediated cellular cholesterol efflux. *J Biol Chem* **272:** 20982-20985.

Jingami H., Brown M. S., Goldstein J. L., Anderson R. G., & Luskey K. L. (1987) Partial deletion of membrane-bound domain of 3-hydroxy-3-methylglutaryl coenzyme A reductase eliminates sterol-enhanced degradation and prevents formation of crystalloid endoplasmic reticulum. *J Cell Biol* **104:** 1693-1704.

Joyce C., Skinner K., Anderson R. A., & Rudel L. L. (1999) Acyl-coenzyme A:cholesteryl acyltransferase 2. *Curr Opin Lipidol* **10:** 89-95.

Joyce C. W., Shelness G. S., Davis M. A., Lee R. G., Skinner K., Anderson R. A., & Rudel L. L. (2000) ACAT1 and ACAT2 membrane topology segregates a serine residue essential for activity to opposite sides of the endoplasmic reticulum membrane. *Mol Biol Cell* **11:** 3675-3687.

Kabbaj O., Holm C., Vitale M. L., & Pelletier R. M. (2001) Expression, activity, and subcellular localization of testicular hormone-sensitive lipase during postnatal development in the guinea pig. *Biol Reprod* **65:** 601-612.

Kabbaj O., Yoon S. R., Holm C., Rose J., Vitale M. L., & Pelletier R. M. (2003) Relationship of the hormone-sensitive lipase-mediated modulation of cholesterol metabolism in individual compartments of the testis to serum pituitary hormone and testosterone concentrations in a seasonal breeder, the mink (Mustela vison). *Biol Reprod* **68:** 722-734.

Kennelly P. J., & Rodwell V. W. (1985) Regulation of 3-hydroxy-3-methylglutaryl coenzyme A reductase by reversible phosphorylation-dephosphorylation. *J Lipid Res* **26:** 903-914.

Kerr J. B., Mayberry R. A., & Irby D. C. (1984) Morphometric studies on lipid inclusions in Sertoli cells during the spermatogenic cycle in the rat. *Cell Tissue Res* **236:** 699-709.

Kim D. H., Iijima H., Goto K., Sakai J., Ishii H., Kim H. J., Suzuki H., Kondo H., Saeki S., & Yamamoto T. (1996) Human apolipoprotein E receptor 2. A novel lipoprotein receptor of the low density lipoprotein receptor family predominantly expressed in brain. *J Biol Chem* **271:** 8373-8380.

Kozarsky K. F., Donahee M. H., Rigotti A., Iqbal S. N., Edelman E. R., & Krieger M. (1997) Overexpression of the HDL receptor SR-BI alters plasma HDL and bile cholesterol levels. *Nature* **387:** 414-417.

Kraemer F. B., Patel S., Saedi M. S., & Sztalryd C. (1993a) Detection of hormone-sensitive lipase in various tissues. I. Expression of an HSL/bacterial fusion protein and generation of anti-HSL antibodies. *J Lipid Res* **34:** 663-671.

Kraemer F. B., Patel S., Singh-Bist A., Gholami S. S., Saedi M. S., & Sztalryd C. (1993b) Detection of hormone-sensitive lipase in various tissues. II. Regulation in the rat testis by human chorionic gonadotropin. *J Lipid Res* **34:** 609-616.

Kraemer F. B., & Shen W. J. (2002) Hormone-sensitive lipase: control of intracellular tri-(di-)acylglycerol and cholesteryl ester hydrolysis. *J Lipid Res* **43:** 1585-1594.

Kraemer F. B., Tavangar K., & Hoffman A. R. (1991) Developmental regulation of hormone-sensitive lipase mRNA in the rat: changes in steroidogenic tissues. *J Lipid Res* **32:** 1303-1310.

Langfort J., Ploug T., Ihlemann J., Saldo M., Holm C., & Galbo H. (1999) Expression of hormone-sensitive lipase and its regulation by adrenaline in skeletal muscle. *Biochem J* **340 (Pt 2):** 459-465.

Langin D., Laurell H., Holst L. S., Belfrage P., & Holm C. (1993) Gene organization and primary structure of human hormone-sensitive lipase: possible significance of a sequence homology with a lipase of Moraxella TA144, an antarctic bacterium. *Proc Natl Acad Sci U S A* **90:** 4897-4901.

Large V., Arner P., Reynisdottir S., Grober J., Van Harmelen V., Holm C., & Langin D. (1998) Hormone-sensitive lipase expression and activity in relation to lipolysis in human fat cells. *J Lipid Res* **39:** 1688-1695.

Leblond C. P., & Clermont Y. (1952) Definition of the stages of the cycle of the seminiferous epithelium in the rat. *Ann N Y Acad Sci* **55:** 548-573.

Lee J. Y., & Carr T. P. (2004) Dietary fatty acids regulate acyl-CoA:cholesterol acyltransferase and cytosolic cholesteryl ester hydrolase in hamsters. *J Nutr* **134:** 3239-3244.

Lee O., Chang C. C., Lee W., & Chang T. Y. (1998) Immunodepletion experiments suggest that acyl-coenzyme A:cholesterol acyltransferase-1 (ACAT-1) protein plays a major catalytic role in adult human liver, adrenal gland, macrophages, and kidney, but not in intestines. *J Lipid Res* **39:** 1722-1727.

Lee R. G., Willingham M. C., Davis M. A., Skinner K. A., & Rudel L. L. (2000) Differential expression of ACAT1 and ACAT2 among cells within liver, intestine, kidney, and adrenal of nonhuman primates. *J Lipid Res* **41:** 1991-2001.

Lee W. S., Lee D. W., Baek Y. I., An S. J., Cho K. H., Choi Y. K., Kim H. C., Park H. Y., Bae K. H., & Jeong T. S. (2004) Human ACAT-1 and -2 inhibitory activities of saucerneol B, manassantin A and B isolated from Saururus chinensis. *Bioorg Med Chem Lett* **14:** 3109-3112.

Leydig F. (1850) Zur anatomie der männlichen Geschlechtsorgane und Analdrusen der Säugethiere. *Zeit Zool* **2:** 1-57.

Li B. L., Li X. L., Duan Z. J., Lee O., Lin S., Ma Z. M., Chang C. C., Yang X. Y., Park J. P., Mohandas T. K., Noll W., Chan L., & Chang T. Y. (1999) Human acyl-CoA:cholesterol acyltransferase-1 (ACAT-1) gene organization and evidence that the 4.3-kilobase ACAT-1 mRNA is produced from two different chromosomes. *J Biol Chem* **274:** 11060-11071.

Lin S., Cheng D., Liu M. S., Chen J., & Chang T. Y. (1999) Human acyl-CoA:cholesterol acyltransferase-1 in the endoplasmic reticulum contains seven transmembrane domains. *J Biol Chem* **274:** 23276-23285.

Lin S., Lu X., Chang C. C., & Chang T. Y. (2003) Human acyl-coenzyme A:cholesterol acyltransferase expressed in chinese hamster ovary cells: membrane topology and active site location. *Mol Biol Cell* **14:** 2447-2460.

Lipsett M. B., Wilson H., Kirschner M. A., Korenman S. G., Fishman L. M., Sarfaty G. A., & Bardin C. W. (1966) Studies on Leydig cell physiology and pathology: secretion and metabolism of testosterone. *Recent Prog Horm Res* **22:** 245-281.

Liscum L., Finer-Moore J., Stroud R. M., Luskey K. L., Brown M. S., & Goldstein J. L. (1985) Domain structure of 3-hydroxy-3-methylglutaryl coenzyme A reductase, a glycoprotein of the endoplasmic reticulum. *J Biol Chem* **260:** 522-530.

Liu J., Chang C. C., Westover E. J., Covey D. F., & Chang T. Y. (2005) Investigating the allosterism of acyl-CoA:cholesterol acyltransferase (ACAT) by using various sterols: in vitro and intact cell studies. *Biochem J* **391:** 389-397.

Lofts B., & Boswell C. (1960) Cyclical changes in the distribution of the testis lipids in the common frog, Rana temporaria. *Nature* **187:** 708-709.

Londos C., Brasaemle D. L., Schultz C. J., Adler-Wailes D. C., Levin D. M., Kimmel A. R., & Rondinone C. M. (1999) On the control of lipolysis in adipocytes. *Ann N Y Acad Sci* **892:** 155-168.

Lufkin T., Lohnes D., Mark M., Dierich A., Gorry P., Gaub M. P., LeMeur M., & Chambon P. (1993) High postnatal lethality and testis degeneration in retinoic acid receptor alpha mutant mice. *Proc Natl Acad Sci U S A* **90:** 7225-7229.

Lukyanenko Y. O., Chen J. J., & Hutson J. C. (2001) Production of 25-hydroxycholesterol by testicular macrophages and its effects on Leydig cells. *Biol Reprod* **64:** 790-796.

Luskey K. L., Faust J. R., Chin D. J., Brown M. S., & Goldstein J. L. (1983) Amplification of the gene for 3-hydroxy-3-methylglutaryl coenzyme A reductase, but not for the 53-kDa protein, in UT-1 cells. *J Biol Chem* **258:** 8462-8469.

Mairal A., Melaine N., Laurell H., Grober J., Holst L. S., Guillaudeux T., Holm C., Jegou B., & Langin D. (2002) Characterization of a novel testicular form of human hormone-sensitive lipase. *Biochem Biophys Res Commun* **291:** 286-290.

Martens L. L., & Guibert R. (1994) Cost-effectiveness analysis of lipid-modifying therapy in Canada: comparison of HMG-CoA reductase inhibitors in the primary prevention of coronary heart disease. *Clin Ther* **16:** 1052-1062; discussion 1036.

McPherson R., & Gauthier A. (2004) Molecular regulation of SREBP function: the Insig-SCAP connection and isoform-specific modulation of lipid synthesis. *Biochem Cell Biol* **82:** 201-211.

Meiner V. L., Cases S., Myers H. M., Sande E. R., Bellosta S., Schambelan M., Pitas R. E., McGuire J., Herz J., & Farese R. V., Jr. (1996) Disruption of the acyl-CoA:cholesterol acyltransferase gene in mice: evidence suggesting multiple cholesterol esterification enzymes in mammals. *Proc Natl Acad Sci U S A* **93:** 14041-14046.

Miettinen H. E., Rayburn H., & Krieger M. (2001) Abnormal lipoprotein metabolism and reversible female infertility in HDL receptor (SR-BI)-deficient mice. *J Clin Invest* **108:** 1717-1722.

Miller S. J., Parker R. A., & Gibson D. M. (1989) Phosphorylation and degradation of HMG CoA reductase. *Adv Enzyme Regul* **28:** 65-77.

Montoudis A., Boileau S., Simoneau L., Mounier C., & Lafond J. (2004) Evaluation of 3-hydroxy-3-methylglutaryl-COA-reductase, cholesterol-7alpha-hydroxylase and acyl-COA:cholesterol acyltransferase activities: alternative chromatographic methods to separate metabolites. *Biomed Chromatogr* **18:** 706-713.

Mulder H., Holst L. S., Svensson H., Degerman E., Sundler F., Ahren B., Rorsman P., & Holm C. (1999) Hormone-sensitive lipase, the rate-limiting enzyme in triglyceride hydrolysis, is expressed and active in beta-cells. *Diabetes* **48:** 228-232.

Mulder H., Sorhede-Winzell M., Contreras J. A., Fex M., Strom K., Ploug T., Galbo H., Arner P., Lundberg C., Sundler F., Ahren B., & Holm C. (2003) Hormone-sensitive lipase null mice exhibit signs of impaired insulin sensitivity whereas insulin secretion is intact. *J Biol Chem* **278:** 36380-36388.

Nes W. D., Lukyanenko Y. O., Jia Z. H., Quideau S., Howald W. N., Pratum T. K., West R. R., & Hutson J. C. (2000) Identification of the lipophilic factor produced by macrophages that stimulates steroidogenesis. *Endocrinology* **141:** 953-958.

Ness G. C. (1994) Developmental regulation of the expression of genes encoding proteins involved in cholesterol homeostasis. *Am J Med Genet* **50:** 355-357.

Ness G. C., & Chambers C. M. (2000) Feedback and hormonal regulation of hepatic 3-hydroxy-3-methylglutaryl coenzyme A reductase: the concept of cholesterol buffering capacity. *Proc Soc Exp Biol Med* **224:** 8-19.

Ness G. C., Eales S., Lopez D., & Zhao Z. (1994) Regulation of 3-hydroxy-3-methylglutaryl coenzyme A reductase gene expression by sterols and nonsterols in rat liver. *Arch Biochem Biophys* **308:** 420-425.

Ness G. C., Gertz K. R., & Holland R. C. (2001) Regulation of hepatic lanosterol 14 alpha-demethylase gene expression by dietary cholesterol and cholesterol-lowering agents. *Arch Biochem Biophys* **395:** 233-238.

Ness G. C., & Nazian S. J. (1992) Developmental expression of multiple forms of 3-hydroxy-3-methylglutaryl coenzyme A reductase mRNA in rat testes. *J Androl* **13:** 318-322.

Nguyen L. B., Shefer S., Salen G., Ness G. C., Tint G. S., Zaki F. G., & Rani I. (1990) A molecular defect in hepatic cholesterol biosynthesis in sitosterolemia with xanthomatosis. *J Clin Invest* **86:** 923-931.

Nwokoro N. A., Wassif C. A., & Porter F. D. (2001) Genetic disorders of cholesterol biosynthesis in mice and humans. *Mol Genet Metab* **74:** 105-119.

Ohata M. (1979) Electron microscope study on the bat testicular interstitial cell with special reference to the cytoplasmic crystalloid. *Arch Histol Jpn* **42:** 103-118.

Osborne T. F., Goldstein J. L., & Brown M. S. (1985) 5' end of HMG CoA reductase gene contains sequences responsible for cholesterol-mediated inhibition of transcription. *Cell* **42:** 203-212.

Osterlund T. (2001) Structure-function relationships of hormone-sensitive lipase. *Eur J Biochem* **268:** 1899-1907.

Osuga J., Ishibashi S., Oka T., Yagyu H., Tozawa R., Fujimoto A., Shionoiri F., Yahagi N., Kraemer F. B., Tsutsumi O., & Yamada N. (2000) Targeted disruption of hormone-sensitive lipase results in male sterility and adipocyte hypertrophy, but not in obesity. *Proc Natl Acad Sci U S A* **97:** 787-792.

Panda T., & Devi V. A. (2004) Regulation and degradation of HMGCo-A reductase. *Appl Microbiol Biotechnol* **66:** 143-152.

Panini S. R., Delate T. A., & Sinensky M. (1992) Post-transcriptional regulation of 3-hydroxy-3-methylglutaryl coenzyme A reductase by 24(S),25-oxidolanosterol. *J Biol Chem* **267:** 12647-12654.

Pape M. E., Schultz P. A., Rea T. J., DeMattos R. B., Kieft K., Bisgaier C. L., Newton R. S., & Krause B. R. (1995) Tissue specific changes in acyl-CoA: cholesterol acyltransferase (ACAT) mRNA levels in rabbits. *J Lipid Res* **36:** 823-838.

Pelletier R. M. (1986) Cyclic formation and decay of the blood-testis barrier in the mink (Mustela vison), a seasonal breeder. *Am J Anat* **175:** 91-117.

Pelletier R. M. (1995) The distribution of connexin 43 is associated with the germ cell differentiation and with the modulation of the Sertoli cell junctional barrier in continual (guinea pig) and seasonal breeders' (mink) testes. *J Androl* **16:** 400-409.

Pelletier R. M., & Byers S. W. (1992) The blood-testis barrier and Sertoli cell junctions: structural considerations. *Microsc Res Tech* **20:** 3-33.

Pelletier R. M., & Friend D. S. (1983) The Sertoli cell junctional complex: structure and permeability to filipin in the neonatal and adult guinea pig. *Am J Anat* **168:** 213-228.

Pelletier R. M., & Friend D. S. (1986) Sertoli cell junctional complexes in gossypol-treated neonatal and adult guinea pigs. *J Androl* **7:** 127-139.

Pelletier R. M., Okawara Y., Vitale M. L., & Anderson J. M. (1997) Differential distribution of the tight-junction-associated protein ZO-1 isoforms alpha+ and alpha- in guinea pig Sertoli cells: a possible association with F-actin and G-actin. *Biol Reprod* **57:** 367-376.

Pelletier R. M., & Vitale M. L. (1994) Filipin vs enzymatic localization of cholesterol in guinea pig, mink, and mallard duck testicular cells. *J Histochem Cytochem* **42:** 1539-1554.

Pelletier R. M., Yoon S. R., Akpovi C. D., Silvas E., & Vitale M. L. (2009) Defects in the regulatory clearance mechanisms favor the breakdown of self-tolerance during spontaneous autoimmune orchitis. *Am J Physiol Regul Integr Comp Physiol* **296:** R743-762.

Pignataro O. P., Radicella J. P., Calvo J. C., & Charreau E. H. (1983) Mitochondrial biosynthesis of cholesterol in Leydig cells from rat testis. *Mol Cell Endocrinol* **33:** 53-67.

Porter F. D. (2002) Malformation syndromes due to inborn errors of cholesterol synthesis. *J Clin Invest* **110:** 715-724.

Potter J. E., Millette C. F., James M. J., & Kandutsch A. A. (1981) Elevated cholesterol and dolichol synthesis in mouse pachytene spermatocytes. *J Biol Chem* **256:** 7150-7154.

Reynisdottir S., Eriksson M., Angelin B., & Arner P. (1995) Impaired activation of adipocyte lipolysis in familial combined hyperlipidemia. *J Clin Invest* **95:** 2161-2169.

Rigotti A., Trigatti B. L., Penman M., Rayburn H., Herz J., & Krieger M. (1997) A targeted mutation in the murine gene encoding the high density lipoprotein (HDL) receptor scavenger receptor class B type I reveals its key role in HDL metabolism. *Proc Natl Acad Sci U S A* **94:** 12610-12615.

Roberts C. K., Liang K., Barnard R. J., Kim C. H., & Vaziri N. D. (2004) HMG-CoA reductase, cholesterol 7alpha-hydroxylase, LDL receptor, SR-B1, and ACAT in diet-induced syndrome X. *Kidney Int* **66:** 1503-1511.

Royo T., Pedragosa M. J., Ayte J., Gil-Gomez G., Vilaro S., & Hegardt F. G. (1993) Testis and ovary express the gene for the ketogenic mitochondrial 3- hydroxy-3-methylglutaryl-CoA synthase. *J Lipid Res* **34:** 1636.

Rudel L. L., Lee R. G., & Cockman T. L. (2001) Acyl coenzyme A: cholesterol acyltransferase types 1 and 2: structure and function in atherosclerosis. *Curr Opin Lipidol* **12:** 121-127.

Sakashita N., Miyazaki A., Chang C. C., Chang T. Y., Kiyota E., Satoh M., Komohara Y., Morganelli P. M., Horiuchi S., & Takeya M. (2003) Acyl-coenzyme A:cholesterol acyltransferase 2 (ACAT2) is induced in monocyte-derived macrophages: in vivo and in vitro studies. *Lab Invest* **83:** 1569-1581.

Sakashita N., Miyazaki A., Takeya M., Horiuchi S., Chang C. C., Chang T. Y., & Takahashi K. (2000) Localization of human acyl-coenzyme A: cholesterol acyltransferase-1 (ACAT-1) in macrophages and in various tissues. *Am J Pathol* **156:** 227-236.

Saladin K. S. (2000) Anatomy & Physiology: The Unity of Form and Function, 2nd Kenneth S. Saladin McGraw-Hill (eds) McGraw-Hill Companies Press Boston MA.

Sertoli E. (1865) Dell'esistenza di particolari cellule ramificate nei canalicoli seminiferi del testicolo umano. . *Morgagni* **7:** 31-40.

Sever N., Yang T., Brown M. S., Goldstein J. L., & DeBose-Boyd R. A. (2003) Accelerated degradation of HMG CoA reductase mediated by binding of insig-1 to its sterol-sensing domain. *Mol Cell* **11:** 25-33.

Shalaby M. A., el-Zorba H. Y., & Kamel G. M. (2004) Effect of alpha-tocopherol and simvastatin on male fertility in hypercholesterolemic rats. *Pharmacol Res* **50:** 137-142.

Shapiro D. J., Nordstrom J. L., Mitschelen J. J., Rodwell V. W., & Schimke R. T. (1974) Micro assay for 3-hydroxy-3-methylglutaryl-CoA reductase in rat liver and in L-cell fibroblasts. *Biochim Biophys Acta* **370:** 369-377.

Shen W. J., Sridhar K., Bernlohr D. A., & Kraemer F. B. (1999) Interaction of rat hormone-sensitive lipase with adipocyte lipid-binding protein. *Proc Natl Acad Sci U S A* **96:** 5528-5532.

Shikita M., & Tamaoki B. I. (1965) Testosterone Formation by Subcellular Particles of Rat Testes. *Endocrinology* **76:** 563-569.

Shimano H. (2001) Sterol regulatory element-binding proteins (SREBPs): transcriptional regulators of lipid synthetic genes. *Prog Lipid Res* **40:** 439-452.

Shimano H. (2002) Sterol regulatory element-binding protein family as global regulators of lipid synthetic genes in energy metabolism. *Vitam Horm* **65:** 167-194.

Simons K., & Ikonen E. (2000) How cells handle cholesterol. *Science* **290:** 1721-1726.

Song B. L., Javitt N. B., & DeBose-Boyd R. A. (2005) Insig-mediated degradation of HMG CoA reductase stimulated by lanosterol, an intermediate in the synthesis of cholesterol. *Cell Metab* **1:** 179-189.

Song B. L., Qi W., Yang X. Y., Chang C. C., Zhu J. Q., Chang T. Y., & Li B. L. (2001) Organization of human ACAT-2 gene and its cell-type-specific promoter activity. *Biochem Biophys Res Commun* **282:** 580-588.

Song B. L., Wang C. H., Yao X. M., Yang L., Zhang W. J., Wang Z. Z., Zhao X. N., Yang J. B., Qi W., Yang X. Y., Inoue K., Lin Z. X., Zhang H. Z., Kodama T., Chang C. C., Liu Y. K., Chang T. Y., & Li B. L. (2006) Human acyl-CoA:cholesterol acyltransferase 2 gene expression in intestinal Caco-2 cells and in hepatocellular carcinoma. *Biochem J* **394:** 617-626.

Stahlberg D., Rudling M., Angelin B., Bjorkhem I., Forsell P., Nilsell K., & Einarsson K. (1997) Hepatic cholesterol metabolism in human obesity. *Hepatology* **25:** 1447-1450.

Steinberger A., & Steinberger E. (1971) Replication pattern of Sertoli cells in maturing rat testis in vivo and in organ culture. *Biol Reprod* **4:** 84-87.

Stubbs C. D., & Smith A. D. (1984) The modification of mammalian membrane polyunsaturated fatty acid composition in relation to membrane fluidity and function. *Biochim Biophys Acta* **779:** 89-137.

Suckling K. E., & Stange E. F. (1985) Role of acyl-CoA: cholesterol acyltransferase in cellular cholesterol metabolism. *J Lipid Res* **26:** 647-671.

Suckling K. E., Stange E. F., & Dietschy J. M. (1983a) Dual modulation of hepatic and intestinal acyl-CoA: cholesterol acyltransferase activity by (de-)phosphorylation and substrate supply in vitro. *FEBS Lett* **151:** 111-116.

Suckling K. E., Stange E. F., & Dietschy J. M. (1983b) In vivo modulation of rat liver acyl-coenzyme A:cholesterol acyltransferase by phosphorylation and substrate supply. *FEBS Lett* **159:** 29-32.

Tacer K. F., Haugen T. B., Baltsen M., Debeljak N., & Rozman D. (2002) Tissue-specific transcriptional regulation of the cholesterol biosynthetic pathway leads to accumulation of testis meiosis-activating sterol (T-MAS). *J Lipid Res* **43:** 82-89.

Taylor F. R., Saucier S. E., Shown E. P., Parish E. J., & Kandutsch A. A. (1984) Correlation between oxysterol binding to a cytosolic binding protein and potency in the repression of hydroxymethylglutaryl coenzyme A reductase. *J Biol Chem* **259:** 12382-12387.

Temel R. E., Gebre A. K., Parks J. S., & Rudel L. L. (2003) Compared with Acyl-CoA:cholesterol O-acyltransferase (ACAT) 1 and lecithin:cholesterol acyltransferase, ACAT2 displays the greatest capacity to differentiate cholesterol from sitosterol. *J Biol Chem* **278:** 47594-47601.

Temel R. E., Trigatti B., DeMattos R. B., Azhar S., Krieger M., & Williams D. L. (1997) Scavenger receptor class B, type I (SR-BI) is the major route for the delivery of high density lipoprotein cholesterol to the steroidogenic pathway in cultured mouse adrenocortical cells. *Proc Natl Acad Sci U S A* **94:** 13600-13605.

Uelmen P. J., Oka K., Sullivan M., Chang C. C., Chang T. Y., & Chan L. (1995) Tissue-specific expression and cholesterol regulation of acylcoenzyme A:cholesterol acyltransferase (ACAT) in mice. Molecular cloning of mouse ACAT cDNA, chromosomal localization, and regulation of ACAT in vivo and in vitro. *J Biol Chem* **270:** 26192-26201.

Vallet-Erdtmann V., Tavernier G., Contreras J. A., Mairal A., Rieu C., Touzalin A. M., Holm C., Jegou B., & Langin D. (2004) The testicular form of hormone-sensitive

lipase HSLtes confers rescue of male infertility in HSL-deficient mice. *J Biol Chem* **279:** 42875-42880.

Wang H., Liu F., Millette C. F., & Kilpatrick D. L. (2002) Expression of a novel, sterol-insensitive form of sterol regulatory element binding protein 2 (SREBP2) in male germ cells suggests important cell- and stage-specific functions for SREBP targets during spermatogenesis. *Mol Cell Biol* **22:** 8478-8490.

Wang S. P., Chung S., Soni K., Bourdages H., Hermo L., Trasler J., & Mitchell G. A. (2004) Expression of human hormone-sensitive lipase (HSL) in postmeiotic germ cells confers normal fertility to HSL-deficient mice. *Endocrinology* **145:** 5688-5693.

Wang S. P., Laurin N., Himms-Hagen J., Rudnicki M. A., Levy E., Robert M. F., Pan L., Oligny L., & Mitchell G. A. (2001) The adipose tissue phenotype of hormone-sensitive lipase deficiency in mice. *Obes Res* **9:** 119-128.

Wechsler A., Brafman A., Shafir M., Heverin M., Gottlieb H., Damari G., Gozlan-Kelner S., Spivak I., Moshkin O., Fridman E., Becker Y., Skaliter R., Einat P., Faerman A., Bjorkhem I., & Feinstein E. (2003) Generation of viable cholesterol-free mice. *Science* **302:** 2087.

Wiebe J. P., & Tilbe K. S. (1979) De novo synthesis of steroids (from acetate) by isolated rat Sertoli cells. *Biochem Biophys Res Commun* **89:** 1107-1113.

Willner E. L., Tow B., Buhman K. K., Wilson M., Sanan D. A., Rudel L. L., & Farese R. V., Jr. (2003) Deficiency of acyl CoA:cholesterol acyltransferase 2 prevents atherosclerosis in apolipoprotein E-deficient mice. *Proc Natl Acad Sci U S A* **100:** 1262-1267.

Wing T. Y., & Lin H. S. (1977) The fine structure of testicular interstitial cells in the adult golden hamster with special reference to seasonal changes. *Cell Tissue Res* **183:** 385-393.

Xu F., Rychnovsky S. D., Belani J. D., Hobbs H. H., Cohen J. C., & Rawson R. B. (2005) Dual roles for cholesterol in mammalian cells. *Proc Natl Acad Sci U S A* **102:** 14551-14556.

Yang T., Espenshade P. J., Wright M. E., Yabe D., Gong Y., Aebersold R., Goldstein J. L., & Brown M. S. (2002) Crucial step in cholesterol homeostasis: sterols promote binding of SCAP to INSIG-1, a membrane protein that facilitates retention of SREBPs in ER. *Cell* **110:** 489-500.

Yeaman S. J. (1990) Hormone-sensitive lipase--a multipurpose enzyme in lipid metabolism. *Biochim Biophys Acta* **1052:** 128-132.

Yu C., Chen J., Lin S., Liu J., Chang C. C., & Chang T. Y. (1999) Human acyl-CoA:cholesterol acyltransferase-1 is a homotetrameric enzyme in intact cells and in vitro. *J Biol Chem* **274:** 36139-36145.

Zammit V. A., Caldwell A. M., & Kolodziej M. P. (1991) Rapid decrease in the expression of 3-hydroxy-3-methylglutaryl-CoA reductase protein owing to inhibition of its rate of synthesis after Ca2+ mobilization in rat hepatocytes. Inability of taurolithocholate to mimic the effect. *Biochem J* **279 (Pt 2):** 377-383.

Zhang Y., Yu C., Liu J., Spencer T. A., Chang C. C., & Chang T. Y. (2003) Cholesterol is superior to 7-ketocholesterol or 7 alpha-hydroxycholesterol as an allosteric activator for acyl-coenzyme A:cholesterol acyltransferase 1. *J Biol Chem* **278:** 11642-11647.

Appendix

Table 2. Reaction mixture for reverse transcription PCR

Component	Volume (25μl)
RT buffer (10×)	2.5 μl
dNTP (5mM)	2.5 μl
Oligo dT (10μM)	2.5 μl
Enzyme RT	1.25μl
RNase inhibitor	0.4μl
RNA	2.5 μg
H_2O	

Table 3. Reaction mixture for PCR

Component	Volume (25μl)
10× QIAGEN PCR buffer	2.5 μl
5×Q-solution	5 μl
dNTP mix (10mM each)	0.5 μl
Primer sense	1.25μl
Primer anti-sense	1.25μl
Taq DNA polymerase	0.125 μl
Distilled water	12.375 μl
Template DNA	2.5 μl

Table 4. PCR standard protocol

Stages	Condition
Stage I: initial denaturation (Reps:1)	95°C 5min
Stage II: PCR (Reps:40)	95°C 1min 60°C 45sec. 72°C 1min
Stage III: Extension	72°C 7min
Stage IV: Cooling	4°C ∞

Table 5. Reaction mixture for real time PCR (SYBR Premix Ex Taq^{TM})

Component	Volume (20μl)
SYBR Premix Ex Taq^{TM} (2×)	10 μl
PCR forward primer (10μM)	0.4 μl
PCR reverse primer (10μM)	0.4 μl
Template (<100ng)	2μl
H_2O	7.2μl

Table 6. Shuttle PCR standard protocol

Stages	Condition
Stage I: initial denaturation (Reps:1)	95°C 30sec. 20°C/sec.
Stage II: PCR (Reps:40)	95°C 5sec. 20°C/sec. 60°C 30sec. 20°C/sec.
Stage III: Melting curve analysis	95°C 0sec. 20°C/sec. 65°C 15sec. 20°C/sec. 95°C 0sec. 20°C/sec.

Table 7. Three-step PCR standard protocol

Stages	Condition
Stage I: initial denaturation (Reps:1)	95°C 30sec. 20°C/sec.
Stage II: PCR (Reps:40)	95°C 5sec. 20°C/sec. 58°C 20sec. 20°C/sec. 72°C 15sec. 20°C/sec.
Stage III: Melting curve analysis	95°C 0sec. 20°C/sec. 65°C 1min. 20°C/sec. 95°C 0sec. 20°C/sec.

Table 8. Gel for separation (10%)

Component	Volume (8ml)
H_2O	1.6ml
1M Tris-0.5M Glycine (0.2M-0.1M)	1.6ml
10% SDS	0.32ml
50% Glycerol	0.8ml
25% Acrylamide/0.25% Bis	3.2ml
4% Persulphate of ammonium	0.4ml
10% TEMED	0.08ml

Table 9. Gel for concentration (4%)

Component	Volume (8ml)
H_2O	1.68ml
0.5M Tris-HCl pH 6.7	0.56ml
50mM EDTA pH 6.7	0.32ml
50% Glycerol	0.4ml
25% Acrylamide/0.25% Bis	0.64ml
4% Persulphate of ammonium	0.2ml
10% TEMED	0.04ml